The Pleiotropic Effects of LC8 on the Anchoring Protein in Flagellar Radial Spoke Complex

Anjali Gupta
Marquette University

THE PLEIOTROPIC EFFECTS OF LC8 ON THE ANCHORING PROTEIN IN FLAGELLAR RADIAL SPOKE COMPLEX

by

Anjali Gupta, M.S.

A Dissertation submitted to the Faculty of the Graduate School,
Marquette University,
in Partial Fulfillment of the Requirements for
the Degree of Doctor of Philosophy

Milwaukee, Wisconsin

December 2011

ABSTRACT
THE PLEIOTROPIC EFFECTS OF LC8 ON THE ANCHORING PROTEIN IN
FLAGELLAR RADIAL SPOKE COMPLEX

Anjali Gupta, M.S.

Marquette University, 2011

The goal of this thesis is to elucidate the assembly mechanism of macromolecular complexes in the microtubule-based axoneme in flagella. The axoneme is comprised of more than 400 distinct polypeptides. While all axonemal proteins are synthesized in the cell body, they need to be imported to the tip of the growing flagella for the final assembly. They are then assembled into distinctive structural complexes and integrated into precise positions relative to each other. The assembled macromolecular complexes operate in concert enabling the axoneme to beat rhythmically as a biological machine. This arduous process involves multiple reactions and meticulous regulation. However, the assembly process in the cell body and at the tip of flagella remains largely unknown.

This thesis took advantage of a flagella model organism *Chlamydomonas* and a rather simple and a well-characterized axonemal complex, the radial spoke, to identify the key assembly mechanisms. Genetic studies have revealed two spoke components, RSP3 and LC8, that are particularly important for the assembly of the entire complex. Mutants defective in either gene generate paralyzed flagella devoid of the RS. Using a variety of approaches that are possible for this model organism, this study revealed that a stack of LC8 dimers directly binds to RSP3 at the tip of the flagella to promote a series of events, including phosphorylation of RSP3, formation of the base of the RS and docking of the spoke to the axoneme.

These findings have shed light on the series of events that occur between transport and assembly. These findings also have broad implications, as LC8 is a promiscuous molecule that interacts with many flagellar and non-flagellar proteins in the cell body. Many of them play vital roles in the normal functioning of cells or in the pathogenesis of microorganisms. Some LC8 target proteins exist in the molecular complexes, as the radial spoke. However, the LC8-involved reactions remain poorly defined. The findings from this thesis show that LC8 bindings can trigger pleiotropic effects on a single target protein. Together, these conclusions shed critical insight on the biology of flagella and LC8.

ACKNOWLEDGEMENTS

Anjali Gupta, M.S.

First I would like to thank my mentor, Dr. Pinfen Yang. Without her guidance, perseverance and constant encouragement the development of my scientific career would have been impossible. She taught me to think critically and creatively and also to write effectively. Her continuous patience and support throughout these five years is greatly appreciated.

I would like to express my gratitude to my graduate committee members, Dr. Stephen Downs, Dr. Kathleen Karrer, Dr. Edward Blumenthal, Dr. Allison Abbott and Dr. David Wagner, for their time, help and support. Their insightful comments and suggestions kept my research focused.

I would like to thank my current and past lab members and friends Priyanka Sivadas, Dr. Radhika Gopal and Dr. Mei Wei for giving me a challenging and fun environment at the same time. We shared great times together.

Finally, the most deserved thanks to my mom and dad. Their blessings and words of wisdom always encouraged me to move forward beyond all the odds. A special thanks to my brother Anshul, for cheering and boosting my spirit and to my brother Mangesh, to whom I dedicate my dissertation. The memories and the encouraging words of him are unforgettable.

And to my fiancé Ankur - for his love, support and for everything he is.

TABLE OF CONTENTS

LIST OF TABLES

LIST OF FIGURES

LIST OF ABBREVIATIONS

2D	Two Dimensional
AH	α-Helix
AKAP	A-Kinase Anchoring Protein
CaM	Calmodulin
CP	Central Pair
CSC	Calmodulin associated Spoke Complex
D/D	Dimerization and Docking domain
DEAE	DiEthylAminoEthyl
DRC	Dynein Regulatory Complex
EM	Electron Microscopy
ERK	Extracellular signal Regulated Kinase
fla	Flagella less
GKAP	Guanylate Kinase Associated Protein
HC	Heavy Chain
HSP40	Heat Shock Protein 40
IC	Intermediate Chain
IDA	Inner Dynein Arm
IFT	Intra-Flagellar Transport
KI	Potassium Iodide
LC	Light Chain
MAPK	Mitogen Activated Protein Kinase
NaCl	Sodium Chloride
NEK9	NIMA related Kinase
nNOS	neuronal Nitric Oxide Synthase
Nup159	Nuclear Pore protein 159
ODA	Outer Dynein Arm
p53BP1	p53 Binding Protein 1
pf	Paralyzed Flagella
PKA	Protein Kinase A
PMM	Paramomysin
RII	Regulatory domain of PKA
RS	Radial Spoke
RSP	Radial Spoke Protein
WT	Wild Type

CHAPTER 1: INTRODUCTION

1.1 Cilia or flagella

Cilia and flagella are similar organelles generated by most eukaryotic organisms ranging from protists to humans. They extend from the cell body to the extracellular environment. Those that are short or appear in a cluster are generally referred to as cilia while those that are longer and less numerous are referred to as flagella. However, these two terms are used interchangeably.

These organelles play two vital roles. First of all, they are cellular antennae. By protruding into the aqueous milieu, these organelles are ideal to detect extracellular stimuli. The chemical signals, like morphogens, growth factors, hormones and nutrients, or physical signals, like light and fluid flow, are transduced through channels and receptors enriched in the ciliary membrane (Singla and Reiter, 2006; Satir and Christensen, 2007; Davenport and Yoder 2005; Pazour and Witman, 2003). The signal transduction is relayed to the nucleus, enabling cells to monitor the environment. Based on the signaling, cells can either maintain the homeostasis or change a wide range of cellular reactions, such as metabolism, movement, differentiation and mitosis. The immotile sensory cilium is often referred as primary cilium. One example is the primary cilium of kidney tubular epithelium. The primary cilium senses the fluid flow with calcium channels. The fluid flow triggers calcium influx that in turns triggers a cleavage of a signaling peptide that is then transported back to nucleus so that the epithelial cells maintain the homeostasis. A defect in any step of this pathway will lead to changes in gene expression and reactions in the epithelium, leading to de-differentiation, loss of

polarity, unchecked mitosis and thus cyst formation. Clinically, the disorder is referred to as polycystic kidney disease (Davenport and Yoder 2005).

Aside from monitoring the surrounding environment, some cilia and flagella are motile, beating rhythmically across surrounding fluid. These motile organelles exhibit distinctive waveform and beat frequency in different cell types. The forces generated by cilia circulate the fluid on the surface or propel the cells to move in an aqueous environment. Most simple organisms generate these dual-functioning cilia for navigation, a behavior crucial to feast, evade and mate, in order to thrive in changing environment (Satir and Christensen, 2007).

Similarly, vertebrates take full advantage of both functions. Although most nucleated cells generate a solitary immotile primary cilium for monitoring purposes, the distributions of motile cilia are more restricted. Clustered motile cilia are a typical feature of the epithelium in the respiratory tract, the ventricle of the central nervous system and the female reproductive tract. These cilia propel the viscous fluid along the epithelial surface and the movement transports particles, chemicals and oocytes directionally. In the male reproductive system, sperm cells generate a single motile flagellum that propels male gametes to oocytes. These organelles play critical roles in normal functioning of each system.

Defects in either sensory or motile function of these organelles cause myriad of serious developmental disorders and diseases that are collectively referred as ciliopathies (Snell et al., 2004; Satir and Christensen, 2007; Marshall, 2008; Sharma et al. 2008; Gerdes et al., 2009). The symptoms vary, depending on which types of cilia are affected and what functions are compromised. The phenotypes include blindness, deafness,

polycystic organs, polydactyly, anosmia, hydrocephaly, situs inverses, diabetes, hypertension, obesity, chronic respiratory tract infections and infertility. These combined symptoms mystified the medical fields for decades. In recent years, it has become clear that the disorders are rooted in anomalies in cilia and flagella. Thus the studies of these organelles have been taken in various directions related to ciliogenesis, sensory function and motility mechanisms. This thesis primarily addresses a molecular interaction that is relevant to these fundamental mechanisms in all types of cilia and flagella.

1.2 *Chlamydomonas* -- the model system

Many fundamental mechanisms in cilia and flagella were discovered in *Chlamydomonas*, a biflagellate green alga with multiple experimental advantages, genetics in particular (Harris, 2001). Most discoveries made in the green algae are directly applicable to mammals because of the conserved structure, function, composition and mechanisms of these organelles. It is easy to generate viable flagellate *Chlamydomonas* mutants. It is also relatively easy to identify defective genes, the encoded proteins and their interacting partners. Studies of the mutants with a myriad of phenotypes in flagellar length, sensory functions and motility revealed invaluable physiology-relevant information. The novel genes and their functions were instrumental in the discoveries of mammalian orthologues and in identifying the genetic and molecular defects underlying a wide spectrum of congenital disorders related to defective cilia (Merchant et al., 2007; reviewed in Pazour and Witman, 2009). This thesis continues to take advantage of this model organism to reveal a key mechanism in the assembly of the axoneme during ciliogenesis.

1.3 Axoneme – the cytoskeleton of cilia and flagella

All cilia and flagella are supported by a microtubule-based scaffold, the axoneme. The details in the axoneme vary to serve the needs of individual cell types. However, the majority of them adopt a 9+2 or a 9+0 format. The 9+2 format is the most common among motile cilia and flagella and in fact is the best characterized (Li et al. 2003; Avidor-Reiss et al., 2004; Li et al., 2004) (Figure 1-1A). The 9+2 axoneme consists of 9 microtubule doublets encircling a pair of singlet microtubules called the central pair (CP). Each microtubule of the CP associates with multiple projections that are encircled by a thin central sheath. The CP is absent in the 9+0 axoneme. The surrounding 9 outer doublets consist of a complete A tubule attached to a partial B tubule. The A tubule anchors three prominent macromolecular complexes-- the outer dynein arm (ODA), the inner dynein arm (IDA) and the radial spoke (RS). These complexes are arranged around the circumference and along the length of the axoneme. The ODA and IDA project toward the B tubule of the adjacent outer doublets while the RS projects inward towards the CP (Figure 1-1A). These complexes are located at precise positions relative to each other in each 96-nm repeat (Figure 1-1B). These basic structures and their biochemical compositions are largely conserved throughout evolution (Mitchell and Sale, 1999; Wargo et al., 2005; Lechtreck and Witman, 2007; Lechtreck et al., 2008).

These structures operate in concert and are central to motility. The concerted action enables this super complex to beat rhythmically with high frequency and a particular waveform. In addition, these structures harbor signal transducers that modulate motility in response to secondary messengers. Together these major axonemal structures

A
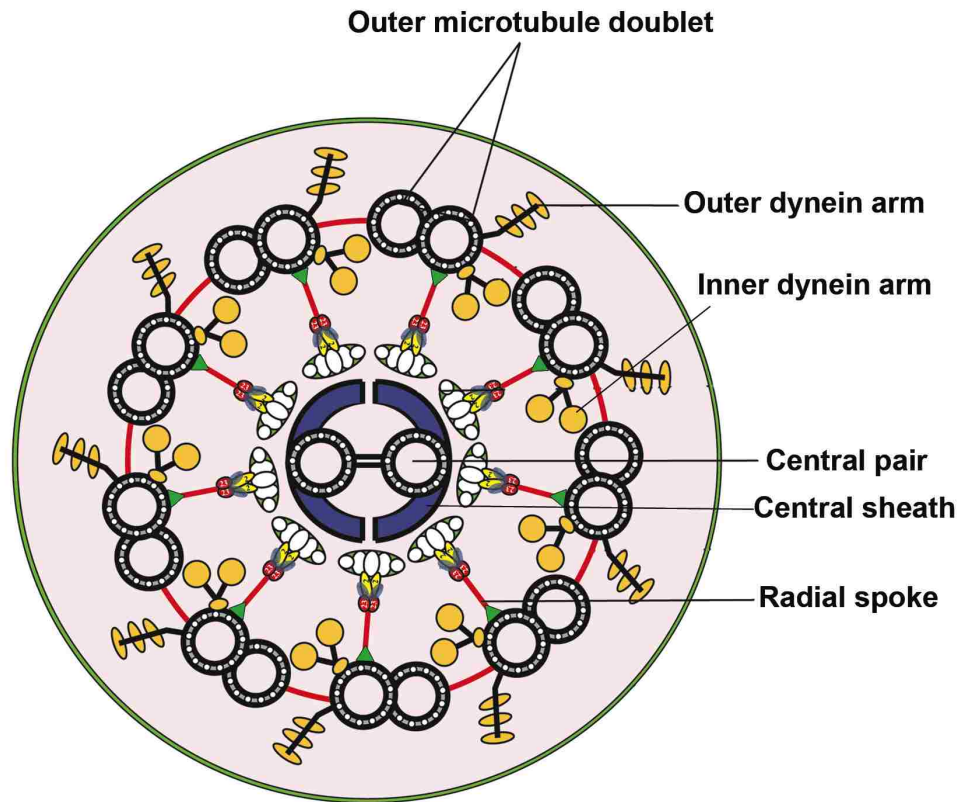
B
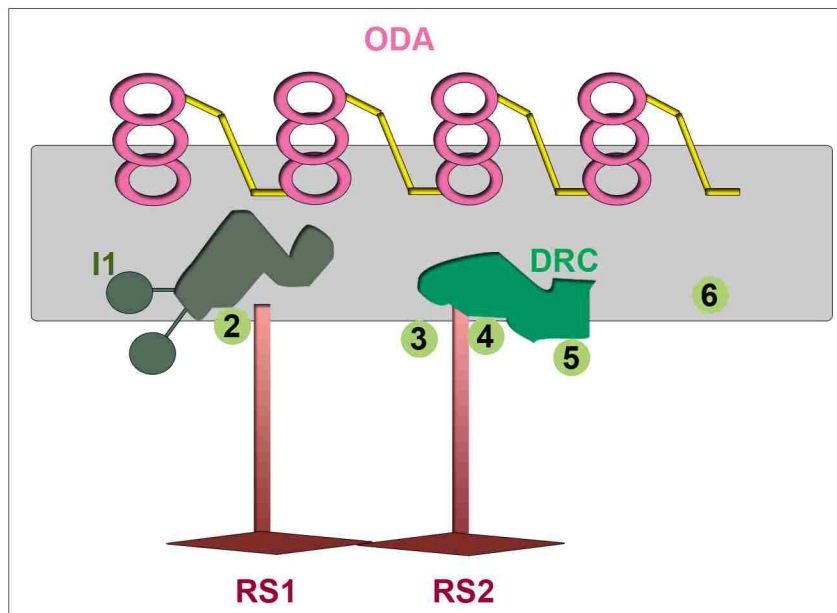
Figure 1-1. The schematic diagrams of the 9+2 axoneme.

(A) A cross section view, with nine microtubule outer doublets surrounding the central pair apparatus. Dynein arms docked to the outer doublets protrude towards the adjacent doublets while the T-shaped radial spoke projects towards the central pair apparatus. **(B)** The averaging of 96-nm repeats on an outer doublet. Each repeat has four outer dynein arms (ODAs), two radial spokes (RS1 and RS2), several inner dynein arm (IDA) species and a dynein regulatory complex (DRC). The base of the RSs is in proximity to IDAs and DRC. I1: is IDA specie 1. #2-6: refers to electron densities of different IDA species that are grouped as I2 and I3.

are the basis of the sophisticated biological nanomachines. Each structure has a unique contribution and will be discussed in more detail as follows.

Axonemal dyneins: Axonemal dyneins are divided into two major categories, ODA and IDA, based on their position on the outer doublets. ODAs are located at the outer perimeter while IDAs are positioned closer to the inner circumference (DiBella and King, 2001). When viewed longitudinally, four ODAs and three IDAs repeat at every 96-nm interval (Figure 1-1B). It is believed that the motors dock to their respective docking complexes on the outer doublets and the docking complexes determine the specific location and the periodicity of the motors (Casey et al. 2003).

The sub-classes of motor complex vary in their protein composition (reviewed in King and Kamiya, 2009). Regardless, their components are usually named heavy chains (HC), intermediate chains (IC) and light chains (LC) based on the molecular mass. Each motor usually contain 1-3 HCs that are ATPases and two ICs that are structural scaffolds located at the base of the motor. ICs associate with LCs to form a subcomplex anchoring the ATPase to the outer doublets. These larger molecules are critical for the assembly of the motor complex. Defects in HCs or ICs result in the absence or deficiencies in the entire complex. In contrast, the roles and the significance of different LCs vary drastically. Some are dispensable or regulatory, while a few are indispensable and are not unique to the dynein motors. They are dimers and present in various flagellar and non-flagellar molecular complexes. The best example is LC8, which is the focus of this dissertation. A later section will be devoted to discuss LC8 in detail.

Contrary to only one type of ODA, there are several species of IDAs. The composition of IDAs is complex and only partially revealed. Electron microscopy reveals three IDAs, I1, I2 and I3, at distinct positions in each axonemal repeat. However, biochemically IDAs can be separated into 7 species/isoforms, each with a different HC composition and a slightly overlapping function in controlling the flagellar waveform (Kagami et al., 1990; Kagami and Kamiya, 1995). While the I1 (specie f) is localized in each 96-nm repeat, the localization of I2 (specie a, c, d, e) and I3 (specie b, g) subspecies varies along the axoneme. Among the subspecies of IDAs, I1 resembles ODA the most, in the composition and morphology. Both have more than 1 HC. In particular, both contain LC8 (Harrison et al., 1998). In contrast, the other IDAs consist of only a single HC and no LC8.

Some of these single-headed IDA are less abundant in the mutants defective in the dynein regulatory complex (DRC). Studies of suppressor mutagenesis discovered that mutations in DRC or the ATPase in outer dynein arm or inner dynein I1 rescue the paralysis of the Radial Spoke or Central Pair mutants without restoring either structure. Based on this study, it was proposed that the Radial Spoke and Central Pair control dynein motors through the DRC. Topographically, the DRC is located at the base of the Radial Spoke near inner dynein arm I2 and I3 (Piperno et al., 1992; Piperno et al. 1994; Rupp and Porter, 2003; Gardner, 1994).

ODA and IDA motors contribute distinctively to the beating properties (Kamiya, 2002). ODAs provide the primary force that powers the oscillatory beating. The flagella of ODA mutants are motile but beat with low frequency. On the contrary, IDAs primarily, but not exclusively, determine the waveform. The flagella of IDA mutants

beat with normal frequency but with a shallower amplitude. The different IDA species are regulated differently. I1 IDA appears to be the key target of the RS-dependent phospho-regulation (Howard et al., 1994; Habermacher and Sale, 1995, 1997).

Radial spoke (RS): The RS is a T-shaped complex with ~ 7-nm thick and ~ 40-nm long stalk and a ~ 20-nm wide bulbous head (Nicastro et al. 2005). They appear as doublets or triplets in every 96-nm repeat depending on the organism, as doublet in *Chlamydomonas* axoneme. The two spokes are in distinct micro-environments. The base of spoke1 is near I1 while the base of spoke 2 is adjacent to DRC and the I2 and I3 (Piperno et al., 1990; Porter et al. 1992). Although conventional EM failed to reveal any differences in the two spokes, recent cryotomography images did show obvious differences between the bases of the two RSs (Nicastro et al., 2006). The distinct topography between the two spokes suggests that the docking mechanism and the role of the two RSs are different. As the RS is a key subject of this thesis, a separate section will be devoted to discuss this molecular complex.

Central pair apparatus: The central pair (CP) apparatus is comprised of two microtubule singlets, CP1 and CP2. They associate with multiple distinct projections that differ in the periodicity as well as the composition (Mitchell and Sale, 1999; Zhang and Mitchell, 2004; Mitchell, 2009). The CP is physically detached from the outer doublets. However, it plays a central role in the control of dynein motors (Wargo and Smith, 2004). It is proposed that CP1, CP2 and their associate projections have distinct functions in

controlling motility. The control is mediated through the intermittent contact between the CP projections and the RS.

1.4 Mechanistic of axonemes

In general, the ATPase activity of dynein motors powers flagellar beating. Motors engage with the neighboring outer doublets and hydrolyze ATP. Hydrolysis of ATP triggers conformational changes in the motor. The conversion of chemical energy into physical energy results in sliding of adjacent microtubules (reviewed in Lindemann and Lesich, 2010). However, the thousands of dynein motors distributed throughout the 9 outer doublets cannot activate simultaneously. Simultaneous firing of all motors would result in a rigid flagellum. Instead, the motors have to take turn in order to generate and propagate a bend. The RS and CP constitute a control system that coordinates the activity of dynein motors.

The primary control mechanism appears mechanical in nature (Lindemann and Lesich, 2010). The inter-doublet sliding generates a longitudinal tension on the RS that are attached to both outer doublets and the CP. This causes the RS to tilt and lengthen slightly at the bend (Figure 1-2). However, the nearby straight regions have vertically oriented RS. This suggests that the RS-CP contact is transient. Furthermore, the tilting and lengthening of RS implies that the RS are relatively rigid but has slight elasticity (Warner and Satir, 1974; Curry and Rosenbaum, 1993; Smith and Yang, 2004). Additionally, the CP rotates once per beat in some cilia or flagella. The rotation of the CP around the axis of the axoneme applies a centrifugal force on the RS, causing the RS to twist and to extend further. These two forces may act on the RS to push or pull dynein

motors locally into an active state (Omoto et al., 1999; Lindemann and Lesich, 2010). This transient contact with the CP and the transduction through the RS is critical as genetic defects abolishing the contact result in completely paralyzed flagella. The subtle defects that interfere with the coupling between the CP and the dynein motors will result in flagella with asynchronized and jerky movement.
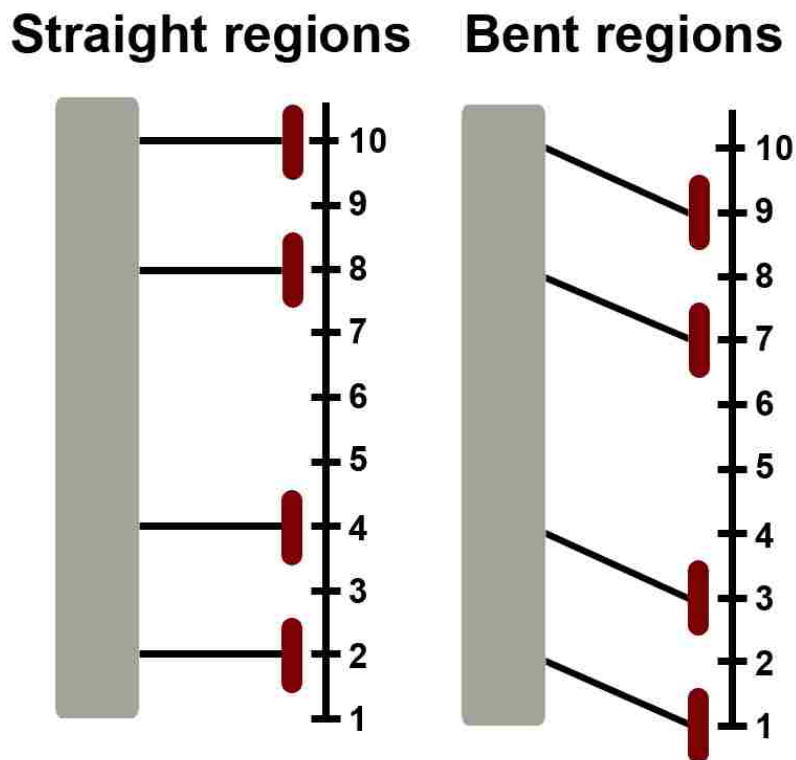
Figure 1-2. Deformation of the RS during oscillatory beating.

RSs (brown-headed T) in resting flagella are oriented vertically to the microtubule outer doublets (grey bars) and the central pair microtubule (black line) that has periodic projections (numbered bars). The sliding between outer doublets applies force on the spokes attached to the central pair projection resulting in the lengthening and tilting of the stalk. Modified after Warner and Satir, 1974.

1.5 Modulation of axonemes

Cilia and flagella are not merely the oscillating machines. They respond to stimuli by changing the beating pattern. These changes are induced by common secondary messengers such as calcium, cAMP and cGMP (Salathe, 2007). The machinery necessary for the regulation of the rhythmic beating are built into the axoneme. This was successfully shown by the reactivation assay. Isolated axonemes, without flagellar membrane and the cytoplasm can be reactivated upon the addition of ATP (Gibbons and Gibbons, 1972). It was found that the reactivated movement responds to secondary messengers largely as intact cilia and flagella indicating that molecular switches that mediate the changes are located in the axoneme. For example, calcium was found to change waveform as well as beat frequency in a reactivation assay (Kamiya and Witman, 1984; Omoto and Brokaw, 1985). Further studies showed that calcium regulates these changes by acting on axonemal dyneins, RS and CP that harbors the proteins that bind calcium or the prototype calcium sensor -- calmodulin (Wakabayashi et al., 2009; Yang et al., 2001; Patel-King et al., 2004; Yang et al., 2004; Wargo et al., 2006; Dymek and Smith, 2007).

In addition, functional studies showed that the cAMP-dependent protein kinases (PKA) inhibit the beating of *Chlamydomonas* flagella (Hasagawa and Kamiya, 1987). This inhibitory effect was reversed by calcium-independent phosphatase, PP1 and PP2A (Habermacher, et al., 1995; 1997; King and Dutcher, 1997). The PKA activity seems to be regulated by RSs that operate to inhibit PKA (Howard et al., 1994) and casein kinase 1 (CK1) (Yang and Sale, 2000) located in axonemes. In the absence of RSs, one of the CK1 substrate I1 inner dynein intermediate chain IC138 becomes hyper-phosphorylated.

The phosphorylation state of IC138 regulates the sliding of the microtubules (Wirschell et al., 2009). Using a similar experimental strategy, it was demonstrated that calcium and calmodulin-dependent kinase also regulate motility through the RS and CP (Smith, 2002). Together, these independent lines of evidence show that a network of calcium-dependent and independent molecular switches are built into the axonemes to concertedly regulate the rhythmic beating.

1.6 Transportation of axonemal components – Intraflagellar transport

The assembly of the axoneme is a complicated process. These organelles are devoid of any translational machinery and thus are built by proteinaceous components synthesized in the cell body. However, they are assembled largely at the tip of the axoneme by a rather efficient process. A deflagellated *Chlamydomonas* can regenerate the full-length flagella containing ~ 1000's 96-nm axonemal repeats in 1 hour. The effective assembly at the distal end of flagella requires the delivery of the axonemal components from the cell body by intraflagellar transport (IFT) (Johnson and Rosenbaum, 1992; Kozminski et al., 1993). The transport system is comprised of trains and motors (Figure 1-3). The train is the protein complex that binds the cargoes at the peri-basal body area (Deane et al., 2001). The anterograde transport of the particles from the cell body to the tip is driven by kinesin motor (Cole et al., 1993) while the retrograde transport from the tip to the cell body is powered by cytoplasmic dynein motor (Pazour et al., 1998). The motors carry train and walk on the axonemal outer doublets to deliver the loaded cargoes comprised of axonemal components as well as proteins in the membrane.
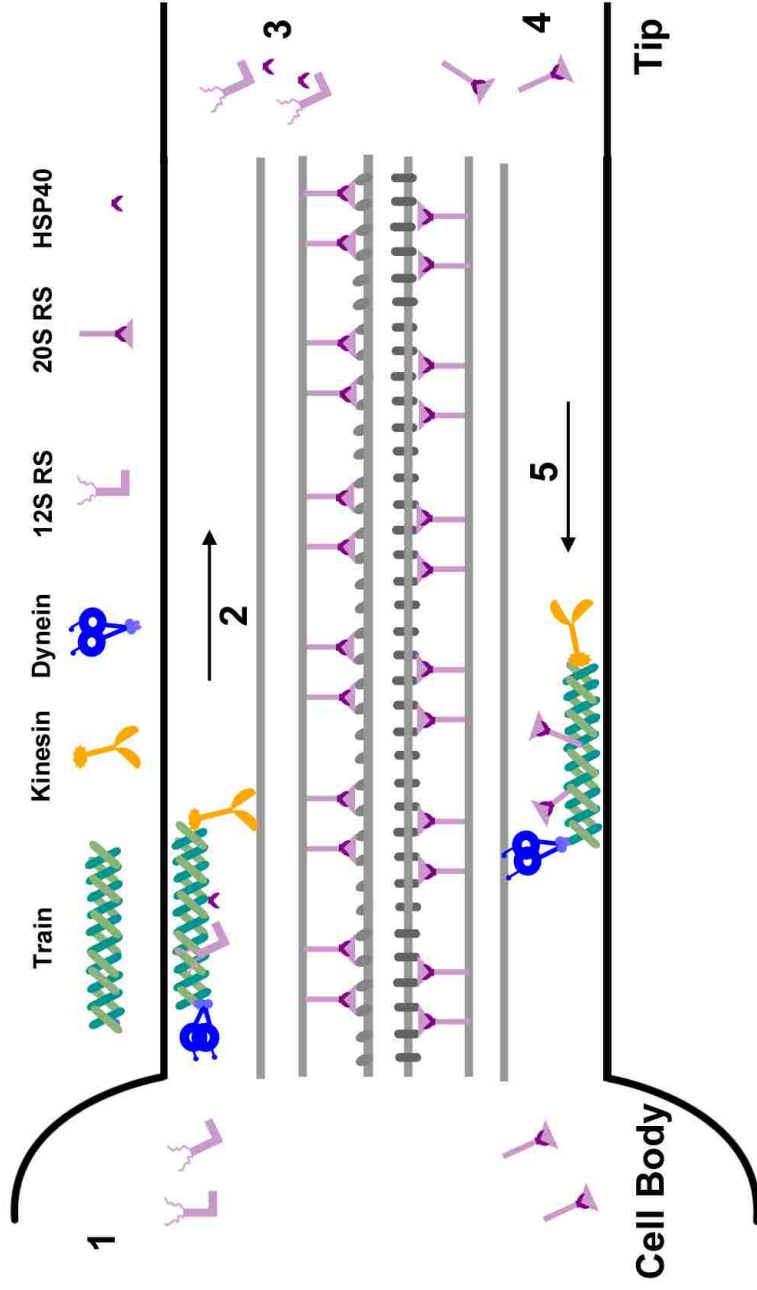
Figure 1-3. The model for the assembly process of the RS complex.

The RS are pre-assembled in the cell body as precursor particles. The precursors are loaded on IFT trains at the peri-basal body area underneath the flagella (Step 1). The loaded trains are driven by kinesin motors to the tip of the flagella (Step 2). At the tip, the precursor complexes are released from the train (Step 3) and then converted into mature spokes and integrated into the axoneme at the precise positions. The disassembled mature RS particles (Step 4) are then delivered back to the cell body by dynein motors (Step 5). The precursor and mature spoke particles differ in the content and morphology. Step 3 and Step 4 are poorly defined.

IFT occurs constantly, even in the established flagella. Studies of the temperature-sensitive kinesin mutant demonstrated that IFT is required for the formation of nascent axonemes during ciliogenesis as well as for the maintenance of the established axonemes (reviewed in Rosenbaum, 2002; Cole et al., 2003; Pedersen et al., 2006; Scholey and Anderson, 2006). Defects in this transport machinery, trains or motors, result in short or no flagella. The discovery of this ongoing machinery originated from the study of the RS.

1.7 Radial spoke

The RS in *Chlamydomonas* flagella has been employed to discover fundamental mechanisms in cilia and flagella because of its unique composition and physical features (reviewed by Yang et al., 2010). The major RSPs have unusually low isoelectric points (pI) that enable their purification from the rest of the axonemal components in 2-D SDS-PAGE. The RS is also extremely stable, and is purified as an intact complex in Potassium Iodide (KI) buffer. The purified spoke polypeptides were used for raising antibodies for tracking the RS complex in a variety of studies. The *Chlamydomonas* RS mutant strains that are defective in different genes are also available for in vivo studies (Table 1-1). Together, these resources have become powerful tools for addressing fundamental questions in cilia and flagella.

For instance, comparisons of the motility deficiencies of various RS mutants have revealed the basic control mechanism of oscillatory beating (Yang et al., 2008). Furthermore, fluorescent microscopy of the distribution of a key spoke protein revealed that RS was added at the growing tip of the axoneme during ciliogenesis, rather than at

the basal end of the axoneme (Johnson and Rosenbaum. 1992), implying that there is a transport mechanism that delivers the axonemal component synthesized in the cell body to the tip of flagella. This prediction, led to the observation of particles moving along the length of flagella in living cells (Kozminsky et al., 1993) and the subsequence discovery of the IFT mechanism and defective human genes responsible for various ciliopathies. This thesis took advantage of the RS to elucidate the assembly mechanism of axonemal complexes. Following is the introduction on this macromolecular complex, with a particular focus on two constitutive RS subunits that are central to the assembly, RSP3 and LC8.

Table 1-1. *Chlamydomonas* radial spoke mutants.

Mutants	Gene product	Motility phenotype	Morphological defect	Missing RSPs	Less abundant RSPs	Phosphorylation
pf1[a]	4	Paralyzed	Spokehead-less	1,4,6,9,10	None	Normal
pf5 [a, c]	?	Paralyzed	?	13,15,11	All	?
pf14 [a]	3	Paralyzed	Spoke-less	All	None	Normal
pf17 [a]	9	Paralyzed	Spokehead-less	1,4,6,9,10	None	Normal
pf24 [a]	2	Paralyzed	?	None	1,4,6,9,10,2, 16,23	Normal
pf25 [a,d]	11	Swimming/ Paralyzed	None	11	8	Normal
pf26ts [a, e]	6	Paralyzed at 32°C	None	None	1,4,6,9,10	Normal
pf27 [a]	?	Paralyzed	?	None	All	Hypo-phosphorylation
fla14-1[b]	LC8	Paralyzed,	Spoke-less; Short flagella	All	All	Normal
fla14-3[c]	LC8-CT	Paralyzed/ twitching	?	13, 15	All	Hypo-phosphorylation

[a] Huang et al., 1981.
[b] Pazour et al., 1998.
[c] Yang et al., 2009.
[d] Yang and Yang, 2006.
[e] Wei et al., 2010.

1.7.1 Composition of the radial spoke

The components of the RS were revealed by both genetic and biochemical methods. The

Chlamydomonas pf14 mutant generates paralyzed flagella lacking the entire T-shaped RS

complex. The comparison of the axonemes from *pf14* and WT in 2-D SDS-PAGE

showed that the morphological deficiency corresponds to the absence of at least 17

axonemal proteins (Piperno et al., 1981). These 17 proteins also appeared in the isolated

RS particles (Yang et al., 2006). These findings indicate that these 17 polypeptides are

unique to the RS. Cytoplasmic complementation showed that the gene encoding one of

the 17 proteins, RSP3, has a premature stop codon in *pf14*. Transformation of the wild

type RSP3 gene into *pf14* mutant rescued the paralysis phenotype. Thus RSP3 plays a

central role in the assembly of the rest of the RSPs. In addition, the isolated RS also

contains calmodulin and LC8 that are present in multiple axonemal complexes (Yang et

al., 2001; reviewed by Yang and Smith, 2009). Together, these 19 components constitute

the RS complex.

  Additional RS mutants with limited deficiencies in the morphology and

composition, revealed the general position of these molecules (Table. 1-2; Yang et al.,

2006). Five RSPs (RSP1, 4, 6, 9, 10) are located in the spokehead that contacts the CP

intermittently, while the rest of the RSPs are located in the stalk (Table 1-2). Among the

stalk proteins, RSP 2, 5, 16, 23, are predicted to locate at the head-stalk junction (neck),

linking and stabilizing the two morphologically distinct spoke modules (Huang et al.,

1981; Curry and Rosenbaum, 1993; Yang et.al., 2004; 2008; Yang and Yang, 2006;

Kohno et al., 2010). The other proteins are thought to be located towards the base of the

stalk.

These RSPs contain a wide range of molecular modules. Interestingly, those implicated in signal transduction are exclusively located in the stalk. The general topography of RSPs is helpful in understanding the localization of these signaling modules and for the study of RS. However, the molecular interactions that underlie this seemingly purposeful arrangement remain unknown. It is only partially revealed that how RSPs become assembled into a single complex and how the RSs anchors near specific dynein motors and DRC on the axoneme. Addressing these questions will reveal the complex arrangement of RSPs that controls flagellar beating both mechanically and chemically.

1.7.2 Phosphorylation of the radial spoke proteins

Indirect evidence has suggested that phosphorylation of axonemal proteins regulate the beating. The in vivo pulse 32P incorporation experiments provided evidence that more than 80 proteins in the axoneme are phosphorylated. Comparison of WT axoneme with *pf14* axoneme showed that five of them are in the RS -- RSP2, 3, 5, 13, 17 and that they are exclusively localized in the stalk (Table 1-2). The difference in the extent of phosphorylation level of these five proteins in two paralyzed RS mutants, *pf27,* suggested that these proteins are hypo-phosphorylated in this mutant. Thus it was proposed that phosphorylation of these RSPs may modulate flagellar beating (Piperno et. al. 1981, Yang and Yang, 2005). However, aside from hypo-phosphorylation, RSPs are less abundant in the axonemes of these two mutants (Table 1-1) and the assembled RSs are no longer KI-resistant (Yang and Yang, 2005; Yang et al., 2009). These observations suggest that phosphorylation is linked to the proper assembly of the RS (Yang and Yang,

2005; Qin et al., 2004); and the defective assembly of the RS, not phosphorylation, is directly responsible for the motility deficiency.

The genetic defect in *pf27* has not been determined yet. The hypophosphorylation of RSP in this mutant is used as a standard for determination of phosphorylation of RSP in other mutants like *fla14-3*. The multiple bands in the SDS-PAGE gels are generally considered as the different levels of phosphorylation of the RSP However, there is no direct experimental evidence that shows the hypo-phosphorylation of the RSPs. The RS deficiencies in *fla14-3* are due to a read through mutation at the stop codon of the LC8 gene, resulting in a LC8 polypeptide with a C-terminal extension (LC8-CT). This mutant has reduced amounts of RS in the axoneme and the multiple bands of RSP3 in this mutant suggest that it is hypo-phosphoryated (Yang et al., 2009). In a more severe mutant, the LC8 null mutant *fla14-1,* RS is not detectable in the axoneme but is still abundant in the soluble flagellar matrix. The RSP3 in the flagellar matrix of this mutant also displays multiple bands suggesting that RSP3 remains hypo-phosphorylated (Table 1-1; Qin et al., 2004). These observations indicate that LC8 is critical for the assembly of the RS and is correlated with RSP3 phosphorylation. This prediction is consistent with the discoveries that multiple protein kinases are involved in the control of the ciliogenesis (Wilson et al., 2010) and cilia resorptions (Pan and Snell, 2007) — the assembly and disassembly of axonemal complexes. The RS could again provide a venue to investigate the role of phosphorylation in assembly.

1.7.3 Assembly of the radial spoke

The assembly of the RS is only partially revealed (Figure 1-3). Fractionation of the cell

body extract and soluble flagellar matrix shows that RSPs are assembled into precursor

complexes in the cell body (Qin et al., 2004)., The precursor complexes are released from

IFT trains and converted into the mature RS complexes at the tip. The bound mature RS

are released from the axoneme and are transported by retrograde IFT back to the cell

body for repair.

It has become evident that the precursor and mature RS particles differ in several

ways. First of all, they sediment differently in the sucrose gradient. The sedimentation

coefficient of precursor particles is 12S and of mature spoke particle is 20S (Qin et al.,

2004). Secondly, they differ in protein composition. The characterization of 12S

particles and the discovery that a spoke protein HSP40 is absent in the 12S precursor

revealed that only a portion of RSPs are present in the precursor particles (Yang et al.,

2008; Diener et. al., 2011). The exact subunits missing in the precursor remain to be

determined (Table 1-2). Lastly, the precursor and the mature particles differ in

morphology (Diener et. al., 2011). The distinctions between the precursors and mature

complexes gives rise to the possibility that the RSPs absent in the precursors, like HSP40,

are transported to the tip independently to join the precursors during or after the

precursors become integrated into the axoneme.

The RSs integrate/dock to two precise locations relative to the dynein species.

Cryotomography has vividly revealed the distinctions between the base of the two RSs,

spoke 1 and spoke 2 (Figure 1-1B; Nicastro et al., 2006; Sui et. al., 2006). Recently,

studies of spoke-associated proteins shed some light on the docking mechanism of RS.

The 20S RS contains all RSPs and a calmodulin-binding spoke-associated complex (CSC) (Dymek et. al. 2007). The CSC complex is also present in the *pf14* axonemes that lack the RS suggesting that CSC binds RS but is assembled in the axoneme independently of the RSPs. This complex is comprised of four components, calmodulin, IP2, IP3 and IP4. In an overlay, recombinant IP-2 was recognized by recombinant RSP3. Also the anti-CSC antibody enhanced the microtubule-sliding velocity of RS mutants suggesting that the CSC complex and dyneins are linked. These independent lines of evidence suggest that CSC is present at the very base of the RS complex in the position to mediate docking of the RS complex. However, in the RNAi knockdown of the CSC components only spoke 2 was selectively lost from some spoke doublets and spoke 1 appeared rather normal (Dymek et. al., 2011). Apparently additional molecules are involved in docking the two sets of RSs at distinct positions in doublets. Thus, extraordinary assembly processes must take place inside the flagella to convert the precursor particles into mature complexes and localize them to precise positions relative to each other on the outer doublets.

Table 1-2. Radial spoke proteins[a]

Name	Mature spoke	Spoke precursor	Relevant features	Locations
RSP1	+	+		
RSP4	+	+		
RSP6	+	+		Head
RSP9	+	+		
RSP10	+	+		
RSP2	+	+	Phosphorylated	
RSP23	+	?		
RSP5	+	+	Phosphorylated	
RSP16	+	- (5S)		Neck
RSP20 (Calmodulin)	+	?		
RSP3	+	+	Phosphorylated; the stalk base; AKAP	
RSP11	+	+	RIIa domain containing	
RSP7	+	+	RIIa domain containing	
RSP12	+	+		
LC8	+	?		Stalk
RSP8	+	?		
RSP14	+	?		
RSP13	+	?	Phosphorylated	
RSP17	+	?	Phosphorylated	

[a] Yang et al., 2006.

1.8 RSP3

RSP3 plays a central role in this elaborate assembly process of the RS. Chemical

crosslinking of axonemes showed that RSP3 exists as a homodimer in the RS complex

(Wirschell et al., 2008). This homodimer interacts with multiple molecules and is

involved in multiple tasks.

RSP3 docks the RS to the axoneme

Independent lines of evidence indicate that RSP3 docks the RS to the axoneme. Firstly,

flagellum of the RSP3 mutant pf14 lacks the entire RS. Secondly, amino acids 42 – 80 of

the RSP3 N-terminus expressed in rabbit reticulolysate was pulled down by the spoke-

less *pf14* axonemes suggesting that the RSP3 N-terminus docks RS to the axoneme.

However, this interaction is mediated by non-tubulin components since RSP3 was not

pulled down by microtubules polymerized from purified tubulins (Diener et. al. 1993).

Lastly, one candidate axonemal protein that docks RSP3 is IP-2 in the CSC complex.

Both molecules interact in an in vitro overlay assay in which recombinant RSP3 is used

as a ligand (Dymek et. al., 2007). Thus, it was predicted that RSP3 is located at the base

of the RS to dock the complex to the axoneme.

Emerging evidence suggests that RSP3 is not merely the base. In the cell body

of *pf14*, without RSP3 the other RSPs assembled into small sub-complexes, instead of a

single RS lacking the base (Diener et al., 2011) suggesting that RSP3 forms the core for

binding of other RSPs.

RSP3 is an atypical AKAP

RSP3 has been considered as an A-kinase anchoring protein (AKAP). AKAPs anchor c-AMP-dependent protein kinase (PKA) near the intended substrates to increase the precision and efficiency of cAMP-dependent regulation. In addition, AKAPs also harbor distinct motifs for anchoring molecular switches for other regulatory pathways. Therefore, AKAPs are considered as signal transduction scaffolds (reviewed by Wong and Scott, 2004). Many AKAPs, including RSP3, were discovered by using RII, the regulatory subunit of PKA, as a probe in an overlay assay (Bregman et al., 1989). The interaction between AKAPs and RII is mediated by an amphipathic helix (AH) in AKAPs and the dimerization and docking (D/D) domain, RIIa, in RII. The RII-binding AH was mapped to a.a.#161-178 in RSP3 (Gaillard et al., 2001; Gaillard et al., 2006). This region is rather conserved among RSP3 orthologues and conservative replacement of two residues in the AH abolishes the RSP3-RII interaction in the overlay.

However, none of RS components bear remote resemblance to PKA except the RIIa domain that mediates the docking, not functioning, of PKA. This docking domain is present in two RSPs, RSP7 and RSP11 (Yang and Yang, 2006). They are co-localized with RSP3 toward the base of the RS complex (Figure 3-1), and they bind to RSP3 in vitro as well. These observations suggest that RSP3 is an atypical AKAP that anchors these two RIIa-domain- containing RSPs.

RSP3 binds to a MAP kinase

Recently, it was shown that the N-terminus unique to a mammalian RSP3 isoform interacts with a MAP Kinase ERK1/2 in the yeast 2-hybrid system (Jivan et. al., 2009).

The MAPK ERK1/2 phosphorylates recombinant RSP3 at the N-terminus and the phosphorylation promotes the interaction of RSP3 and RII. This is thought to regulate the interactions of RSP3 and PKA. It is not clear what this means to the *Chlamydomonas* RS yet. RSP3 is hypo-phosphorylated in the preassembled 12S particles while it becomes phosphorylated in the 20S mature complex. However, though the 12S RS has hypo-phosphorylated RSP3 it still contains the RIIa domain containing RSP11 and RSP7 (Diener et al., 2011). Therefore the in vivo relevance of RSP3 phosphorylation remains unclear. Addressing this question could reveal the significance of phosphorylation of RSP3 and axonemal proteins in general.

1.9 LC8

The other protein that is important for the assembly of the RS is LC8. In fact the importance of LC8 is beyond the RS and cilia. LC8 is one of the most conserved proteins in eukaryotic cells. This 10-kD protein consists of 89 a.a., except for a few orthologues that have some additional a.a. at the N-terminus. The residues of human LC8 sequence are 100%, 94% and 88% identical to the LC8 in rat, *Drosophila,* and *Chlamydomonas*, respectively (Liang et.al., 1999). The importance of LC8 is well recognized, but the role of LC8 is still emerging.

1.9.1 The importance of LC8

As indicated by the extraordinary sequence conservation, LC8 is a crucial molecule. Null mutation in the LC8 gene results in rampant apoptosis and embryonic lethality in *Drosophila* (Dick et al., 1996); abnormal nuclear migration in *Aspergillus* (Beckwith et al., 1998); and half-length flagella and lower rate of cell division in *Chlamydomonas* (Pazour et al. 1998). LC8 is shown to work with dynein motors that transport a wide range of cargoes (Puthalakath et al., 1999; Lo et al., 2006). Though most studies were focused on the dynein-dependent role of LC8, emerging evidence has shown the role of LC8 independent of dyneins. For example, a study of interaction of LC8 with the phosphoprotein in rabies virus showed that LC8 binding promotes efficient viral transcription, a role independent of the molecular motors (Raux et al., 2000; Tan et al., 2007). However, the lethality and the dynein-dependent phenotypes obfuscate the broad impact of LC8 on numerous proteins that bind LC8 in vivo.

1.9.2 LC8-binding proteins

LC8 was first identified as a subunit of ODA in *Chlamydomonas* flagella (King and Patel-King, 1995). Subsequently, LC8 was discovered as a subunit of many other target proteins by immunoprecipitation and in yeast 2-hybrid experiments (Rodriguez-Crespo et al., 1998; Rodriguez-Crespo et al., 2001). With the advent of proteomic tools, like various high throughput hybrid systems, pepscans and bioinformatic data-mining, more than 100 proteins in eukaryotes and viruses are found to be capable of binding LC8 (NCBI interactome database; Lerida et. al., 2004; Rapali et. al., 2011). Although many interactions remain to be verified experimentally, the bona fide LC8-binding proteins are

involved in a wide spectrum of cellular functions and pathogenesis, such as apoptosis (Bim and Bmf) (Puthalakath et al., 1999; Puthalakath et al., 2001), nuclear transport (Nup159) (Stelter et al., 2007), DNA repair (p53BP1) (Lo et al., 2005), nNOS inhibition (Jaffrey and Snyders, 1996), transcription of viral particles (P protein) (Jacob et al., 2000) and cancer progression (Pak1) (Vadlamudi et al., 2004). LC8 also functions in the presynaptic cytomatrix (Bassoon) (Fejtova et al., 2009) and in postsynaptic density (GKAP) (Naisbitt et al. 2000). The diversity of LC8-binding proteins is consistent with the omnipresence and abundance of this small molecule.

1.9.3 The structure

Crystallography of LC8 with or without a peptide from nNOS revealed that LC8 is a rectangular dimer (Liang et. al., 1999). Each monomer contributes two α-helices located at the opposing end of the dimer (Figure 1-4A). The five β-strands from each monomer wrap around each other to form a symmetric core. The less conserved N-termini are facing the periphery, while the highly conserved C-termini are embedded at the interface (Figure 1-4B). The buried C-terminus seems to be functionally significant, as mutant LC8 with an additional C-terminus compromises the assembly of the RS in the flagella (Yang et al., 2009). The β-strands from two monomers create two deep hydrophobic grooves at the interface. Two 13 a.a. peptides of nNOS bind to the two grooves to form sixth β-strand (Arrows, Figure 1-4A). The interaction induces dimeric LC8 to undergo a slight conformational change. It is the two hydrophobic grooves that are responsible for the promiscuous interaction of LC8 with a wide range of target proteins (Fan et al., 2001; Benison et al., 2007).

A
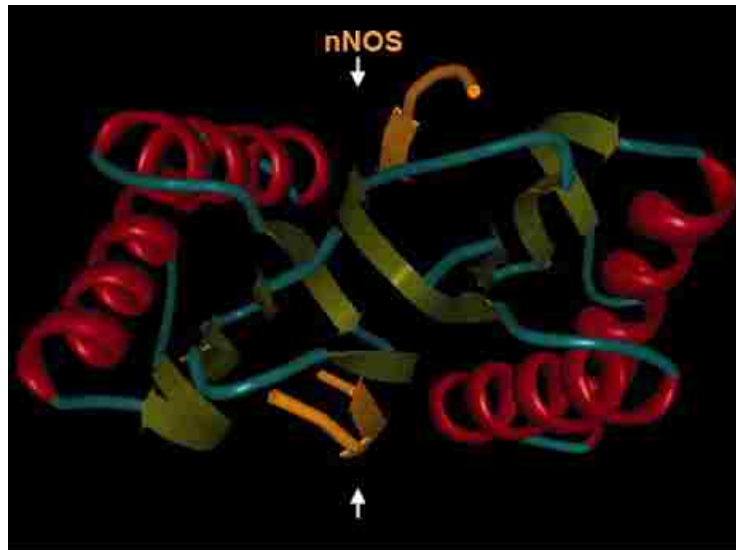
B
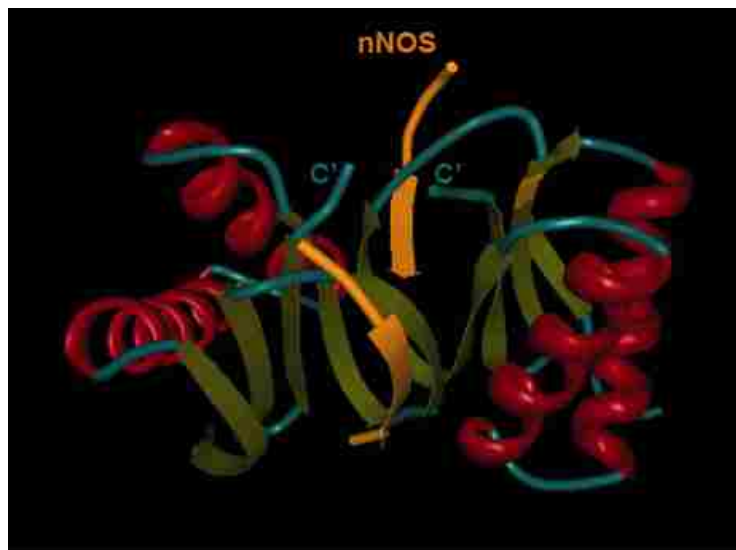
Figure 1-4. The crystal structure of dimeric LC8 and the binding peptides.
(A) The α-helices (red ribbons) are located at the periphery of LC8 dimer and the β-strands form the central core and two identical grooves (arrow). The grooves bind to the peptides from nNOS (yellow); **(B)** A view rotating near -90° around the X-axis shows that the LC8 C-terminus is nearly embedded at the dimeric interface.

1.9.4 LC8-binding sequences

The LC8 binding sequences in many target proteins have been mapped. A few target proteins even harbor multiple binding sites, aligned in tandem (Table 1-3). Although the inter-monomeric groove can accommodate 13 a.a., the first common pattern found by comparing the IC in dyneins and several other target proteins was only contain 5 a.a., (K/R) XTQT (Lo et al., 2001). This motif was then used for genome-wide search. Many proteins with this motif were identified and shown to bind LC8 in vitro (Rodriguez-Crespo et al., 2001). However, many verified binding sequences do not contain the basic residue (K/R) and their T residues are replaced by non-charged residues like S, I, V or C (Rapali et. al., 2011). A typical example for the diverged binding sequences is the GIQVD sequence present in several target proteins including nNOS (Rodriguez-Crespo et al., 2001). A few target sequences, like that from myosin V and Pak21, do not bear any resemblance to this motif, including the seemingly conserved Q residue (Table 1-3; Rapali et. al., 2011).

Despite the a.a. divergence in the LC8-binding sequences, structural studies predicted that they are present within a region with a high degree of local disorder—like an unfolded state or lack of prominent secondary or tertiary structures (Barbar, 2008). The hydrophobic interactions between the inherently flexible LC8-binding peptides and the inter-monomeric grooves explain the partnership of LC8 dimer with vastly different target proteins (Nyarko et. al., 2011).

Table 1-3. Some of the known LC8 binding partners[a].

Protein name	Sequence	a.a.#	Oligomerization
Adenain	LVKSTQTV	107	-
Bassoon	ANYGSQTE	1426	Predicted coiled coil
Bassoon	VAQGTQTP	1530	Predicted coiled coil
Bassoon	AEFSTQTP	1502	Predicted coiled coil
Bcl-2-like protein 11, BimL	CDKSTQTP	110	-
Bcl-2-modifying factor, Bmf	EDKATQTL	66	-
Breast carcinoma-amplified sequence 1	LDAQVQTD	566	Homodimer
Cytoplasmic dynein 1 intermediate chain 1	YSKETQTP	149	Homodimer
DNA (cytosine-5)-methyltransferase 3A	KDLGIQVD	651	Homodimer
Human papillomavirus E4	QDKQTQTP	21	-
Egalitarian	VDAESQTL	950	Predicted coiled coil
Guanylate kinase-associated protein, GKAP	QSVGVQVE	675	Predicted coiled coil
Guanylate kinase-associated protein, GKAP	LSIGIQVD	650	Predicted coiled coil
Microtubule-associated protein 4	GSKSTQTV	800	-
Myeloid leukemia factor 1, Mlf1	FQASTQTR	124	-
Myosin Va	DDKNTMTD	1284	Homodimer
Nitric oxide synthase, brain	KDMGIQVD	239	Homodimer
Nuclear respiratory factor 1	EHGVTQTE	3	Homodimer
Nucleoporin NUP159	ADFDVQTS	1105	Predicted coiled coil
Nucleoporin NUP159	AESGIQTD	1118	Predicted coiled coil
Nucleoporin NUP159	CNFSVQTF	1167	Predicted coiled coil
Nucleoporin NUP159	KHNSTQTV	1143	Predicted coiled coil
Nucleoporin NUP159	VDNGLQTE	1155	Predicted coiled coil
Lyssavirus phosphoprotein.	EDKSTQTP	142	Homotrimer
Rabiesvirus P protein	EDKSTQTT	142	Homotrimer
African swine fever virus p54	QNTASQTM	142	-
Swallow	SAKATQTD	289	Homodimer
Ras guanyl-releasing protein 3	TSQATQTE	610	homodimer
Replication origin-binding protein	MAKSTQTF	744	Homodimer
Radial Spoke Protein RSP3	RHIDIQTD	99	Homodimer
Radial Spoke Protein RSP3	ADTSTQTD	119	Homodimer
Radial Spoke Protein RSP3	TDAITQIE	144	Homodimer
Serine/threonine-protein kinase Nek9	HSKGTQTA	943	Homodimer
Serine/threonine-protein kinase PAK 1	RDVATSPI	215	Homodimer.
Tumor suppressor p53-binding protein 1	NNIGIQTM	1150	Homooligomers

Tumor suppressor p53-binding protein 1	VSAATQTI	1167	Homooligomers
Zinc finger MYND domain-containing protein 11	LHRSTQTT	411	Predicted coiled coil
Zinc finger protein 354A	TTKSTQTQ	94	-
Gephyrin	EDKGVQCE	219	Homooligomers
Zinc finger transcription factor, Trps1	VDRSTQDE	1205	-
Heat shock cognate 71 kDa protein, Hsc73	PTKQTQTF	430	Predicted coiled coil
Guanine nucleotide-binding protein subunit beta-2-like 1, Rack1	CKYTVQDE	138	-
Zaire Ebola virus; Polymerase cofactor, VP35	RNSQTQTD	69	Homooligomers
Syntaphilin	QERAIQTD	310	Predicted coiled coil

*Orange rows, the proteins with multiple LC8-binding sites, aligned in tandem.

*Green rows, RSP3 and its three LC8-binding sites (this study).

[a]Modified from Rapali et al., 2011

1.9.5 LC8-like molecules

LC8 is one of the molecules that represents a group of small promiscuous homodimers.

Characterization of *Chlamydomonas* ODA and I1 IDA revealed that several LCs

resemble LC8 in sequence or structure. They are evolutionarily conserved and could be

categorized into three families: the light chain 8 family (LC6, LC8, LC10); the

Tctex1/Tctex2 family (LC2 and LC9) and the LC7/Roadblock family (Pfister et al.,

2006). These LCs function as dimers and bind the intermediate chains (ICs) in an array

at the base of the motor complex that is involved in attachment of the motor to its target

site in the axoneme (Figure 1-5D; King et al., 1991; Wilkerson et al., 1995; reviewed in

King and Kamiya, 2009). Although each LC has a specific binding site on the IC, studies

of mutants suggest that some of these LC dimers are partially redundant. However, a

few, like Tctex-1, Tctex-2, and LC7 are irreplaceable for motor complexes (Mok et al.,

2001; DiBella et al., 2004; DiBella et al. 2005). Similar to LC8, some of the LCs, like

Tctex1 and Tctex2, also interact with non-motor molecules (O'Neill et al., 1995).

Studies of LC8 will help to understand various cellular processes that employ these

similar small molecules.

1.9.6. Function of LC8

Although the structures of LC8 and LC8-binding peptides are well defined, the functions

of such interactions are not yet established. Several theories have been proposed (Figure

1-5). The earlier theories were influenced by the discoveries of the first few LC8-binding

proteins.

LC8 as a regulator

LC8 was initially recognized as a protein inhibitor of nNOS activity (Jaffrey and Snyder, 1996) and thus was considered to be a regulator. However subsequent studies were unable to confirm this role (Hemmens et al. 1998). As more and more LC8 target proteins were discovered that are dynein cargoes, this theory has waned, and the role of LC8 was reinforced in transportation instead of regulation (Rodriguez-Crespo et al., 1998).

LC8 is an adapter for the dynein cargos

The interaction of LC8 with the intermediate chain (IC) and a wide range of cellular proteins led to the proposal that the dimeric LC8 functions as a motor-cargo adaptor, with one groove adhering to the intermediate chain and the other tethering to various cargo proteins (Puthalakath et al., 1999; Lo et al., 2006). However, accumulated evidence has challenged this model. Although it is possible that the LC8 dimer may glue two different molecules together, the motor-cargo adaptor theory has not yet been substantiated by any experimental evidence.

LC8 is a stabilizer for molecular complexes

Whereas the cargo model explains the numerous cargoes that dynein motors transport, the kinetic and structural studies of reconstituted IC peptides, LC8 and LC8-like molecules showed that these small dimers substantially enhance the stability of the homodimeric IC chains (Williams et. al., 2007) that are the scaffold of the motor complex. Interaction of one IC with only one of the two LC8 grooves, as proposed for motor-cargo adapter theory, would destabilize the motor complex. Thus, the small dimer most likely binds to two polypeptide chains in the same complex to enhance complex stability.

LC8 dimerizes target proteins

This idea is similar to the stabilizer model except that it only emphasizes on the LC8

dimers bringing two target peptides in close proximity to each other (Figure 1-5A). NMR

structures of LC8 and dynein's IC or swallow in *Drosophila* have shown that the

monomer-dimer equilibrium is shifted towards the dimer in the presence of LC8 binding

(Wang et al., 2004; Benison et al., 2006; Lo et. al., 2006).

LC8 refolds target proteins

This theory is founded on the basis of localization of the LC8 binding sequences in the

disordered region of the peptides (Barbar, 2008). The NMR and kinetic studies showed

that upon LC8 dimer binding, the helical content of two homodimeric IC increased,

leading to coiled coil formation of the ICs (Figure 1-5A; Nyarko et. al. 2004, Benison et.

al., 2006). Thus, it was proposed that LC8 binding would promote protein refolding and

consequently formation of a more ordered structure.

LC8 promotes higher-level complex formation

Independent lines of evidence support this theory. First, the monomer-dimer equilibrium

of myosin V is shifted towards dimer-tetramer equilibrium in the presence of LC8,

resulting in formation of a larger complex (Wagner et. al., 2006; Hodi et al. 2006).

Another line of evidence comes from *Chlamydomonas* LC8 mutant, *fla14-3*. The LC8 in

this mutant has an extended C-terminal that alters LC8 conformation. This change in

dimeric interface is insufficient to abrogate the binding to the target proteins but is

sufficient to interfere with interaction between ICs and other molecules, suggesting that

proper binding of LC8 to ICs promotes further association of the IC with other subunits

unique to individual dynein motors (Figure 1-5B; Yang et al., 2009). In the same vein, binding of one LC8 dimer increases the binding efficiency of another LC8 dimer or LC8-like molecule by 1000-fold, suggesting that the binding of LC8 promotes the binding of other molecules resulting in higher-level complex formation (Hall et al., 2009).

A stack of LC8 dimers targets protein to form a rigid rod

More recently, it was found that the dimeric Nup159 in the nuclear pore complex of yeast associates with a stack of 5 LC8 dimers. The complex forms a 20-nm rod that is proposed to confer rigidity to the transmembrane region in the nuclear pore complex (Figure 1-5C; Stelter et. al., 2007). However, the studies on dimeric IC and two LC8 dimers aligned in tandem predicted flexibility between the LC8 binding sites (Williams et al., 2007; Hall et al., 2009). Thus the role of multiple LC8 dimers aligned in tandem remains to be resolved.

LC8 promotes phosphorylation

This idea is still emerging. The only observation is that LC8 binds to the unphosphorylated NEK9, a NIMA family protein kinase. Upon binding, LC8 promotes the oligomerization and auto-phosphorylation of NEK9 (Figure 1-5B; Regue et. al., 2011).

A

B

C

D
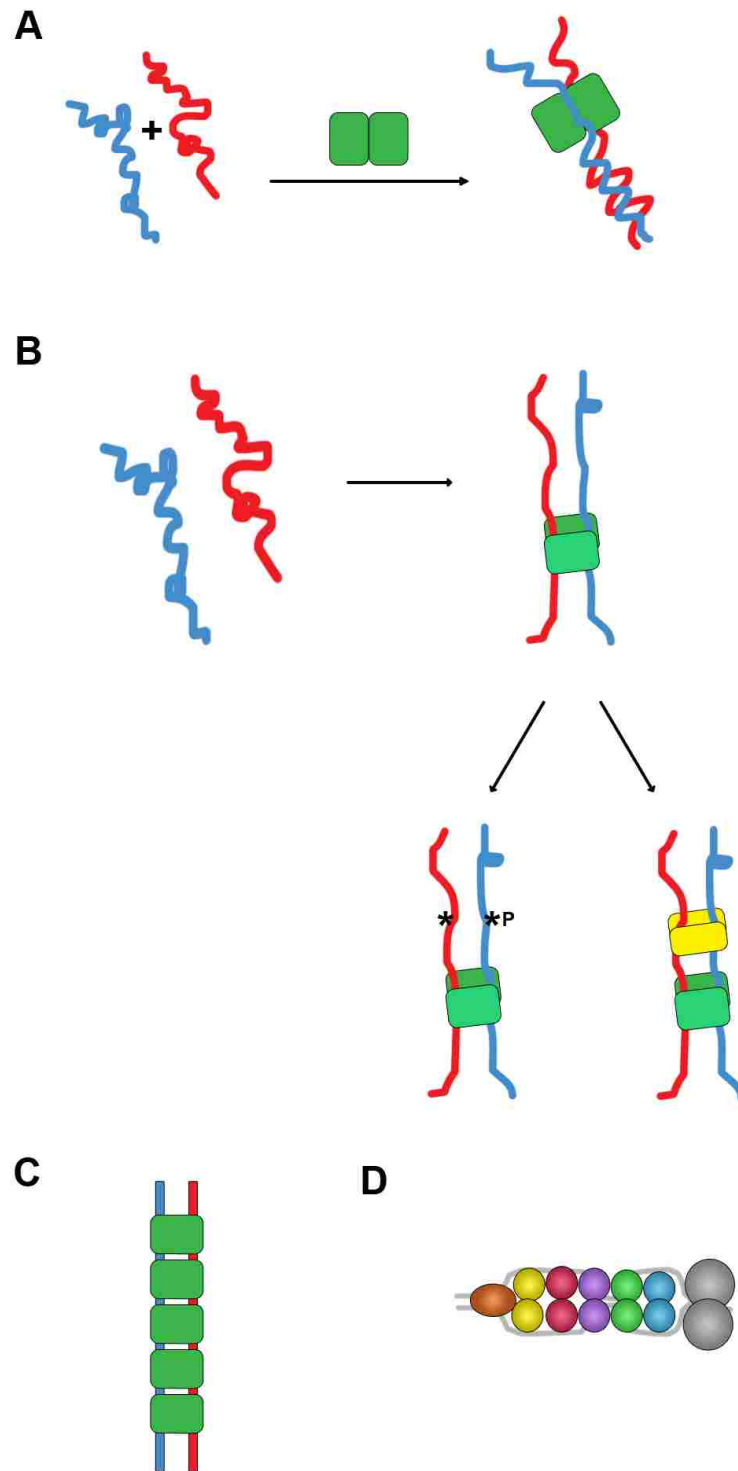
Figure 1-5. The predicted roles of LC8.

(A) Binding to a LC8 dimer promotes dimerization and refolding of target proteins (Barbar, 2008). (B) LC8 dimer promotes phosphorylation (Regue et. al., 2011) and additional molecular interactions of target proteins (Yang et al., 2008). (C) A stack of LC8 dimers promotes the formation of a rigid rod (Stelter et al., 2007). (D) A stack of LC8 and LC8-like molecules binds to target proteins (King and Kamiya, 2009). LC8 dimer, green rectangle; LC8 target proteins, red and blue random coils; LC8-like molecules, all other colored objects; asterisk, phosphorylation.

1.9.7 The role of LC8 in flagella

Chlamydomonas flagellum provides an unusual opportunity to study the role of LC8 in vivo. LC8 is present in four molecular complexes in flagella, the ODA (King and Patel-King 1995), the I1 IDA (Harrison et al., 1998), the RS (Yang et al., 2001) and the cytoplasmic dynein (Pazour et al., 1998; Rompolas et al., 2007) that mediates the retrograde IFT. Because LC8 binds numerous proteins in higher organisms, the majority of the studies on LC8 are conducted in vitro. Importantly, the LC8 mutants in the higher organisms are lethal in contrast to the *Chlamydomonas* LC8 null mutant which is viable (Dick et al., 1996). Thus, the studies of LC8-containing complexes in *Chlamydomonas* flagella will provide a platform to test the various theories regarding the role of LC8 in molecular complexes.

The importance of LC8 in flagella is revealed by the severe deficiency in the LC8 null mutant *fla14-1*. The flagella of this mutant are only half-length and re-absorb easily (Pazour et al., 1998; Yang et al., 2008). The axoneme is devoid of the RS and ODA while I1 is reduced. The cytoplasmic dynein for the retrograde IFT fails to enter flagella. Despite the absence of RS in the *fla14-1* axoneme, the 12S and 20S RS precursor particles are present in the flagellar matrix (Qin et. al., 2004), suggesting that LC8 is critical for docking-- the integration of the RS into the axoneme. However, these rampant defects did not occur in an allelic mutant, *fla14-3*. In *fla14-3*, LC8 has an extended C-terminal tail due to the TAA to TTA read-through mutation. In its axoneme, ODA and I1 display marginal defects, however the RS is reduced at least by 50%, the KI-resistance is lost and RSP3 is hypo-phosphorylated (Yang et al., 2008). These data suggest that the LC8 C-terminal tail affects the RS disproportionately in comparison to

axonemal dyneins. In other words, LC8 may play a more prominent role in the RS

complex than in others. Elucidation of the basis of differential impacts will further the

understanding of the RS assembly and provide insight into flagella biology and the role

of LC8 in general.

1.10 Objectives of this dissertation

RSs are absent in the axonemes of both RSP3 and LC8 mutants. Based on the common

phenotype, this dissertation tested the central hypothesis that **LC8 directly binds to**

RSP3 to promote the assembly of the RS complex.

The first objective was **to determine whether LC8 interacts directly with**

RSP3. To test this, RSP3 sequence was searched for the canonical LC8 binding motifs.

Surprisingly, RSP3 N-terminus harbors not just one, but five TQT-like motifs aligned in

tandem. To test if this region indeed binds LC8, two independent experiments were

conducted. One was to cleave RS complexes into sub-particles by proteolysis and

examine if LC8 co-fractionate with RSP3 N-terminus. Another approach was to express

tagged recombinant RSP3 N-terminus and LC8 in bacteria and test their direct

interaction.

The second objective was **to determine whether LC8 promotes the docking of**

RSP3 to the axoneme. Two independent approaches were taken. The first approach was

to perform the in-vitro reconstitution of RSP3 N-terminus with the spoke-less *pf14*

axonemes in the presence or absence of LC8. Axonemes were then sedimented and the

samples were analyzed to compare the amounts of RSP3 co-purified with axonemes. The

second approach was to purify the RS particles from the axonemes of a mutant strain that

expresses only the RSP3 N-terminus. The hypothesis predicts that, the pull down shall contain LC8 as well as the RS-docking proteins.

The third objective was **to determine whether the interaction of RSP3 with multiple LC8 molecules is crucial for the RS-mediated control of synchronized oscillatory beating**. An in vivo approach was taken to generate *Chlamydomonas* mutants expressing RSP3 with some or all of the five LC8 binding motifs perturbed by site-directed mutagenesis. The mutant strains were assessed for the flagellar beating, the deficiencies in LC8 and RS and finally for the phosphorylation state of RSP3.

These three objectives were achieved successfully. The combined results from these multiple approaches support the central hypothesis and reveal the processes occurring during the final assembly of RS complex. These findings show that multiple LC8 binds to RSP3 in tandem to the RS precursors in flagella and the binding has three impacts: the formation of rigid stalk at the base, the docking of the spoke base to two distinct positions on each axonemal unit and the phosphorylation of RSP3. This finding also provides an explanation of the molecular basis of oscillatory beating. Lastly, the pleiotropic effects of LC8 on RSP3 and the entire RS complex integrate multiple prevailing models. This conclusion will inspire a global view of LC8 in macromolecular complexes.

The materials and methods used in this study are described in detail in Chapter 2. Chapter 3 explains all of the experiments and results founded on the three objectives. Finally, Chapter 4 discusses the implications of the findings and proposes a model for the assembly of the RS and axonemal complexes in general.

CHAPTER 2: MATERIALS AND METHODS

2.1 Strains and Culture

The *Chlamydomonas reinhardtii* strains used in this work included: cc124 (wild type),

pf14 (lacking radial spokes), *fla14-1* (LC8 null-mutant), *fla14-3* (LC8-CT) and *pf28pf30*

(lacking outer dynein arms and I1 inner dynein). They were obtained from

Chlamydomonas Resource Center (Harris, 2001). Cells were cultured in Tris-acetate-

phosphate (TAP) medium with aeration on 14/10 hr light/dark cycle (Yang et al., 2008).

2.2 Sequence Analysis

The RSP3 homologs were identified by *BLAST* search against the protein database at

http://www.ncbi.nlm.nih.gov/BLAST/. The *ClustalW* (1.83) program at

http://www.ebi.ac.uk/clustalw/ was used to generate multiple sequence alignment of

RSP3 homologs. *Jpred* program available at http://www.compbio.dundee.ac.uk/www-

jpred/ was used for secondary structure prediction. Regional disorder was predicted

using *RONN* at http://www.strubi.ox.ac.uk/RONN.

2.3 Molecular Biology

2.3.1 Bacterial expression constructs

The S-tagged RSP3$_{1-160}$ construct was generated by PCR amplification using a GST-

RSP3 cDNA construct (Diener et al., 1993) as a template and primers #23S and #24AS

(Table 2-2) with built-in BglII and XhoI restriction sites, respectively. The PCR product

was cloned in-frame into pET Duet-1 vector (Novagen) that produced RSP3 with a C-

terminal S tag. The His-tagged LC8 construct was generated by PCR amplification using LC8 cDNA clone (Yang et. al. 2009) as a template and primers #27S and #28AS with a built-in NdeI and EcoRI restriction sites, respectively. The PCR fragment was cloned in frame into pET28-a vector (Novagen). The construct expresses LC8 with a 6-His tag at the N-terminus. These expression constructs were transformed in *E.coli* strain, BL21(DE3). Expression was induced with 1 mM IPTG at 18°C overnight.

2.3.2 *Chlamydomonas* transformation constructs

Genomic pPMM-RSP3-HAHis construct

A NcoI fragment containing the RSP3 genomic DNA was released from a BAC clone and inserted into pGEM-T Easy vector (Promega). The SacI site and its downstream sequence at the 3'-end flanking region were eliminated by limited restriction digest followed by the treatment with T4 DNA polymerase. To add a tag with 3 HA epitopes and 12 His residues, PCR was performed using modified primers to add an XhoI site, 6 His codons before the endogenous stop codon and an XbaI site after the stop codon. Subsequently a PCR fragment encoding 3 HA (Silflow, et al., 2001) and 6 His codons was inserted into the XhoI site. For single plasmid transformation, the paromomycin (PMM) expression cassette was amplified from pSI103 (Yang et al., 2009) and inserted into the AatI site in the vector with the help of the primers #1S and #2AS (Table 2-2) containing in built AatI site. The final plasmid was named pPMM-RSP3-HAHis and was transformed into RSP3 mutant *pf14*. This *Chlamydomonas* strain was used as a control.

RSP3 point mutation constructs

The cloning strategy is summarized in the Figure 2-1. For site-directed mutagenesis, the RSP3 genomic DNA flanked by two SpeI sites was PCR-amplified using #29S and #30AS primers. This region contains all the LC8 binding motifs. The second SpeI site was replaced with XbaI, an isoschizomer, for cloning purposes. The PCR product was cloned into pGEM-T Easy vector (Promega). This construct with only 831-bp insert was used as a template to generate point mutations using the QuikChange strategy (Stratagene).

Primers used for creating the mutations are summarized in the Table 2-1. Briefly, the primers with mutated sequence at each LC8 binding motif were used to mutate either the first two or the last three or all the five sites. The first set of primer pairs was used to mutate the Threonine (T) and Glutamine (Q) residues in the LC8 binding motifs to Alanine (A) and Asparagine (N) residues, respectively, while the second sets of primer pairs mutated all the residues in the motif to Alanine (A).

The mutated PCR fragment was cloned into pGEM-T Easy vector (Promega). The mutations were verified by DNA sequencing. The fragment was released by digestion with SpeI and XbaI enzymes and used to replace the wild type SpeI-SpeI fragment in pPMM-RSP3-HAHis. The clones were assessed by SpeI digest that linearized the mutant construct and released the SpeI fragment from the parental construct. These RSP3-3HA12His constructs with mutated motifs were transformed into RSP3 mutant *pf14*.
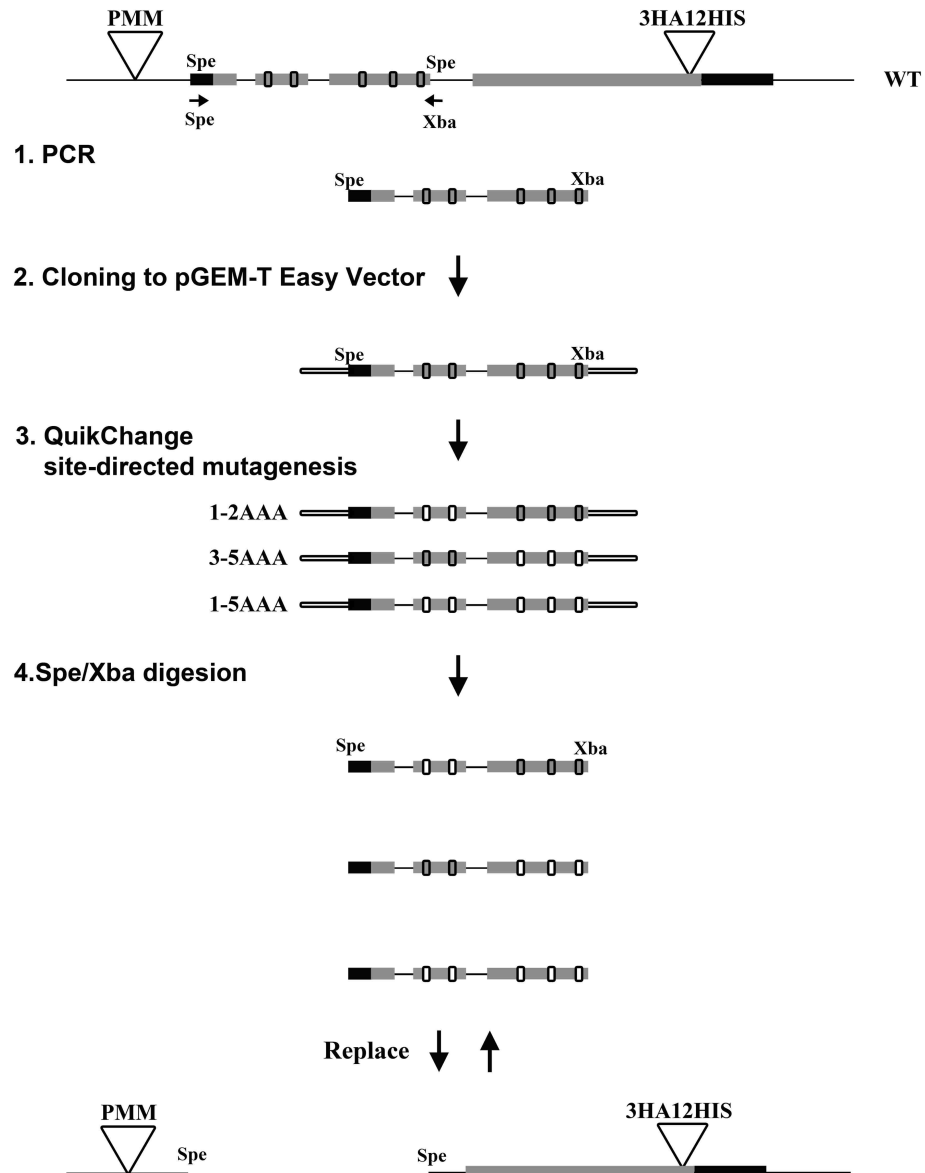
Figure 2-1. Site-directed mutagenesis of LC8 binding motifs in genomic RSP3-3HA12His construct.

A 831-bp fragment at the 5' end of the RSP3 gene was PCR amplified and cloned. The plasmid was used as a template for mutagenesis of the LC8-binding motifs. Mutations were created by using primers harboring the mutated sequences for LC8-binding motifs. The mutated Spe-Xba fragment was used to replace the Spe-Spe fragment in the full length RSP3-3HA12His construct. Grey bars: Exons; Black bars: UTR's

Table 2-1: Mutation and primers for the TQT-like LC8-binding motifs. The mutated sequences were built into the primers.

LC8 binding motifs	1st TQT	2nd TQTQT	3rd IQT	4th TQT	5th TQI
AN mutation	ANT	TNANT	INA	ANT	ANI
Primer pairs	#3S #4AS	#5S #6AS	#7S #8AS	#9 S #10 AS	#11 S #12 AS
AAA mutation	AAA	AAAAA	AAA	AAA	AAA
Primer pairs	#13S #14AS	#15S #16AS	#17S #18AS	#19S #20AS	#21S #22AS

RSP3$_{1-170}$ constructs

To create a construct of truncated RSP3, the PMM-RSP3-HAHis genomic construct was used as a template for mutagenesis (Figure 2-2). The DNA fragment encoding the N-terminal 170 a.a. was PCR amplified with the primer pair #31S and #26AS and the 3' UTR including the flanking sequence was amplified with the primer pair #32S and #33AS. Both the primer pairs had built in EcoRI and XbaI sites. For single plasmid transformation, the PMM cassette was amplified from pSI103, as described before, and inserted into AatI site of pGEM-T Easy vector. The two PCR products were ligated and cloned into EcoRI site of this pGEM-T Easy plasmid containing the PMM cassette. The ligation at the XbaI site eliminated the endogenous stop codon in the RSP3 gene, resulting in the translation of 23 a.a., including 3 cysteine residues, encoded by the 3' UTR. A PCR product encoding 3 HA and 12 His codons was cloned into the XbaI site preceding the stop codon to generate the pRSP3$_{1-170}$–HAHis construct. RSP3$_{1-178}$ was prepared by a similar strategy.
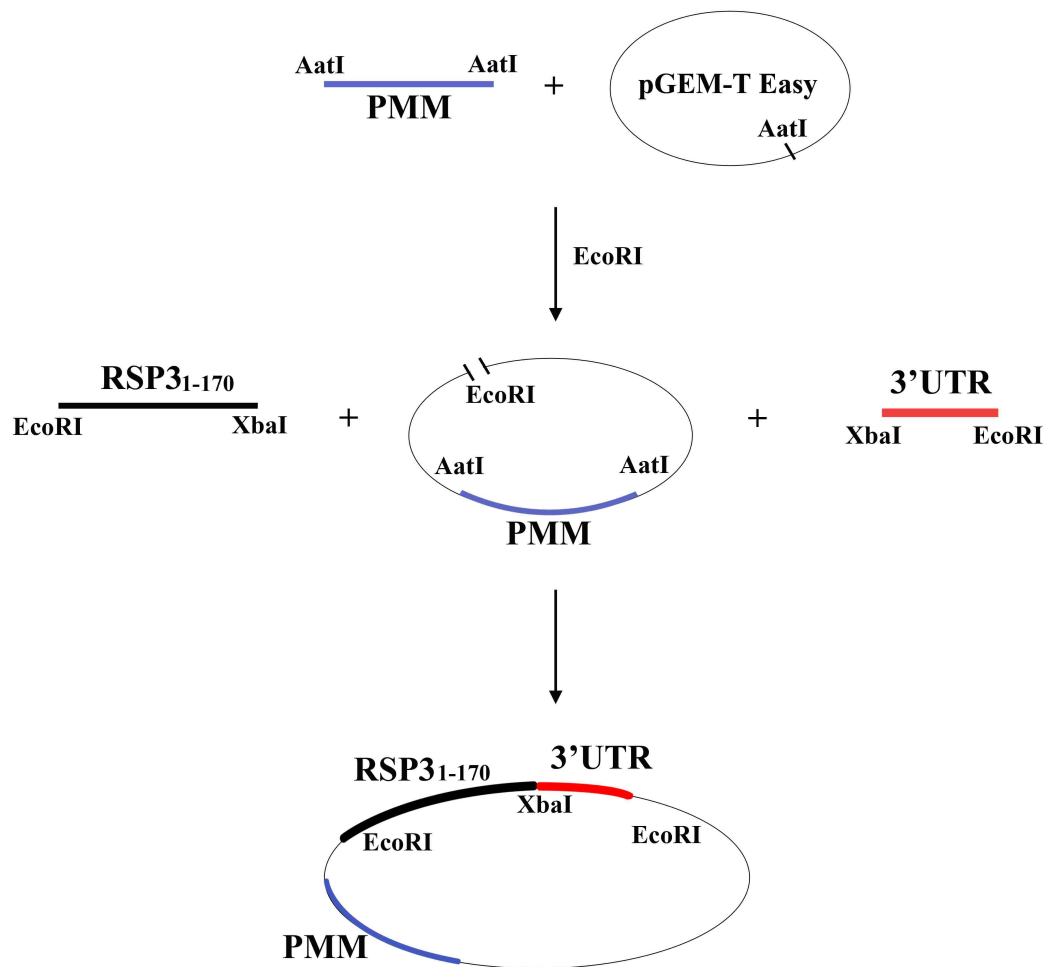
Figure 2-2. Cloning strategy for RSP3$_{1-170}$ -3Cys genomic construct.

RSP3$_{1-170}$ and the 3'UTR fragment were PCR amplified from the RSP3-3HA12His construct. Both the fragments were ligated into the EcoRI site in the pGEM-T Easy vector containing a PMM expression cassette at the AatI site.

2.4 Transformation

For single plasmid transformation, the glass beads method was used to introduce

individual pPMM-RSP3 genomic constructs carrying a PMM selection cassette into the

RSP3 mutant, *pf14* (Kindle, 1990; Diener et al., 1993). The cells were then plated on

TAP plates supplemented with 10 μg/ml PMM for selection. After 4 days, a fraction of

each surviving clone was resuspended in water for microscopic observations.

2.5 Biochemistry

2.5.1 Axoneme preparation and serial extraction

The *Chlamydomonas* cells were centrifuged and the flagella were isolated by the

dibucaine method (Yang et al., 2001). For axoneme preparation, the isolated flagella were

demembranated by 0.5% NP-40 in buffer A (10 mM Hepes, pH 7.2, 5 mM $MgSO_4$, 1

mM dithiothreitol (DTT), 50 mM EDTA, 30 mM NaCl) supplemented with protease

inhibitors, 0.1 mM PMSF and 0.5 TIU/ml Aprotinin.   For the extraction of dyneins,

axonemes were resuspended in 0.6 M NaCl/buffer A at 2-5 mg protein/ml on ice for 30

mins. After incubation, the suspension was centrifuged at 12,000 rpm for 10 mins in a

TA-15 rotor using an Allegra 25 centrifuge (Beckman Coulter). The supernatant

contained dyneins. For RS extraction, the pellet after the NaCl extraction was

resuspended in 0.6 M KI in buffer A. After incubation on ice for 30 mins, centrifugation

was performed at 12,000 rpm for 10 mins to obtain the supernatant that contained RSs.

2.5.2 Limited proteolysis

The *pf28pf30* axonemes were isolated as described above except that DTT, EDTA,

EGTA, PMSF and Aprotinin were omitted throughout the experiment. The axonemal

pellet was resuspended in buffer A at a concentration of 2 mg/ml and treated with trypsin

at different concentrations for 40 min at room temperature. The digestion was terminated

by the addition of an excess of trypsin-inhibitor (Summer and Gibbons, 1971).

2.5.3 Two-Dimensional Electrophoresis

The trypsin-treated axonemes were extracted with 0.6 M KI/buffer A. Following dialysis

against buffer A, the supernatant was resuspended in Laemmli sample buffer without

SDS and was fractionated on 6% native gels. For western blotting, the native gel was

transferred to nitrocellulose membrane. For the 2nd-D analysis, native gel strips were

equilibrated in 5X SDS sample buffer at room temperature for 1 hr. Each strip was then

inserted into a (6% to 16%) gradient gel for SDS-PAGE followed by western blot

analyses.

2.5.4 Affinity purification of bacterial recombinant proteins

For recombinant RSP3$_{1-160}$-S-tag and His-tagged LC8, the IPTG-induced overnight

bacterial culture was centrifuged and the cell suspension was sonicated followed by

centrifugation at 12,000 rpm. The interaction of RSP3$_{1-160}$ and His-LC8 was tested by the

incubation of equal volumes of the two bacterial extracts containing each protein for 1 hr

at room temperature. The mixture was then subjected to affinity purification by S-agarose

(Novagen) and Ni-NTA (Qiagen), following procedures recommended by the

manufacturers, respectively. Proteins were eluted and analyzed by SDS-PAGE and commassie.

Protein quantification of the RSP3$_{1-160}$ and LC8 bands in S-tag pull down was performed by optical densitometry using the GelDoc-It^{Tm} (UVP). The density of each band was measured three times and the average density was calculated. The ratio of the average total densities divided by the ratio of molecular mass was used to determine the molar ratio of LC8 to RSP3.

2.5.5 Affinity purification of axonemal proteins

For purification of truncated tagged spoke particles, the axonemes from RSP3$_{1-178}$-HAHis strain and control *pf14* were extracted with 0.6 M KI/buffer A at the protein concentration of 5 mg/ml. The extracts were diluted to 0.3 M KI with 10 mM imidazole buffer. The supernatant was subjected to Ni-NTA purification. The eluate was fractionated by SDS-PAGE. The proteins were revealed by western blotting and non-formaldehyde silver staining. The novel band seen in silver stain was excised for mass spectroscopy performed by the Shared Mass Spectrometry Facility at the Medical College of Wisconsin.

2.5.6 Reconstitution

Equal amounts of bacterial extracts containing S-tagged RSP3$_{1-160}$ and His-LC8 were added into increasing concentrations of *pf14* or WT axonemes. Following 1-hr incubation at room temperature, the axonemes were spun down at 8000 rpm for 10 min and the supernatant, containing the unbound protein, was removed. The axonemal pellets were washed with Buffer A containing 150mM NaCl and resuspended in Laemmli

sample buffer. The bound proteins contained in the pellet were analyzed by western blotting. RSP3$_{1-160}$ and LC8 were revealed by Fox14 and LC8 antibody, respectively. The amount of axonemes was revealed by p28 antibody.

2.5.7 Preparation of flagellar membrane matrix extract

Flagella were isolated from a 30-liter culture of *pf28pf30* cells and extracted with 0.05% NP-40 in buffer A supplemented with protease inhibitors (Qin et al., 2004). The mixture was centrifuged at 12,000 rpm for 10 mins in a TA-15 rotor using Allegra 25 centrifuge (Beckman Coulter) to obtain the supernatant.

2.5.8 Chemical Crosslinking

Axonemes prepared in DTT-free Buffer A at a concentration of 2 mg/ml was treated with 1-Ethyl-3-(3-dimethylaminopropyl) carbodiimide HCl (EDC; Pierce Chemicals) at a series of concentrations for 1 hr at room temperature. The reaction was terminated by adding Laemmli sample buffer with 140 mM β–mercaptoethanol.

2.5.9 Antibodies

The antibodies used in this study recognized p28 (Dr. G. Piperno, Mount Sinai Medical School), dynein light intermediate chain, DLIC (Dr. M. E. Porter. University of Minnesota), IC140, *Chlamydomonas* RSP3 (Dr. W. S. Sale, Emory University), calmodulin, IP2, IP3 (Dr. E. F. Smith, Dartmouth college), HA (Covance Inc.), and RSP2, RSP3, LC8, and RSP11 (Yang et al., 2006). The pan RSP3 rabbit antibody was raised against the affinity-purified 418-a.a. isoform of recombinant human RSP3.

2.6 Motility analysis

The log-phase *Chlamydomonas* culture was observed by light microscopy and the percentage of swimmers was estimated by the method described in Yang et al., 2005. Images were captured at a rate of 12.5 frames/sec by CoolSnap CCD camera (Photometrics), at 200X magnification. The trajectory of swimmers was tracked by MetaMorph software.

Table 2-2: Oligonucleotides used in this study.

Name	Sequence
#1 S	GGACGTCGACGGCGGGGAGCTCGCTG
#2 AS	GGACGTCGGTACCCGCTTCAAATACGCC
#3 S	CGCGAGGATGAGACGGCGAACACGCTGCCCACGGC
#4 AS	GCCGTGGGCAGCGTGTTCGCCGTCTCATCCTCGCG
#5 S	CCGCCGATGCCACGAACGCGAACACCAAGGGACCCTCG
#6 AS	CGAGGGTCCCTTGGTGTTCGCGTTCGTGGCATCGGC GG
#7 S	CGGCACATCGACATCAACGCGGACGTGTATCTGG
#8 AS	CCAGATACACGTCCGCGTTGATGTCGATGTGCCG
#9 S	GGCTGACACCTCCACGAACGCGGATGCCTTCCTGG
#10 AS	CCAGGAAGGCATCCGCGTTCGTGGAGGTGTCAGCC
#11 S	GCACGGACGCCATCGCGAACATCGAGAACGGTGAG
#12 AS	CTCACCGTTCTCGATGTTCGCGATGGCGTCCGTGC
#13 S	CGAGGATGAGACGGCGGCCGCGCTGCCCACGGC
#14 AS	GCCGTGGGCAGCGCGGCCGCCGCTTCATCCTCG
#15 S	GCCCGCCGATGCCGCGGCCGCGGCAGCCAAGGGACCCTCG
#16 AS	CGAGGGTCCCTTGGCTGCCGCGGCCGCGGCATCGGCGGGC
#17 S	CGGCGGCACATCGACGCCGCAGCGGACGTGTATCTGG
#18 AS	CCAGATACACGTCCGCTGCGGCGTCGATGTGCCGCCG
#19 S	GGAGGCTGACACCTCCGCGGCAGCCGATGCCTTCCTGG
#20 AS	CCAGGAAGGCATCGGCTGCCGCGGAGGTGTCAGCCTCC
#21 S	GGCACGGACGCCATCGCGGCAGCCGAGAACGGTGAGC
# 22 AS	GCTCACCGTTCTCGGCTGCCGCGATGGCGTCCGTGCC
#23 S	CCAGATCTAGTGCAGGCTAAGGCGCAG

#24 AS	CC<u>CTCGAG</u>TTAGGGCTCCACCTCGAAGTC
#25 AS	CC<u>CTCGAG</u>GGGCTCCACCTCGAAGTC
#26 AS	GC<u>TCTAGA</u>CAGCACCTTGCCCACCAGCACCTCCAG
#27 S	GGAATTC<u>CATATG</u>ATGGCGTCGGGCAGCTCC
#28 AS	CG<u>GAATTC</u>TTAGCCCGACTTGAACAGCAG
#29 S	CCGCAAGCTCACTCGTTCACCATAAAC
#30 AS	AG<u>CTCTAGA</u>ATGCGACCGCTCCCTGTCCTGG
#31 S	G<u>GAATTC</u>CCGCTCTGCTCTCCAGTCCGACTAGGG
#32 S	GC<u>TCTAGA</u>CAGGCGCTGGCGGTGCACGCGCTGGG
#33 AS	G<u>GAATTC</u>TGTTGCCTGAGAGCTCCGCCTCGGCC

* The restriction sites in each primer are underlined.

CHAPTER 3: RESULTS

Abstract

LC8 dimer interacts with numerous proteins. However, its function is not well understood. For example, while LC8 is present in both the radial spoke (RS) and dynein motors in *Chlamydomonas* flagella, the RS is particularly vulnerable to loss of LC8 activity. We found that multiple LC8 dimers associate with the N-terminus of RSP3. The interaction enhances the reconstitution of RSP3 N-terminus to the spoke-less axoneme. Interestingly, the pull down of RSP3 N-terminal fragment contains LC8 and the putative RS docking proteins. Furthermore, LC8 is undetectable in RS precursor particles in flagella. Finally, perturbations of the LC8-binding sites result in asynchronous flagella with hypo-phosphorylated RSP3, less LC8 and reduced stability of RS-axoneme association. We propose that in flagella, binding of a stack of LC8 dimers triggers RSP3 phosphorylation, stalk base formation and association with RS docking proteins. These LC8-dependent processes shed light on the biology of flagella and LC8.

Introduction

LC8 is a small yet extraordinarily versatile polypeptide. The dimer of this 10-kDa

molecule is shown to bind more than 100 vital proteins in eukaryotes and viruses (Lo et

al., 2001; Rodriguez-Crespo et. al., 2001; Navarro-Lerida et. al., 2004). The target

proteins are present in a wider range of cellular compartments and are remarkably

diverse, such as apoptotic factor BimL (Puthalakath, et al., 1999), intermediate chains of

dynein motors (Lo et al., 2001), Bassoon that associate with vesicular membrane (Fejtova

, et al., 2009) and phosphoprotein that is involved in viral transcription (Tan et al., 2007).

Some exist in macromolecular complexes while some may simply interact with LC8

(Pfister et al., 2006; Barbar, 2008: Puthalakath, et al., 1999). Many LC8-involved

reactions remain poorly defined.

The role of LC8 differs. It could be for regulation (Jaffrey and Snyder, 1996);

assembly (Pazour et al., 1998; Yang et al., 2008); inhibition (Jaffrey and Snyder, 1996;

Jung et al., 2008); excitation (Tan et al., 2007); dispensable or pivotal (Dick et al., 1996;

Pazour et al., 1998; Yang et al., 2008; Lightcap et al., 2009). And the interaction could be

modulated by phosphorylation (Vadlamudi et al., 2004; Regue et al., 2011) and the redox

state (Jung et al., 2008) of LC8.

The various roles are founded on the association of the two identical grooves at

LC8 inter-monomer interface with 12-a.a. peptides (Liang et al., 1999) in target proteins.

Majority of LC8 target proteins contain one binding site, while a few target proteins

harbor two (Lo et al., 2005; Rompolas et al., 2007) or multiple aligned in tandem (Stelter

et al., 2007; Fejtova et al., 2009). The sequences are not strictly conserved. Some

contain a (K/R) XTQT motif (Lo et. al., 2001). But in many cases, the basic residue is

absent while T residues are replaced by non-charged amino acids (a.a.) like S, I, V or C.

A typical example is GIQVD sequence in nNOS and several target proteins (Jaffrey and

Snyder, 1996). However, some binding sequences, like those in myosin V and PAK1,

are much more diverged, lacking even the conserved Q residue (Espindola et al., 2000;

Lightcap et al., 2009). Despite the variations, the LC8-binding sequences may be located

in inherently disordered regions (Barbar, 2008).

Various functions have been proposed for the bivalent interactions of LC8. The

first model is founded on cytoplasmic dynein (Fan et al., 2001). It contends that the

dimeric LC8 functions as a motor-cargo adaptor, with one groove adhering to the

intermediate chain and the other tethering to various cargo proteins (Sakato and King,

2004). Whereas this model explains the numerous cargoes that dynein motors transport,

accumulated evidence indicated that the role of LC8 is independent to cargo-

transportations of dynein motors (Tan et al., 2007; Williams et al., 2007; Yang et al.,

2008). It was proposed that the bivalency interactions are intended to bind the

homodimer within a complex and the interaction of an LC8 dimer with only one chain of

dimeric IC will destabilize the motor complex (Williams et al., 2007). Another theory

contends that binding to the dimeric grooves in the LC8 dimer promotes the refolding of

structurally disordered region (Barbar, 2008). More recently, it was found that the

dimeric Nup159 in nuclear pore complex could associate with a stack of 5 LC8 dimers to

form a 20-nm transmembrane rod (Stelter et al., 2007). In addition, LC8 binding was

shown to promote phosphorylation of the target proteins (Regue et. al., 2011).

These proposed functions may underlie the phenotypes of *Chlamydomonas* LC8

mutants (Yang et al., 2009). LC8 is present in four key molecular complexes in flagella:

the cytoplasmic dynein that transports cargoes from flagella back to the cell body; two axonemal dynein arms that power the sliding of neighboring microtubule outer doublets (King and Patel-King, 1995; Kamiya, 2002); and the radial spoke (RS) complex that coordinate the activities of the axonemal dyneins (Yang et. al., 2001; 2008). The LC8 null mutant, *fla14-1* and *fla14-2*, generate short and paralyzed flagella in which these complexes are absent or reduced (Pazour et al., 1998). However, the defects of these four complexes in *fla14-3* flagella are very different (Yang et al., 2009). The phenotypes are caused by a stop codon mutation in *fla14-3*'s LC8 gene, resulting in an extended C-terminus, presumably protruding out of a third interface far away from the target-binding grooves. The axonemal dynein motors appear largely spared. However, the flagellar length is shorter, indicating compromised cytoplasmic dynein. Most interestingly, the RS is unstable and drastically reduced in abundance. And radial spoke proteins (RSPs) become hypo-phosphorylated (Huang et al., 1981; Piperno et al., 1981; Yang et al., 2009). The disparate impacts suggest that the role of LC8 in each complex is independent and different. Yet it is unclear why the RS is particularly sensitive to the C-terminal extension in LC8.

The RS is a T-shaped complex with a thinner stalk connected to a bulbous head. The complex is comprised of LC8 and at least 18 other distinct radial spoke proteins (RSPs) (Huang et al., 1981; Piperno et al., 1981; Patel-King et al., 2004; Yang et. al., 2001; 2006). Some of them are partially assembled in the cell body first (Diener et. al., 2011). The prepackaged particles are delivered by the kinesin-driven anterograde intraflagellar transport (IFT) into the flagellar compartment. The partial precursors are converted into mature particles and integrated into the 9 outer doublets of the 9+2

axoneme at the tip of flagella (Johnson and Rosenbaum, 1992; Qin et al., 2004). The severe RS deficiency in the LC8 mutants suggest that LC8 plays a critical role in this complicated assembly process.

One RSP, RSP3, is as vital for RS assembly as LC8. RSP3 exists as a dimer in the RS (Wirschell et al., 2008). A premature stop codon mutation in the RSP3 gene, in the *pf14* mutant, results in low expression of truncated RSP3 that lacks the N-terminal 42 a.a. residues, yet this mutant has paralyzed axoneme devoid of RS suggesting that RSP3 N-terminus is essential for RS assembly (Williams et al., 1989). In line with the genetic evidence, recombinant RSP3 or its N-terminus can be reconstituted to the spoke-less *pf14* axonemes, but not purified microtubules (Diener et. al., 1993). Thus it is predicted that RSP3 is located at the spoke base and its N-terminus is involved in docking RSP3 and hence the entire RS complex to unknown proteins on the microtubule outer doublets. In the same vein, RSP3 binds to a subunit in a CSC complex, a putative spoke docking complex that co-sediments with the RS particles extracted from axonemes (Dymek et. al., 2007).

Based on the common importance of LC8 and RSP3 in RS assembly, we tested the hypothesis that LC8 directly interacts with dimeric RSP3 to promote RS assembly. The results showed that RSP3 interacts with LC8 dimers, in fact multiple in tandem. The interactions affect RSP3 phosphorylation and are critical for at least two aspects of assembly-- forming part of the rigid stalk and targeting the stalk to the RS docking complex on the axoneme. The multiple effects of LC8 on a key molecule in an axonemal complex reveal the mechanisms for the ciliogenesis and motility control; and may be applicable for other complexes in the cell body.

Results

3.1 LC8-binding motifs are present at RSP3 N-terminus

3.1.1 Five LC8-binding motifs are present at RSP3 N-terminus

To identify the LC8-binding proteins in the radial spoke, we visually inspected the

sequences of all *Chlamydomonas* radial spoke proteins (RSPs) for canonical LC8-binding

motif. The canonical LC8-binding motifs have either typical TQT motif or motifs in

which T's are replaced by S, I, V or C (Lo et al., 2001; Rodriguez-Crespo et. al., 2001).

Unexpectedly, we found an array of five TQT-like LC8-binding motifs at RSP3 N-

terminal 160 a.a. (Figure 3-1A). The five LC8 binding motifs are 17-30 a.a. apart and

precede the α-Helix (AH) that binds RII at a.a. #160-178 (Gaillard et al., 2001). In

contrast, no such motifs were evident in other RSPs.

The presence of LC8 binding domains in the N-terminus of RSP3 is

intriguing because this region is central for the docking of the RS. A premature stop

codon mutation in the RSP3 gene in the *pf14* mutant results in paralyzed axonemes

devoid of RSs (Williams et al., 1989), while RSP3 synthesized in the rabbit reticulocyte

lysate can bind to the spoke-less *pf14* axonemes (Diener et. al., 1993). The binding site

was mapped within the first 80 a.a. (Figure 2A, underlined). In addition, in vitro, RSP3

binds to a subunit in a putative calmodulin- and spoke-associated complex (CSC) that

may be involved in docking RS (Dymek et. al., 2007; 2011). Lastly, like many LC8

target proteins, RSP3 exists in RSs as a homodimer (Wirschell et al., 2008).

The first two motifs are located in the axoneme-binding region at the first 80 a.a.

residues (Diener et al., 1993) of RSP3. However, the two sites are not evident in the

corresponding area in the other RSP3 orthologues (Figure 3-1A). For the last three

motifs, Q is absolutely conserved among the orthologues while the flanking residues are

either T or the residues of similar properties. The conservation of last three motifs

suggests that atleast 3 LC8 dimers bind to RSP3 and that the first two motifs are

dispensable. Motifs like these were reported in nuclear pore protein Nup-159 where array

of 5 consensus LC8 motifs are present (Stelter et al., 2007).

3.1.2 LC8 binding region of RSP3 is disordered

The LC8 binding partners are predicted to contain the region of local disorder and low

secondary structure near the LC8 binding sites (Barbar, 2008; Nyitray 2010). Sequence

based analysis of RSP3 N-terminal region using RONN and Jpred servers, predicted that

these sites are present in regions of high disorder and of low propensity to form extensive

α-helices and β-sheets (Figure 3-1B). On the contrary, the rest of RSP3 polypeptide is

largely helical as indicated by the AH just following the LC8 binding sites. Thus, the

sequence analyses suggest that RSP3 is the LC8-binding protein in the RS complex and

the binding region is at its N-terminus.
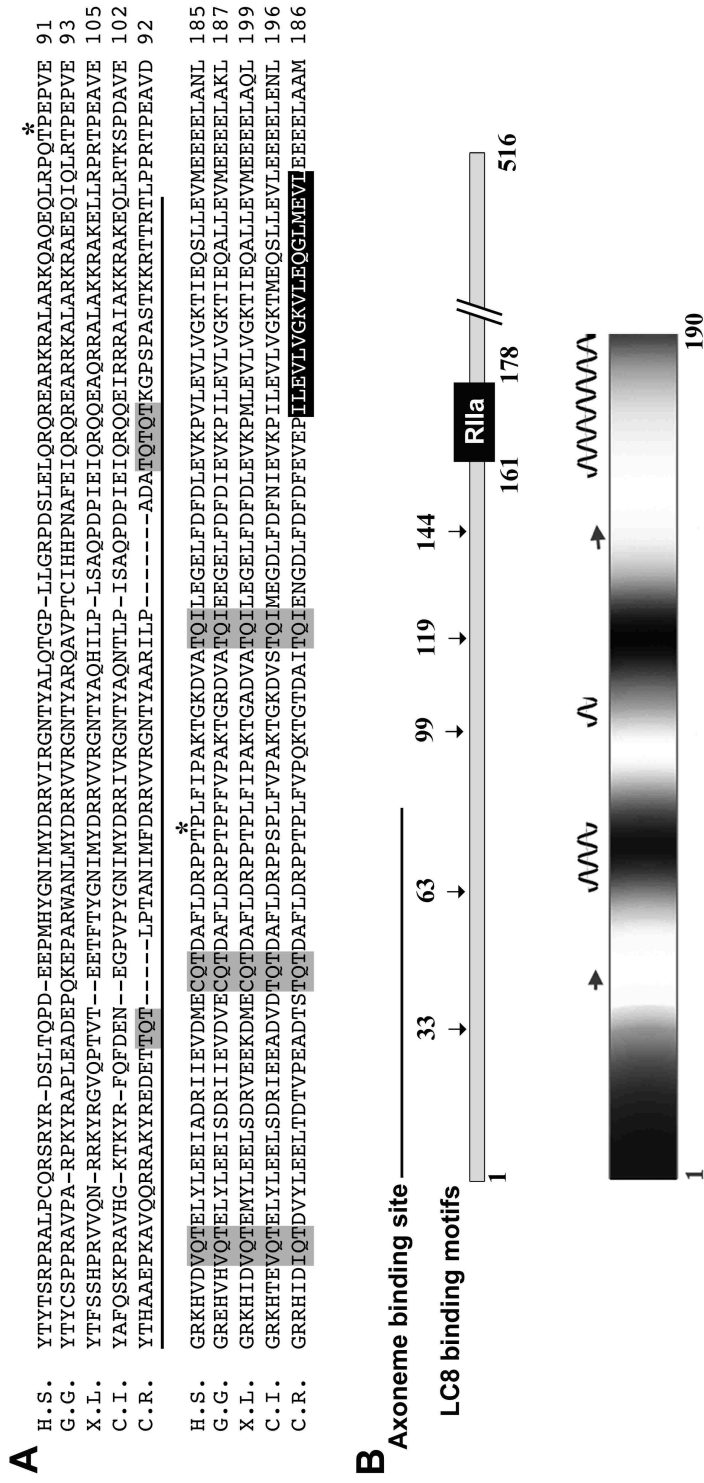
Figure 3-1. Sequence analyses of RSP3. (A) Multiple sequence alignment of the RSP3 N-terminus. Highlighted in grey boxes are five TQT-like LC8-binding motifs in the first 150 a.a. of *Chlamydomonas* RSP3, upstream to the amphipathic helix that binds the RIIa domain (in black; 161-178 a.a.). The first two motifs, in the axoneme-binding region (underlined), are diverged among the orthologues, while the homology of the last three motifs is higher. Asterisks, ERK phosphorylation sites. H.s., *Homo sapiens*; G.g., *Gallus gallus* (chicken); X.l., *Xenopus laevis*; C.i., *Ciona intestinalis*; C.r., *Chlamydomonas reinhardtii*. (B) The schematic depicting the location of LC8-binding motifs in the full-length *Chlamydomonas* RSP3. Black line, the axoneme-binding region. The predicted disordered region (bottom) in RSP3 N-terminus. White, <50% disorder. Black, >50% disorder. The predicted α-helix (coil) and β-strand (arrow)

3.2 Trypsin-digested spoke particles contain both RSP3 N-terminus and LC8

To test the prediction that LC8 binds RSP3, we took advantage of an observation that RS

can be cleaved into fragments by limited trypsin digestion. Trypsin is a protease that

cleaves unprotected peptides at Arg or Lys. The EM images of trypsin treated axonemes

has shown that the RS are digested into smaller sub-particles based on the amounts of

protease added. The EM images also showed the absence of spoke head but the presence

of small stalks of RS in the axonemes on digestion (Summers and Gibbons, 1971). This

suggests that the base of the RS proposed to contain RSP3 and LC8 remains

undigested/protected on treatment. If the hypothesis is right, the RS sub-particle extracted

from the digested axonemes will contain RSP3 N-terminal fragment and LC8 localized at

the stalk base.

3.2.1 Limited digestion of RS yields two sub-particles that contains RSP3 N-terminus

Toward this end, *pf28pf30* mutant axonemes lacking both the outer and inner dyneins

were used with the objective of removing any LC8 contamination due to dyneins. The

axoneme was isolated and treated with increasing concentration of trypsin. The trypsin-

treated axonemes were then suspended in the KI buffer to extract the RS. The digestion

of axoneme followed by RS extraction allows purification of small digested RS stalks

seen in the EM. Following extraction the KI buffer was dialyzed against no salt buffer to

neutralize the salts. The de-salted extract was suspended in sample buffer without SDS

and fractionated on a low percentage native gel (Figure 3-2A).

The native conditions allow the sub-particles to run as a complex. The RS particles with RSP3 N-terminus were revealed by western blots using a pan-RSP3 antibody raised against human RSP3 that is largely comprised of the conserved N-terminal sequence in *Chlamydomonas* RSP3 (Figure 3-1A). Compared with the untreated control (lane 1), the extract from the axonemes treated with trypsin at a ratio of 100:1 by weight contained two smaller RSP3-positive particles. These sub-particles became diminished if the trypsin concentration was two-fold higher (lane 3). Thus, the sample with 100:1 axoneme:trypsin ratio, having two N-terminal containing sub-particles was analyzed further.

For further analysis, SDS-PAGE gel was run. The trypsin treated samples were resuspended in sample buffer containing SDS. The denaturation condition causes the dissociation of the sub-particles into individual polypeptides. The SDS-PAGE shows that RSP3 in this sample migrated as 30- and 20-kDa polypeptides (Figure 3-2B, upper panel), sufficiently large to contain multiple TQT-like motifs. Importantly, LC8 remained intact (Figure 3-2B, lower panel).

3.2.2 The sub-particles contains LC8 of different amounts

To determine whether LC8 and RSP3 fragments were in the same RS sub-particles, the extract was fractionated by 2-D electrophoresis— a native gel in the first dimension separation followed by a SDS-PAGE in the second dimension. This particular 2-D electrophoresis first separates the sub-particles as a complex in the native conditions and then separates each sub-particle into individual polypeptides in the denaturation

conditions. The native gel separates the complex on the basis of charge-to-mass ratio while the SDS-PAGE separates the polypeptides based on the mass alone.

The 2-D SDS-PAGE blot was sequentially probed for LC8 (Figure 3-2C, upper panel) and RSP3 (middle panel). The alignment of the two major LC8 spots with the 30-kDa or 20-kDa RSP3 spots indicates that LC8 and RSP3 N-terminus are present in the two RS sub-particles (Figure 3-2C, middle panel). Notably, the larger particle had the longer RSP3 fragment and the more intense LC8 spot. To position the two RSP3 fragments, the membrane was further probed for RSP11 (lower panel) that binds to the AH at $RSP3_{160-178}$ (Gillard et al., 2001; Yang and Yang, 2006) adjacent to the LC8-binding motifs. Consistently, RSP11 co-migrated with the RSP3 fragments and LC8.

The similar intensities of the two RSP11 and two RSP3 spots suggest that even on the truncation of RSP3 to a smaller particle, the RSP11 binding is not affected. On the contrary the two RSP3 spots co-migrate with different intensities of LC8 spots suggesting that the two RSP3 fragments may differ at the extreme N-terminus and the larger fragment contains more LC8 binding sites than the smaller one (Figure 3-2D).
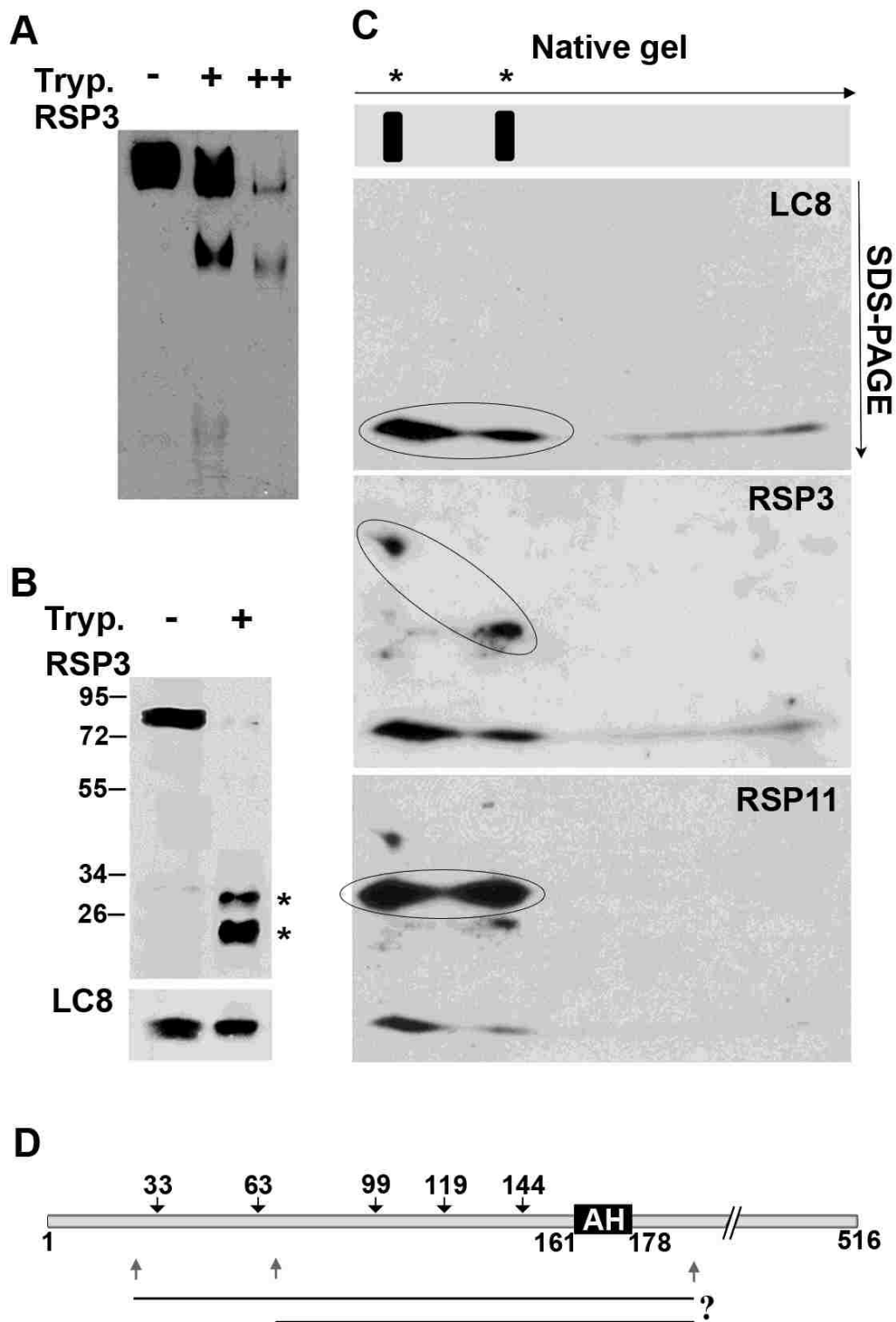
Figure 3-2. Co-migration of LC8 and RSP3 N-terminal proteolytic fragments in electrophoresis. Axonemes of *pf28pf30* that lacks the LC8-containing dyneins were treated with the trypsin solution at the ratio of 1:0, 1:8000, 1:16000 by volume. The KI axonemal extract was fractionated by (A) native gel, (B) SDS-PAGE or (C) the two electrophotretic methods sequentially. The schematic depicts the native gel strip with two RS proteolytic particles. Arrows, the directions of electrophoresis. The blots were probed for RSP3 N-terminus, LC8 and RSP11 that contains a RIIa domain. Note that while RSP11 appeared equally abundant in the two particles, the spot of LC8 that co-migrated with the smaller RSP3 fragment appeared less abundant. (D) The approximate proteolytic sites for the two RSP3 N-terminal fragments are depicted by arrows in the schematic.

3.3 Direct interaction of recombinant LC8 and RSP3 N-terminal region

To test that RSP3 N-terminal region and LC8 directly bind to each other, co-purification

was performed. The assays were carried out with C-terminal S-tagged RSP3 (Amino

acids 1-160) consisting of all five putative LC8 binding motifs and N-terminal His-tagged

LC8. The cloning strategy for both the constructs is described in materials and methods.

The S-tag $RSP3_{1-160}$ and His-LC8 were separately expressed in bacteria and their extracts

were incubated together to allow interaction before affinity purification by two

independent methods.

3.3.1 Affinity purification by Ni-NTA

The mixture of bacterial extract containing S-tag $RSP3_{1-160}$ and His-LC8 were subjected

to Ni-NTA purification. The results were assessed by SDS-PAGE and Coomassie stain.

The protein gel showed that Ni-NTA pulled down $RSP3_{1-160}$ along with His-LC8 (Figure

3-3A). The control containing only one polypeptide showed that the S-tag RSP3 alone

had a low affinity for Ni-NTA.

3.3.2 Affinity purification by S-agarose

Similarly, the mixture containing the S-tag $RSP3_{1-160}$ and His-LC8 was subjected to S-

agarose affinity purification. The results showed S-agarose pulled down LC8 along with

S-tag $RSP3_{1-160}$ (Figure 3-3B). Without S-tag $RSP3_{1-160}$, the control containing only His-

LC8 was not pulled down by S-agarose. Thus, in vitro the N-terminal region of RSP3

binds directly and specifically to LC8.

3.3.3 RSP3 N-terminus interacts with 3 LC8 dimers

To assess the stoichiometry of LC8 and RSP3$_{1-160}$ in the pull down, the two polypeptides

were quantified. The expression of His-tagged LC8 appeared more robust than the RSP3

fragment and, thus, the pull down from Ni-NTA was not suitable for stoichiometry. Thus,

the ratio of RSP3/LC8 was obtained from the S-agarose sample that pulled down the less

abundant S-tag RSP3$_{1-160}$ instead. The average density of Coomassie-stained RSP3 band

and LC8 band was measured by densitometry. Comparison of the average densities

divided by the molecular mass revealed that the stoichiometry of RSP3 N-terminus

versus LC8 was 1: 3 (Figure 3-3B). Similar ratio was obtained when the RSP3 N-

terminus was pulled down with LC8 by Ni-NTA in a separate experiment where the

saturating amount of RSP3 was added. The serial dilution of this sample gave the ratio of

1:3.5 indicating the protein load and stain was within the linear range for densitometry

(Figure 3-4). This ratio is consistent with the three conserved LC8-binding sites in RSP3.
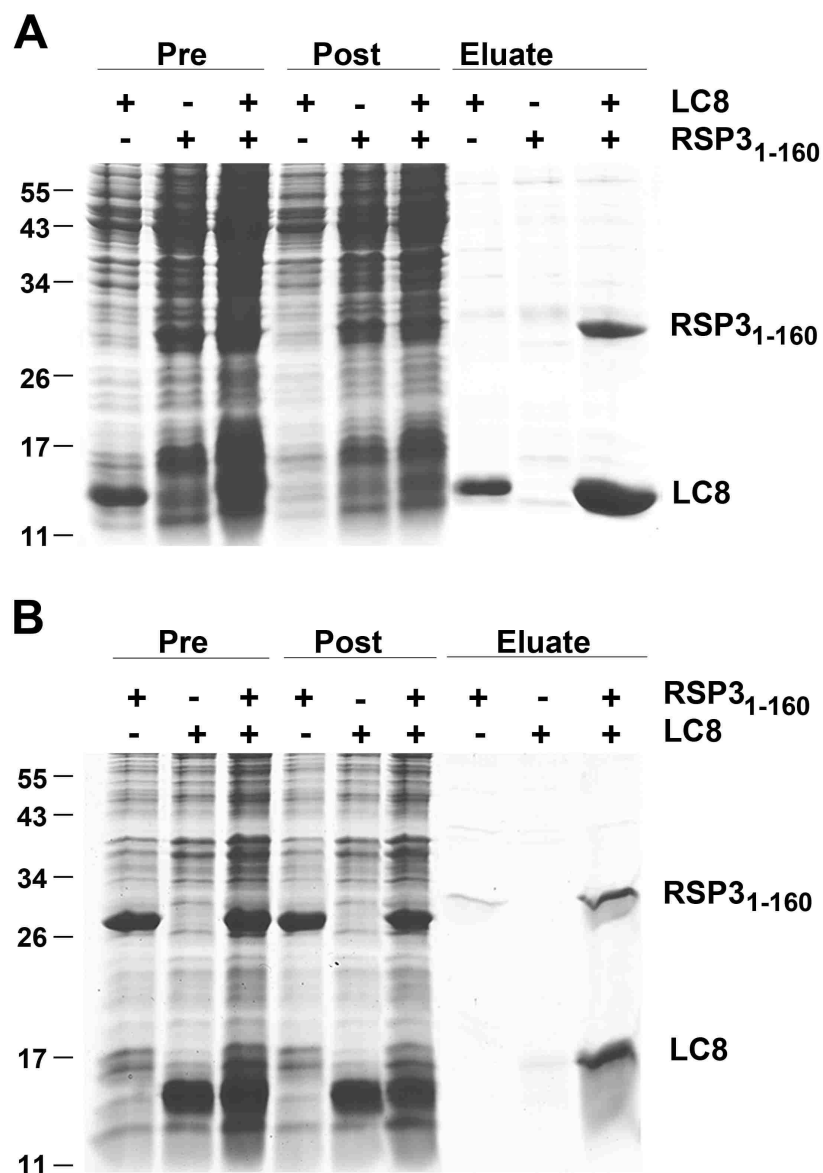
Figure 3-3. Direct interaction of recombinant LC8 and RSP3$_{1-160}$. Bacterial extracts containing His-tagged LC8, S-tag RSP3$_{1-160}$ or the mixture were subjected to Ni-NTA (A) and S-agarose beads (B). Protein samples were fractionated by SDS-PAGE and revealed by Coomassie stain. Pre, bacterial extract; Post, flow through. The aberrant migration of the S-tag elute is due to the 3 M MgCl$_2$ in the elution buffer.
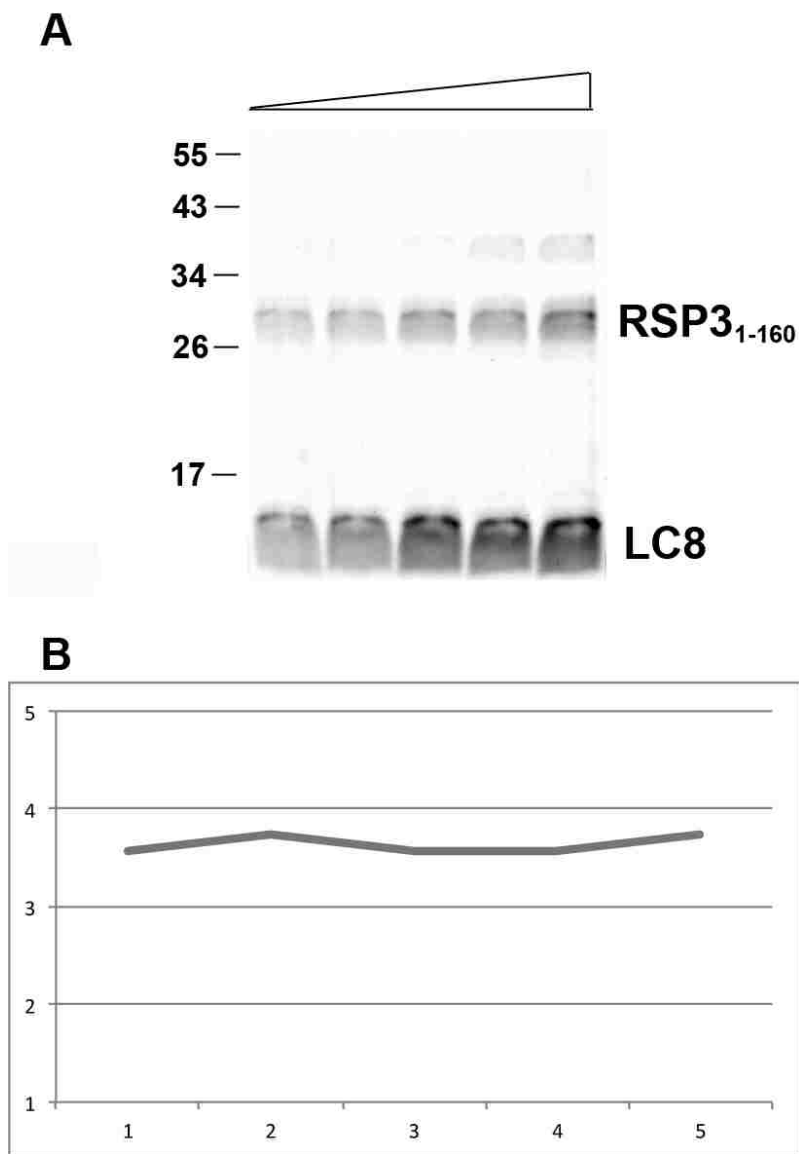
Figure 3-4. RSP3$_{1\text{-}160}$ interacts with ~ 3.5 LC8 dimers. Bacterial extracts containing the mixture of His-tagged LC8 and S-tag RSP3$_{1\text{-}160}$ was subjected to Ni-NTA beads. (A) The co-purified sample was further subjected to serial dilution and was fractionated by SDS-PAGE and revealed by Coomassie stain. (B) The ratio of average density divided molecular mass of serially diluted sample in (A) led to an approximate stoichiometry ratio of 1:3.5 for RSP3:LC8.

3.4 LC8 enhances the reconstitution of RSP3 to the spoke-less axoneme

Although the RS is not detectable in the axoneme of the LC8 null-mutant (Pazour et al., 1998), it is still rather abundant in its flagellar matrix (Qin et al., 2004). Based on this we propose that LC8 is involved in docking the RS to the axoneme. In order to understand if LC8 binding to RSP3 N-terminus promotes its docking to the axoneme an in vitro reconstitution experiment was performed.

Previously it was demonstrated that the spoke-less *pf14* axonemes pulled down more RSP3 N-terminus expressed in the rabbit reticulocyte lysate than the wild type (WT) axonemes (Diener et. al., 1993). However, RSP3 N-terminus cannot be pulled down by microtubules alone. These results led to the conclusion that RSP3 N-terminus specifically associates with the spoke docking proteins on the axoneme. Although this experiment did not add LC8, the rabbit reticulolysate likely supplemented LC8 that is extraordinarily conserved throughout evolution. To determine whether LC8 improves this reconstitution, the $RSP3_{1-160}$-containing bacterial extract was incubated with axonemes in the presence or absence of the bacterial extract containing His-LC8 (Figure 3-5). To perform the experiment, equal amounts of bacterial extracts were incubated with the axoneme added in two-fold increments. If the hypothesis is right, the axoneme will pull down a larger amount of RSP3 in presence of LC8. The experimental group used *pf14* axonemes without RS while the control group used WT axonemes that contain RS.

After incubation, the axoneme was spun down and the unbound supernatant was removed. The contents of the axoneme pellet with reconstituted polypeptides were assessed by western blots. The quantity of axonemes was reflected by p28, a subunit in I2/I3 inner dyneins. The amount of $RSP3_{1-160}$ pulled down by the *pf14* axonemes was

much greater in the presence of LC8 than without LC8 (Figure 3-5, compare lane 3&4); and than the WT group (compare lane 10&11). This indicates that LC8 promotes the reconstitution of RSP3 to the spoke-less axoneme.

It is worthwhile to point out that endogenous un-tagged LC8 in *pf14* axonemes is less abundant than that in an equal amount of WT axonemes (compare lane 1 & 8) and about equivalent to the half amount in WT axonemes (compare lane 1 & 12). This suggests that the amount of LC8 molecules in the RS is equivalent to the combination of LC8 in both outer dynein arms and I1 inner dynein. This is interesting because of the 2:5 ratio of the RS versus the two LC8-containing dyneins in each 96-nm axonemal unit (Nicastro et al., 2006) and each dynein likely contains 1 LC8 dimer (Pfister et al., 2006; DiBella et al., 2005). Thus, based on this semi-quantitative western blot, each RS particle contains ~2.5 LC8 dimers.
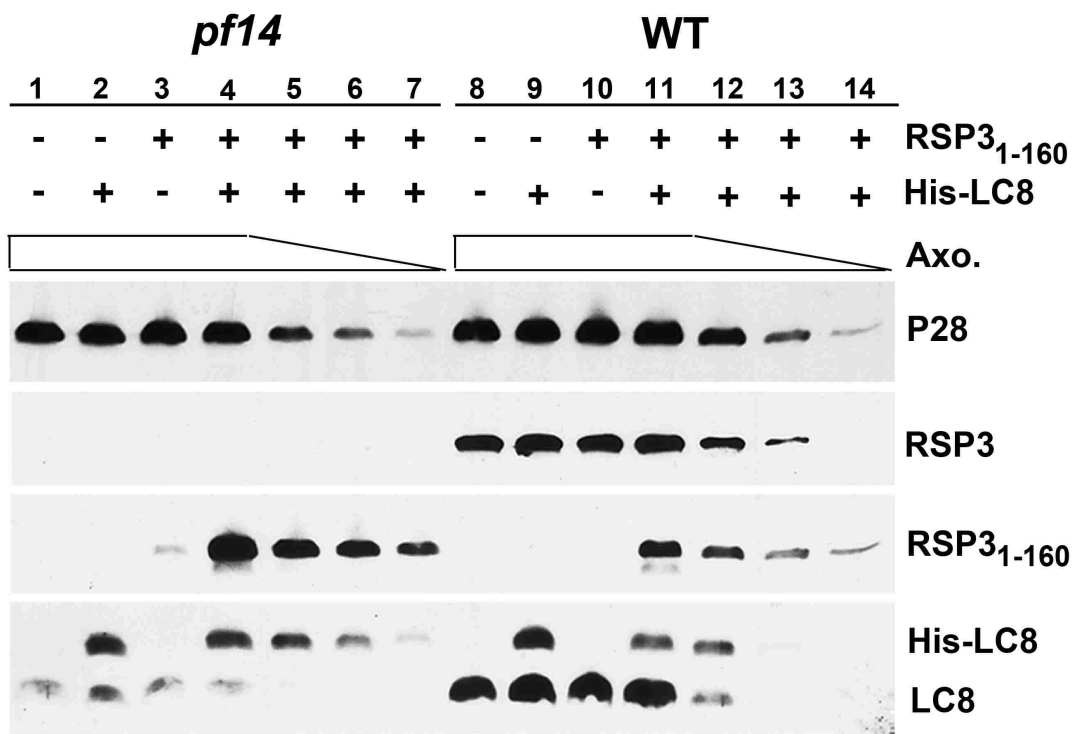
Figure 3-5. LC8 promotes the reconstitution of RSP3 N-terminus to the spoke-less *pf14* axonemes. Bacterial extract containing RSP3$_{1\text{-}160}$, His-LC8 or both were incubated with axonemes from *pf14* or the wild type (WT) of decreasing concentrations by 2-fold (clear bars). The axoneme pellets were fractionated by SDS-PAGE and the blots were probed as indicated. The subunit in inner dyneins, p28, is used to indicate the amounts of axonemes.

3.5 Homodimerization and phosphorylation of RSP3 N-terminus

To characterize the RSP3 N-terminus in vivo, two RSP3 truncation genomic constructs

were transformed into the *pf14* cells to express RSP3$_{1-170}$ a.a. The 1-170 a.a. of RSP3

includes all 5 TQT-like motifs and only about half of the AH that binds the RIIa domain.

To protect the truncated end, the first construct abrogated the endogenous stop codon

leading to an additional 29 a.a. encoded by the 3' UTR at the C-terminus. The 29 a.a.

contained three cysteine residues (Figure 3-6A). On the other hand, the second construct

had a C-terminal HAHis tag, with 3 HA epitopes and 12 His residues (Figure 3-6B). The

cloning strategy of the two constructs is discussed in Chapter 2 - material and methods.

The control, Δ1 (lane 1) is the RS from a mutant expressing a longer truncated HA-His

tagged RSP3, generated for a separate project in the lab.

3.5.1 RSP3 N-terminus is phosphorylated

Interestingly, both RSP3$_{1-170}$-3Cys and RSP3$_{1-170}$-HAHis polypeptides migrated as

multiple bands (arrows). The multiple bands are the result of different phosphorylation

levels of RSP3. This is evident from several RS mutants that show multiple bands due to

hypo-phosphorylation in comparison to RSP3 from the WT that is phosphorylated

(Huang et al., 1981; Yang and Yang, 2006; Yang et al., 2009). The presence of multiple

bands suggests that RSP3 N-terminal fragments in the axoneme are phosphorylated and

some phosphor-residues in RSP3 are located at the N-terminus. In fact, as mentioned in

Chapter 1, there are two T/S residues in this region that are predicted to be

phosphorylated by ERK MAP kinase in mammalian RSP3 in vitro (Jivan et. al., 2009).

One site is between the 2nd and 3rd TQT motifs and the other site is between the 4th and 5th TQT motifs (Figure 3-1A, asterisks).

3.5.2 RSP3 N-terminus forms homodimer

A fraction of RSP3$_{1-170}$-Cys in axonemes migrated as homodimer-like larger particles even in the reducing SDS-PAGE (Figure 3-6A, asterisk). The larger band disappeared when the sample contained an excess of reducing agent. This result suggests that the N-terminal fragment became cross-linked into homodimers by disulfide bonds from the three cysteine residues in the tag. To clarify that the larger band is not due to any artifact RSP3$_{1-170}$-HAHis was treated with the zero-length cross-linker (EDC) to see the larger band of twice the size. Consistent with this interpretation, axonemes with RSP3$_{1-170}$-HAHis treated with EDC also contain the dimer-like band (Figure 3-6B, asterisk). Thus, this region exists as a homodimer in the axoneme. Full-length RSP3 in axonemes also exists as a homodimers and the N-terminus is inherently dimeric in the bacterial system (Wirschell et al., 2008). This finding is consistent with the proposed model that the LC8 dimer associates with polypeptides with inherent dimeric tendency (Barbar, 2008). However, RSP3$_{1-170}$ in axonemes was much less abundant than the longer RSP3 polypeptides from a mutant expressing RSP3 lacking a.a. # 161-244 (Figure 3-6, compare the HA western of the tagged RSP3$_{1-170}$ and a tagged control RSP3). Thus, additional downstream sequence of RSP3 promotes the assembly efficiently.

A

Control 1-170-Cys

− + β-ME

170 —
72 —
55 —
43 —
34 —

α-RSP3

B

Control 1-170-HAHis

1-170-HAHis

EDC 0 0.2 0.4 1 3 5 10 mM

170 —
72 —
55 —
43 —

95 —
72 —

43 —

α-HA

α-RSP3
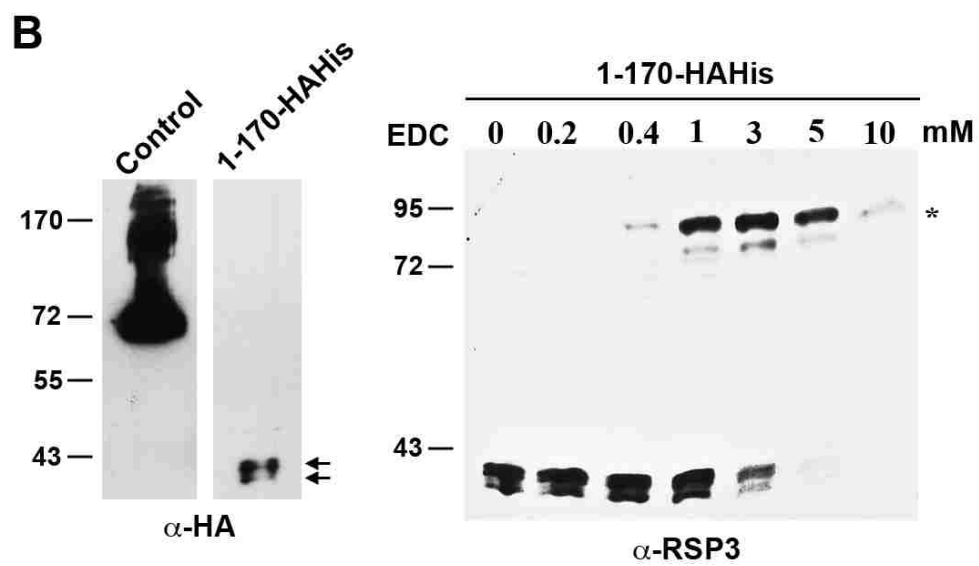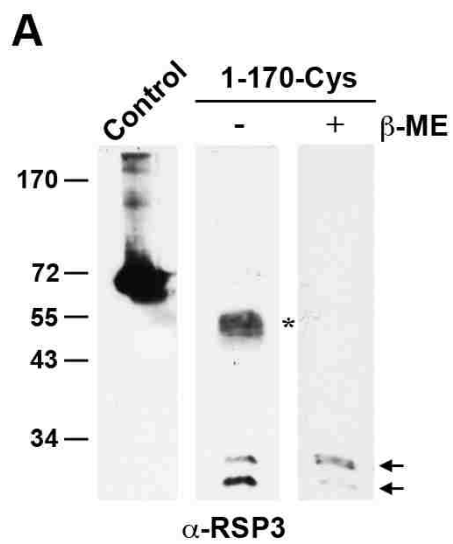
Figure 3-6. The dimeric propensity of RSP3 N-terminus. The axonemes of the *pf14* transformants expressing RSP3$_{1-170}$ with a C-terminal 3-cysteine tag (A) or 3HA12His (B). Monomers of the RSP3$_{1-170}$ fragments migrated as multiple bands (arrows). A fraction of Cys-tagged RSP3$_{1-170}$ migrated as homodimers (asterisk) even in SDS-PAGE. The dimer-like band disappeared in the sample containing 140 mM β-mercaptoethanol (β-ME). Dimeric band (asterisk) also appear in the RSP3$_{1-170}$ HAHis samples treated with increasing amounts of chemical crosslinker, EDC. Control is RSP3ΔCoil1 axoneme, in which RSP3$_{161-244}$ was deleted. Note the blots probed for RSP3 or HA show that this fragment is much less abundant than the longer control RSP3 polypeptide.

3.6 Pull down of extracted RSP3 contains LC8 and putative RS docking proteins

The binding of LC8 at the RSP3 N-terminus and the effect of LC8 in enhancing the

reconstitution of RSP3 N-terminus and the spoke-less axoneme suggest that the complex

of RSP3 N-terminus and LC8 interacts with the spoke docking proteins in the axoneme.

If the hypothesis is correct, the RSP3 N-terminus extracted from axoneme may contain

LC8 as well as the docking proteins.

To test this, we used Ni-NTA to affinity purify RSP3 N-terminus extracted from

axonemes. Because of the low abundance of $RSP3_{1-170}$ in the axoneme, for this

experiment we used the strain that expressed $RSP3_{1-178}$–HAHis (Sivadas et al.,

unpublished data) that has 8 more amino acids than $RSP3_{1-170}$, corresponding to the intact

RIIa-binding site (Gaillard et al., 2001) immediately upstream to the LC8-binding region.

3.6.1 The pull down contains several radial spoke proteins

The RS was extracted from the axoneme of $RSP3_{1-178}$–HAHis strain and affinity purified

by Ni-NTA. The spoke-less axoneme *pf14* was used as the control. The candidate protein

approach was taken to detect the proteins in the pull down. Western blots showed that in

addition to $RSP3_{1-178}$, the pull down also contained the RIIa-containing RSP11 and LC8

as expected (Figure 3-7A). Silver staining also revealed these two polypeptides (Figure 3-

7B) as well as the second RIIa containing protein, RSP7, that is slightly bigger than

tubulin (Figure 3-7B, Yang et al., 2006).

3.6.2 The pull down contains RS docking complex

In addition, western blots (Figure 3-7A) and silver stain (Figure 3-7B) showed that the

pull down also selectively enriched IP2 and IP3 in the CSC complex. The protein gel also

contains a band corresponding to IP4 in the CSC complex. IP-4 was previously identified

determined by mass spectrometry. As the antibody of IP4 is not available due to its non-

antigenic nature, the ~100 kDa band seen in the silver stain was identified as IP4 based

on the similar stoichiometry to IP2 and IP3 and the molecular mass in SDS-PAGE

(Dymek et. al., 2007). The absence of these bands from *pf14* suggests that these proteins

are specific to RS. As most of the RSPs located towards the spoke head were absent in

this truncated strain, this result strongly suggests that CSC complex is located in the

vicinity of the axoneme-binding region of RSP3 and that the CSC complex associates

through first 178 a.a. of RSP3. Additionally, the binding of LC8 to this region suggests

that LC8 promotes the docking of RSP3 to the CSC complex.

Interestingly, western blot analysis showed that calmodulin was not detectable in

the $RSP3_{1-178}$ pull down (Figure 3-7A). Yet previously the CSC complex, including IP2,

IP3 and IP4, was pulled down along with calmodulin (CaM) by anti-calmodulin

immunoprecipitation (IP) from *pf14* axonemal extract (Dymek et al., 2007). The

discrepancy may be due to two reasons. Firstly, this could be due to different proteins

used for the pull down. The previous study used calmodulin IP, which possibly pulled

down only a small fraction of CSC complex that associates with calmodulin. In contrast,

this study used Ni-NTA that pulled down most of the RS and significant amounts of CSC

complex. Thus it is predicted that not all the CSC complex associates with CaM and the

RSP3 pull down contains low amounts of calmodulin, which is undetectable. Secondly, it is possible that CaM dissociates from the CSC complex during the experimentation.

3.6.3 The pull down contains a novel RS docking protein

Interestingly, silver stain also revealed an 85-kDa band (Figure 3-7B, asterisk) in the RSP3$_{1-178}$-HAHis pull down. As IP3 and IP4 in the CSC complex, this band was absent in the *pf14* control and has a similar stoichiometry. Note this protein was not pulled down by the calmodulin IP (Dymek et al., 2007). Thus this protein is novel. In order to identify the protein, the band was excised from the silver stained gel and subjected to mass spectrophotometry.

Mass spectrometry of this purified band revealed eight peptide sequences (Table 3-1) that are encoded by the gene for the flagellar associated protein, FAP206. This protein of predicted 712 a.a. was identified in the flagellar proteome (Pazour et al., 2005). It is rare in the NaCl extract and enriched in the residual axoneme after the NaCl extraction. Thus, this novel polypeptide is a flagellar molecule and like RSPs in the axonemes, FAP206 is resistant to the NaCl extraction (Yang et al., 2001). The FAP206 homologues included human C6ORF165 (Accession #, NP_001026913), which is widely found in mammalian genomes. As expected, the EST profile in the NCBI suggested that its transcripts are particularly enriched in testis. Thus the function of FAP206 is likely conserved.
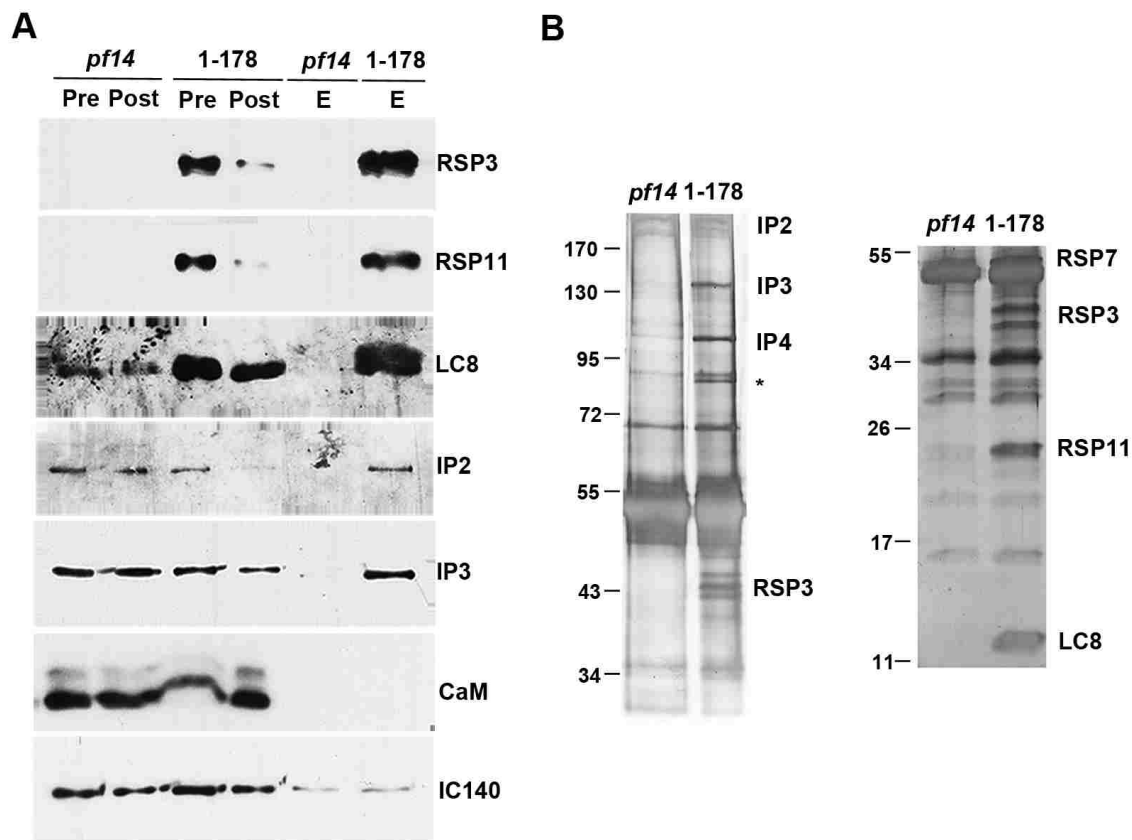
Figure 3-7. Pull down of RSP3$_{1-178}$ contained LC8 and putative RS docking proteins. RSP3$_{178}$-HisHA was pulled down by Ni-NTA from the KI axonemal extract of *pf14* strain expressing the tagged truncated RSP3. The samples were analyzed by western blots (A) and silvered stained protein gel (B). LC8 as well as IP2, IP3 and IP4 in the spoke associated CSC complex were co-purified with RSP3$_{178}$. Controls included *pf14* axonemal extract and the inner dynein arm intermediate chain, IC140. IP4 was not probed by western blots because it was not immunogenic and was identified based on the co-purification with IP-2 and IP-3 and its molecular mass. Note, an unknown 85-kDa protein was co-purified as well (asterisk) and its stoichiometry was equivalent to that of IP3 and IP4.

Table 3-1. The peptide sequences of the new axonemal protein co-purified with truncated RSP3. The sequences, revealed by mass spectrometry, correspond to flagella associated protein FAP206.

Score	Sequence
7	LTQLAELAR
6	VDPYVVAYVTSLEDAR
5	AFLSDPAAVLAGVAAAVAR
4	VYGFSSNADMR
3	GALQSLVPDVSLK
3	AALESVFPVSAVSR
1	AGAVSSEAVAAIGGYVAGLVGDAR
1	FVTLAEGER

3.7 LC8 is undetectable in the RS precursor

The collective evidence supports the hypothesis that LC8 aids the axoneme docking of RSP3 and thus the RS. The question is when and where does LC8 binds to RSP3. Note in the LC8-null *fla14-1* mutant, although RS is absent in the axoneme (Pazour et al., 1998), the soluble RS particles, including the 12S precursor and mature RS, are present in the flagellar membrane matrix (M+M) (Qin et al., 2004). Thus without LC8, the precursor was synthesized in the cell body, delivered to the flagella and converted to 20S in flagella. The RS just cannot dock without LC8. Based on these results, we postulate that LC8 binds to 12S in flagella immediately preceding the docking of the RS. If the hypothesis is correct, LC8 and 12S RS precursor particles will exist as separate particles.

It has been demonstrated previously that LC8 sediments throughout the sucrose gradients of detergent-solublized flagellar membrane matrix (M+M), since LC8 is present in the RS as well as in the 18-20S axonemal dyneins and cytoplasmic dynein. Interestingly, most of the LC8 sediments near the top as small particles (Rompola et al., 2007). To test the hypothesis, we examined if LC8 and RSP3 in the M+M co-fractionate. The 20S and 12S RS fractions from the wild type (WT) M+M gradient were subjected to a second round of fractionation, DEAE ionic chromatography. The goal is to biochemically separate RS particles from other co-sedimented components in the velocity sedimentation. Results from western blots showed that the re-purified 20S and 12S particles contained RSP3 but only the former contained LC8 (Figure 3-8; Unpublished data from Dennis Diener, Yale University). These two independent methods consistently showed that LC8 is undetectable in the 12S particles. We also fractionated the cell body extract and found that LC8 still sedimented primarily at the top of the gradients (not

shown). The sedimentation pattern of LC8 in the cell body or the flagellar matrix is

clearly distinct from most of the other RSPs (Qin et al., 2004; Yang et al., 2006). It is

either not in the 12S precursor or it is easily dissociated from the 12S.
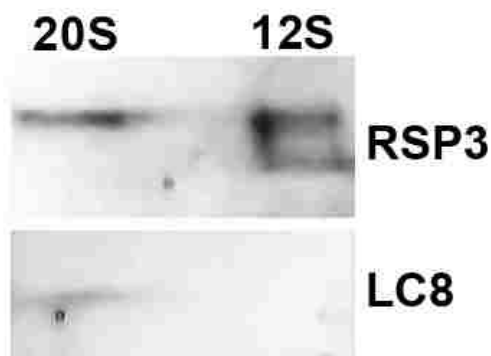
Figure 3-8. LC8 is absent from radial spoke prescursors. **(A)** The membrane matrix extract from *pf28pf30* flagella were sedimented through a 5-25% sucrose gradient. Western blots showed that LC8 sedimented near the top of the gradient, far away from RSP3 or LIC in the cytoplasmic dynein. (B) The anionic chromatography purification of the 20S and 12S radial spoke fractions from the sucrose gradient of WT flagellar membrane matrix extract. Western blot showed the presence of LC8 only in the 20S fractions.

3.8 Perturbation of RSP3's LC8-binding motifs results in hypo-phosphorylated RSP3 and abnormal associations among RS, LC8 and outer doublets

To test the effect of LC8 binding in vivo, RSP3 mutant strains were generated by transformation of *pf14* cells with full-length RSP3-HAHis genomic constructs in which the TQT-like motifs were mutated. For each construct, the mutations were made in clusters; either the first two sites (1-2), the last three sites (3-5) or all the five sites (1-5) were mutated. The AN strains were mutated conservatively, in which one T residue in the TQT-like motif was replaced by A; and Q was changed into N. We also generated AAA strains, in which the three TQT-like residues were completely replaced by AAA as it was reported that the conservative mutations were insufficient to perturb the LC8-binding sites aligned in tandem in Bassoon (Fejtova et. al., 2009). The cloning strategy for these mutants is mentioned in Chapter 2, materials and methods. The control is the tagged WT construct. An antibiotic-resistant cassette was inserted in each construct to distinguish the transformants from the parental *pf14* strain, in case the transformants were paralyzed as well. Each construct was individually transformed into the *pf14* strain. The transformants were first selected based on antibiotic resistance. The results are summarized in Table 3-2.

Table 3-2. Summary of the RSP3 mutants defective in the LC8 binding motifs.

	1st TQT	2nd TQTQT	3rd IQT	4th TQT	5th TQI	Phenotype	% of swimmers
Control						WT	95
1-2 AN	ANT	TNANT				WT	96
3-5 AN			INA	ANT	ANI	WT	92
1-5 AN	ANT	TNANT	INA	ANT	ANI	WT	90
1-2 AAA	AAA	AAAAA				WT	97
3-5 AAA			AAA	AAA	AAA	**Twitch/Slow**	**40 - 60**
1-5 AAA	AAA	AAAAA	AAA	AAA	AAA	**Twitch/Slow**	**40 - 60**

3.8.1 AAA mutants are defective in motility

For each construct that was designed for the single-plasmid transformation, at least 50

antibiotic-resistant transformants were screened microscopically. All constructs were

capable of restoring the motility to *pf14* albeit to different degrees. The mixed population

of swimmers is a common feature of the RS mutants with less severe defects (Gaillard et

al., 2006; Wei, et al., 2010). The 1-2AAA strains and all AN strains were

indistinguishable from the WT control (Table 3-2; Figure 3-9A and 3-9B). The 3-5AAA

or 1-5AAA strains exhibited the most severe motility phenotype.). About 50% of the

cells in the liquid culture were immotile with paralyzed or twitching flagella. The rest

were motile. The percentage of motile cells varied and the motile ones easily became

attached to the glass surface during video microscopy. Furthermore, the flagella

frequently lost synchrony, leading to irregular trajectories (Figure 3-9C and 3-9D.
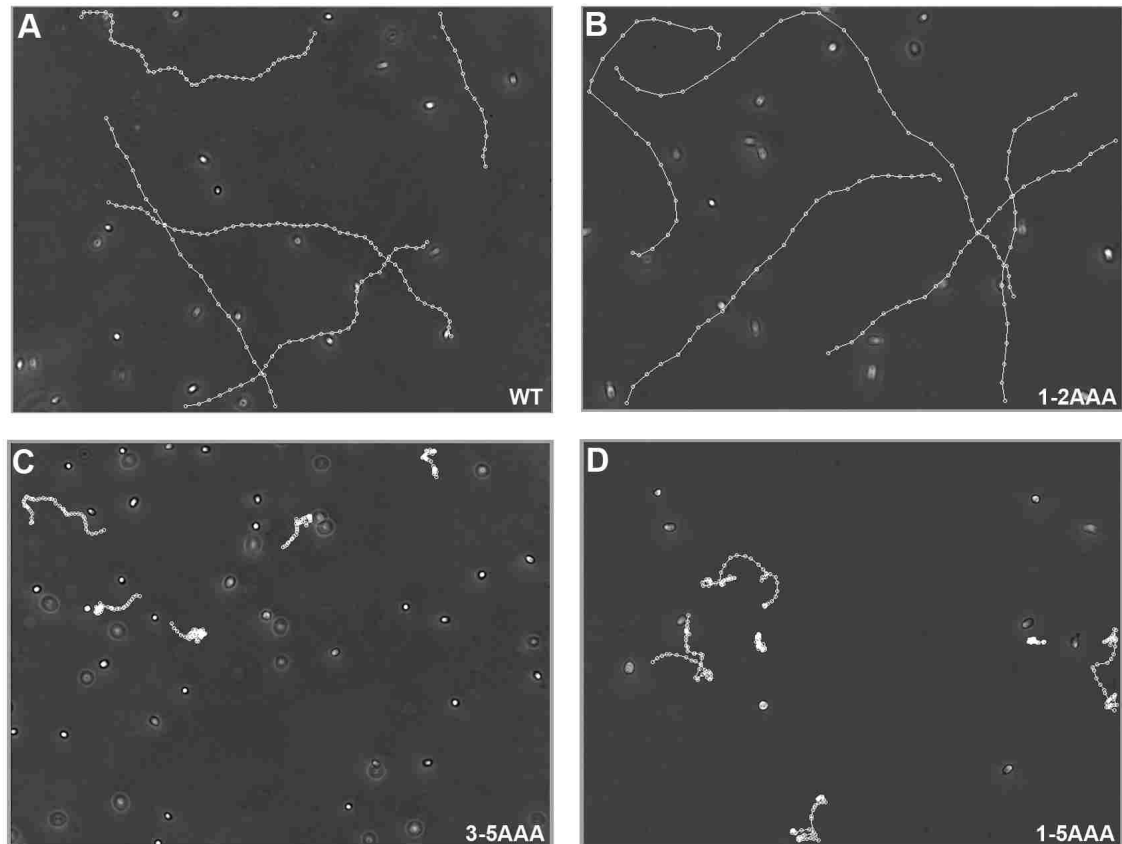
Figure 3-9. The mutants defective in 3-5 LC8 binding motifs in RSP3 exhibit severe motility deficiencies. The 1-5AAA, 3-5AAA and 1-2AAA mutants were recorded at 12.5 frames/sec and tracked to reveal the trajectories. The 3-5AAA and 1-5AAA strains exhibit paralyzed or twitching flagella with occasional slow swimming cells.

3.8.2 AAA mutants results in abnormal associations among RS, LC8 and outer doublets

For each construct, axonemes from 2-3 transformant strains with the highest population

of motile cells were prepared for western blots. The blots were probed for RSP3. RSP3

in the 1-2AAA and 1-5AN strains were restored to WT levels (Figure 3-10; 3-11). The

RSP3 level in 3-5AAA and 1-5AAA axonemes varied in each preparation suggesting

compromised assembly efficiencies (Compare Figure 3-10A and 3-11). The variation in

the assembly level is consistent with the variation of the ratio of swimmers and paralyzed

cells. Because of the variations, we were not certain if the severity of 3-5AAA and 1-

5AAA phenotypes differed.

Since both 3-5AAA and 1-5AAA displayed the most sever phenotypes, we

examined 3-5AAA to determine whether 3-5AAA mutations perturbed RSP3-LC8

binding. In order to see the decrease in amount of LC8 binding to RSP3, it is necessary to

separate RS from the LC8-containing dyneins. For this, axonemes were isolated and

dyneins were largely extracted by 0.6 M NaCl. The RSs were then extracted from the

pellet with the KI buffer. The samples were assessed by western blots. Interestingly, a

small fraction of RS from 3-5AAA mutants solublilized, as dyneins, by the NaCl buffer

(Figure 3-10B), indicating that the axoneme association of the 3-5AAA RS was less

NaCl-resistant than WT RS. Importantly, in the KI extracts that contained most RSP3

and a residual amount of dyneins, as indicated by IC140 western, LC8 amounts in the 3-

5AAA sample were significantly reduced (Figure 3-10B), indicating that the LC8-RSP3

interactions were indeed perturbed by the AAA mutations. The residual LC8 in the KI

fraction could be from the residual dyneins and/or reduced association of LC8 and RSP3.
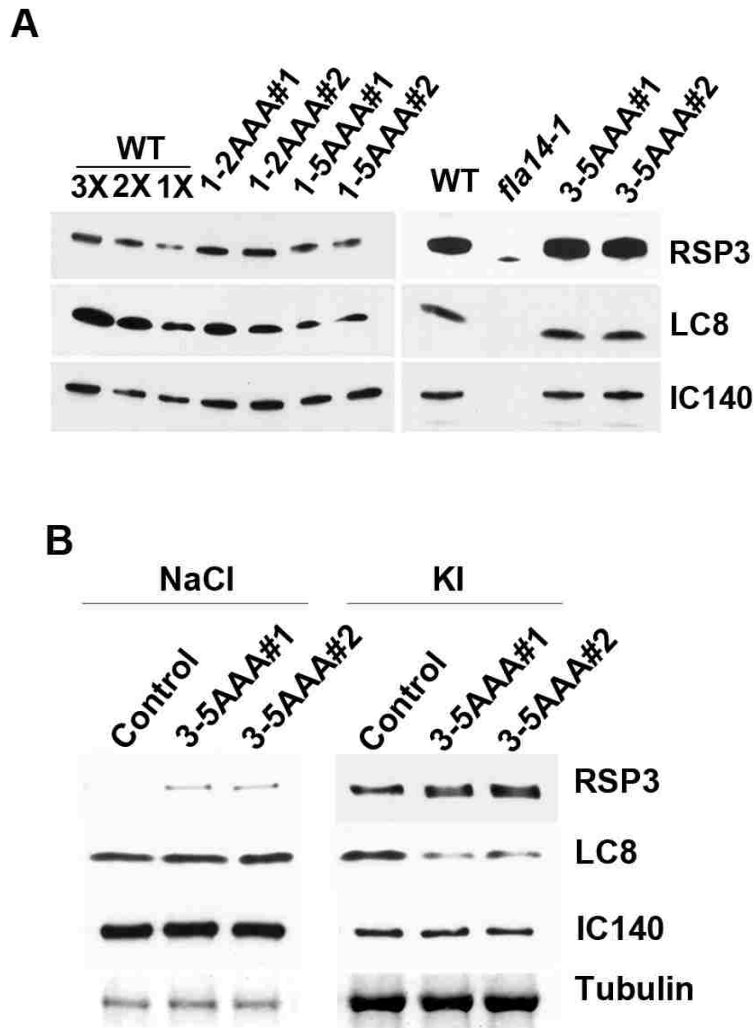
Figure 3-10. The axonemes with 3-5AAA mutations are deficient in the RS and LC8.

(A) Axonemes from the strains as indicated are analyzed by western blots. The axonemes of 1-5AAA strains contain less LC8 and RSP3 than that of 1-2AAA, 3-5AAA and WT strains. The reduction in levels of RSP3 and LC8 in some preparations of 1-5AAA and 3-5AAA was not as evident. 3X; 2X; 1X represents different concentration of axonemes, (B) Western blots of the NaCl extract and the KI extract. Contrary to WT control, a fraction of the RS from the 3-5AAA axonemes is extracted by NaCl as dyneins. The KI extract that contain RSP3 has less amount of LC8 than the WT control. Note mutated RSP3 appears as tightly

3.8.3 AAA mutants are hypo-phosphorylated

In gradient gels, the mutated tagged RSP3 sometimes appeared tightly packed double bands, contrary to the single band of WT RSP3 (Figure 3-10B, right panel). In 6% SDS-PAGE the RSP3 molecules from 3-5AAA, 1-5AAA or 1-5AN strains were all clearly resolved into two bands (Figure 3-11, upper panel, dot and line)— the upper band (dot) co-migrating with WT RSP3. The double tagged RSP3 bands from the RSP3 mutants resemble the double untagged RSP3 bands from the LC8 mutant *fla14-3* and the spoke mutant *pf27* of an unknown genetic defect (Figure 3-11, lower panel; Yang et al., 2009; Yang and Yang, 2006). The axonemes of *pf27* contain less RSs and in vivo ^{32}P labeling showed that phosphorylation of RSP3 and the other spoke phosphoproteins was absent or diminished (Huang et al., 1981; Yang and Yang, 2006). To test for RSP3 phosphorylation level in mutant axonemes, a blot of axonemes was probed with a monoclonal antibody that recognized epitopes containing phospho-threonine-proline (p-thr-pro), the phosphorylation sites of proline-directed protein kinases. Two only sites of such were near the TQT-like motifs (Figure 3-2A, asterisks) and these two sites in human RSP3 were phosphorylated in vitro by ERK1/2 (Jivan et al., 2009). The protein loads were adjusted so that RSP3 amount in each lane was similar, except the negative control *pf14*. The p-thr-pro antibody recognized the upper RSP3 band (dot) but not the lower band (line) in the axonemes with mutated LC8 (*fla14-3*) or mutated RSP3 (3-5AAA) (compare RSP3 and p-thr-pro blots in Fig. 3-11 lower panel). It did not decorate either band of *pf27* RSP3. Together, these data indicate that RSP3 is a substrate of a proline-directed protein kinase; and one or both conserved phosphorylation sites near the LC8 binding region are hypo-phosphorylated due to the mutations in LC8 or the LC8-binding sites in RSP3.
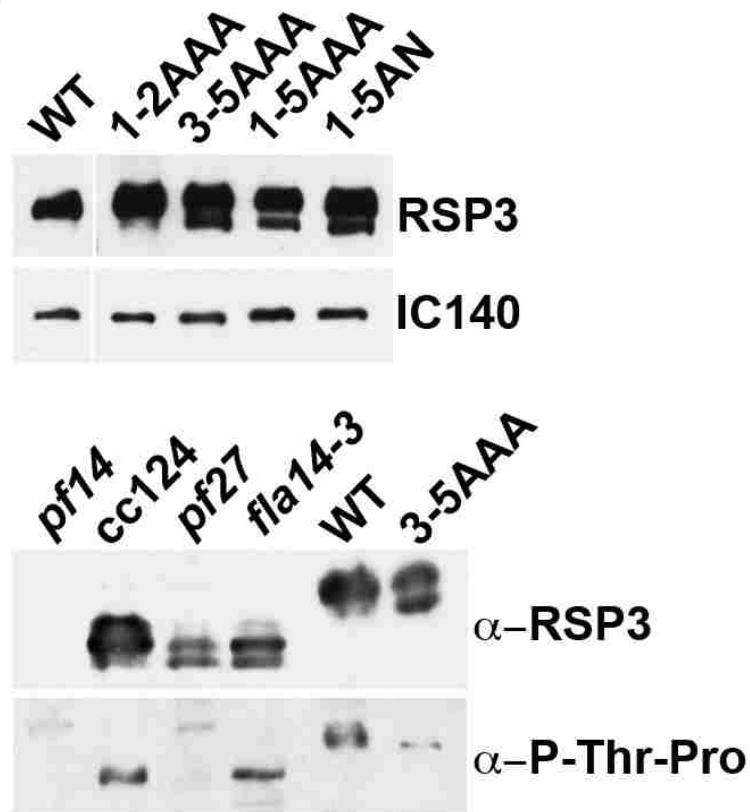
Figure 3-11. The axonemes with 3-5AAA, 1-5AAA and 1-5AN mutations are deficient in phosphorylation. Western blots of the 6% SDS-PAGE revealed hypo-phosphorylated RSP3 in the axonemes of RSP3 and LC8 mutants. The tagged RSP3 defective in the last three LC8-binding motifs migrates as double bands, contrary to the smear in the WT control and 1-2AAA strain (upper panel). The untagged RSP3 polypeptides in *pf27* and *fla14-3* axonemes were less abundant than WT RSP3 and migrated as double bands as well (bottom panel). The upper RSP3 band (dot) in RSP3 mutant or LC8 mutant *fla14-3* was recognized by a phosphor-threonine-proline monoclonal antibody, whereas the lower band (line) was not. Both RSP3 bands in *pf27* were not recognized by the antibody.

Summary

This dissertation set out to test the hypothesis that **LC8 directly binds to RSP3 to promote the assembly of the RS complex**. The findings from independent approaches confirmed this hypothesis and revealed multiple effects from this interaction:

1) There are multiple LC8 binding sites at the N-terminal region of RSP3.
Sequence analysis of RSP3 revealed that there are five TQT-like LC8-binding motifs at the N-terminus of RSP3 (Figure 3-1A). This is unusual since ICs in axonemal dynein contain only one site and the IC in the cytoplasmic dynein that drives IFT has two sites (Rompolas et al., 2007). Like other LC8-binding sequences, this region in RSP3 is predicted to be disordered in contrast to the C-terminus of RSP3 that is largely helical with strong propensity to form coiled coils (Figure 3-1B).

2) Multiple LC8s bind directly to RSP3 N-terminus. RSP3 N-terminus and LC8 from trypsin-treated axonemes co-migrated in the native gel as two RS sub-particles (Figure 3-2). This finding also supported the prediction that the RSP3 N-terminus contains multiple LC8-binding sites to directly interact with LC8. This finding was substantiated by in vitro co-purification of S-tagged RSP3 N-terminus and His-LC8 by either Ni-NTA or S-agarose affinity matrixes (Figure 3-3). Densitometry indicates that the first 160 a.a- fragment of the dimeric RSP3 could directly associate with at-least 3 LC8 dimers.

3) RSP3 N-terminus is phosphorylated and forms homo-dimers. The two RSP3 N-terminal 1-170 a.a. constructs expressing His-tag or Cys-tag RSP3 in axonemes

migrated in SDS-PAGE as monomers and dimers (Figure 3-5). This indicated that the region that binds to multiple LC8 exists as a homodimer. The monomeric polypeptide from both constructs also migrated as multiple bands. This suggests that at least some phosphorylated residues in RSP3 reside in the N-terminal region that binds LC8.

4) LC8 binding promotes docking of the RSP3 N-terminus. In presence of LC8, more RSP3 N-terminus fragments can be reconstituted to the spoke-less axoneme *pf14* than in the absence of LC8. This suggests that association with LC8 enhances the binding of RSP3 N-terminus to axonemes (Figure 3-4).

5) Pull down of RSP3 N-terminus contains LC8 and the putative RS docking proteins. The LC8, RSP11, RSP7 in the RS; the IP2, IP3 and IP4 in the CSC complex and a novel docking protein, FAP206 are co-purified with His tagged $RSP3_{1-178}$ (Figure 3-6). Thus, the CSC complex and FAP206 are located near the base of the RS, likely for directly interacting with RSP3 N-terminus.

6) LC8 is not detectable in RS precursors in the flagellar matrix. Although LC8 is present in the mature RS, the fractionation of soluble flagellar matrix showed that LC8 is not detectable in the 12S RS precursor fractions (Figure 3-7). This supports an interesting idea that LC8 binds the other major RSPs after they arrive in the flagella, possibly at the tip.

7) Mutation of LC8 binding sites in RSP3 results in multiple defects. The mutation of the TQT-like motif into AAA results in defective motility, (Figure 3-8); less LC8 in the RS and reduced stability of RS-axoneme association (Figure 3-9); and more hypo-phosphorylated RSP3 (Figure 3-10). These pleiotropic effects from LC8 mutations

provide the in vivo evidence supporting the results described above from independent approaches.

Collectively, these results shed light on the long-standing questions regarding molecular assembly in motile cilia. Chapter 4 will thoroughly discuss these findings and their implications.

CHAPTER 4: DISCUSSION

The investigation of the role of LC8 in the assembly of the RS complex showed that multiple LC8 dimers bind to the RSP3 N-terminus and the binding has three effects on RSP3: to promote phosphorylation, to form the stalk and to associate with the docking proteins. These results shed new light on LC8, RSP3 and the assembly of axonemal complexes during ciliogenesis.

Multiple LC8 binding sites in RSP3

Independent lines of evidence indicate that RSP3 N-terminus binds to multiple LC8 dimers in tandem. First of all, quantification of the in vitro binding assay of bacterially expressed RSP3 N-terminus and LC8 demonstrated RSP3 binds to LC8 at a ratio of 1:3 (Figure 3-3). Secondly, the comparison of LC8 amounts in spokeless and WT axonemes suggests that the amount of LC8 in the RS fraction accounts for about a half of the total LC8 content in axonemes (Figure 3-5). Furthermore, the trypsin digested RS particle with longer RSP3 fragments contains more LC8 molecules than the smaller one with shorter RSP3 fragments (Figure 3-2). Moreover, perturbations of the last three LC8-binding sites in RSP3 result in significant reduction of LC8 in the RS-containing KI extract (Figure 3-10). Thus it is likely that each RSP3 dimer associates with at least 3 LC8 dimers.

While conservative mutagenesis is sufficient to perturb the LC8-binding site effectively in several target polypeptides with a single binding site (Puthalakath et al., 1999; Bergen and Pun, 2007), it is necessary to mutate TQT-like motifs into AAA in

RSP3 (Table 3-1) as well as in Bassoon (Fejtova et al., 2009) for mutants to exhibit phenotypes. Both molecules have at least 3 binding sites aligned in tandem. In the same vein, truncation mutagenesis of all binding sites was taken to investigate the functions of the 2 and 5 LC8-binding sites in p53BP1 and Nup159, respectively (Lo et al., 2005; Stelter et al., 2007). The difficulty in perturbing tandem-aligned LC8 binding sites may be related to the synergistic effect on the affinity (Williams, et al., 2007). For the target peptides that associate with two LC8 dimers in tandem, binding of the first dimer enhances the affinity for the 2nd dimer by 1000 fold (Hall et al., 2009). Therefore, in the region with an array of LC8 binding sites, the conservative mutagenesis may not reduce the affinity for LC8 enough after the neighboring site associates with LC8.

The role of a stack of LC8 dimers in the RS

Each RSP3 dimer with multiple LC8 dimers in tandem will account for part of the spoke stalk. High-resolution EM of reconstituted dimeric Nup159 peptides and LC8 revealed a 20-nm rigid rod of 5 tightly packed LC8 dimers despite varied distances between the LC8-binding sites (Stelter, et al., 2007). These sites were 9 – 22 a.a apart in contrast to the LC8 binding sites in RSP3 that are 17 – 30 a.a apart. The larger distance between the LC8 binding sites but formation of close stack as seen in Nup159 will result in longer sequences protruding out of stacks forming secondary structure (Figure 4-1A).

However, the crystallography of dynein IC peptides with two LC dimers has inconsistent results. The study predicts that there is bending between the two sites that binds two LC8 dimers (IC.LC8.LC8) in tandem. The bending between the two LC dimers suggests that there is flexibility in this complex (Williams et al., 2007; Hall et al., 2009).

This flexibility was observed when the two LC8 sites were 12 a.a. apart and could vary according to the distance between the binding sites.

Regardless of rigidity or flexibility, a stack of 3-5 LC8 dimers between RSP3 dimers may contribute 12-20 nm to the 40-nm long spoke stalk (Nicastro et al., 2005) (Figure 4-1). It is possible that the longer sequences between LC8-binding sites protrude from the stack (Figure 4-1A) to interact with other molecules, like docking proteins or kinases; or they may account for additional length during RS tilting while flagellar beating (Figure 1-2). Either way LC8 binding could change the physical property of the stalk. Appropriate rigidity and elasticity of the stalk is predicted to underlie the RS-mediated coupling of the CP and the outer doublets (Warner and Satir, 1974). Missing LC8 in the RS may result in pliable RSs, consistent with the paralyzed or asynchronous flagella of 1-5AAA and 3-5AAA strains (Figure 3-9).

A recent study has shown that RSP3 is a structural scaffold extending throughout the entire RS complex (Sivadas et al., unpublished data). Other scaffold molecules, including the dimeric IC scaffold in the cargo-associating sub-complex in dynein motors (Sakato and King, 2004); Bassoon, the dimeric scaffold that is involved in the trafficking and organization of vesicles (Fejota et al., 2009); and GKAP, the dimeric neuronal scaffold protein that is involved in trafficking of postsynaptic density (Naisbitt et al. 2000) bind to multiple LC8 dimers. Thus dimeric scaffold molecules with multiple binding sites for the small dimers, spaced at varied distances, may be a common way to form part of an elongated structure with proper physical properties.

The role of LC8 in RSP3 phosphorylation

This study shows that at least one of the two threonine residues near the LC8-binding sites in RSP3 is phosphorylated by a proline-directed protein kinase and mutations in either LC8 or the last three LC8-binding motifs in RSP3 perturb phosphorylation (Figure 3-1A and 3-11). This finding is consistent with the in vitro phosphorylation of these sites by ERK1/2 (Jivan et. al., 2009) and the double bands of RSP3$_{1-170}$ in SDS-PAGE (Figure 3-6). These observations raise the possibility that these sites are also hypo-phosphorylated in the fast migrating RSP3 in the RS particles that lack LC8, i.e. the 12S RS in the LC8-containing M+M (Figure 3-8) and the 20S and 12S RSs in the LC8-null M+M (Qin et al., 2004). In the yeast 2-hybrid system, ERK1/2 binds to an N-terminal extension of a mammalian-unique alternative spliced RSP3 variant. Perhaps this isoform allows RSP3 in selected cell types to tether ERK1/2 into flagella to enhance LC8-dependent phosphorylation efficiency. For RSP3 molecules that lack this extension, these sites may be phosphorylated by one of the proline-directed kinases found in flagellar proteome (Pazour et al., 2005). Note despite complete replacement of TQT-like motifs in 1-5AAA RSP3, there are still a fraction of phosphorylated RSP3 (Figure 3-11). Perhaps the mutations do not completely block LC8 binding; or LC8 binding merely enhances phosphorylation efficiency.

Phosphorylation has been implicated in the regulation of flagellar beating (Piperno et al., 1981; Segal and Luck, 1985; Porter and Sale, 2000); and the assembly and disassembly of axonemal complexes (Qin et al., 2004; Luo et al., 2011). RSP3 phosphorylation is tightly linked to RS assembly process but its significance is not clear yet. Hypo-phosphorylated RSP3 could be assembled into the axonemes of 1-5AN, 3-

5AAA and 1-5AAA strains, while RS assembly and the motility of the 1-5AN flagella appear normal. Several possibilities that are not mutually exclusive could be considered. Firstly, the fraction of hypo-phosphorylated RSP3 may be too low to cause phenotypes. Or phosphorylation facilitates rather than necessitates certain molecular interactions and some of which are dispensable. For example, in HEK293 cells inhibition of ERK activity negatively affect the interaction of recombinant RSP3, presumably the amphipathic helix specifically with PKA's RII subunit (Jivan et. al., 2009). Perhaps in *Chlamydomonas* flagella, threonine phosphorylation modulates the interaction of the nearby region to interact with the spoke docking proteins or the amphipathic helix (Figure 4-1A, AH) and the RIIa-domain in the RSP7 and RSP11 (Sivadas et al.) (Figure 4-1B, R) that are dispensable but beneficial for consistent flagellar beating (Yang and Yang, 2006; Gaillard et al., 2006).

The role of LC8 in axonemal docking of RSP3

Independent lines of evidence indicate that LC8 promotes the docking of RSP3 and thus RS to the axonemes. Firstly, in vitro reconstitution assays performed using the bacterially expressed RSP3 N-terminus with spokeless axonemes showed that RSP3 binds poorly to the axoneme. The binding of RSP3 to axoneme suggests that RSP3 has tendency to bind axoneme by itself. However the enhanced reconstitution of RSP3 to spokeless axoneme in presence of LC8 suggests that LC8 promotes the docking of RSP3 (Figure 3-5). Secondly, the truncated RS particle expressing His-tagged-RSP3-N-terminus in vivo, while lacking most of the RSPs contained LC8 and the putative docking proteins like IP2, IP3 and IP4 of the CSC complex (Figure 3-7). Furthermore, the LC8

binding sites are either inside or at the downstream region of the axoneme-binding site in

RSP3 (Figure 3-1). Lastly, despite the abundance of LC8 in mature 20S RS isolated from

axoneme or the flagellar matrix, it is not detectable in the 12S precursor particles (Figure

3-8). The large portion of LC8 sediments as free particle at the top of the gradient both in

the matrix and cell body extracts. The simplest interpretation is that LC8 binds to RSP3

in the 12S RS precursors to promote the association of RSP3 with the docking proteins

for becoming part of the axoneme. The process of binding LC8 to 12S in flagella could

serve as a control mechanism to prevent premature assembly of RS with the axoneme

(Figure 4-2).

The pull down of FAP206 as well as CSC complex with RSP3 N-terminus shed

light on the molecular mechanism underlying the precise architecture of the axoneme

(Nicastro et al., 2006). As mentioned in Chapter 1, there are two RS in each 96-nm

longitudinal repeat (Figure 1-1A). The bases of the first and the second spokes are in

proximity to different dynein motors that confer distinct features to the oscillatory beating

and are regulated differently (Porter and Sale, 1999; Kamiya, 2002). The structures in

these two regions have discreet morphologies and are believed to be important for

anchoring and linking the RS to distinct subsets of dynein motors (Huang et al., 1982;

Piperno et al., 1992; Heusero, et al., 2009). A recent RNAi study has implicated the CSC

complex in the assembly of the spoke 2 only (Dymek et al., 2011). Furthermore, the pull

down of CSC did not contain additional polypeptide the size of FAP206 (Dymek et al.,

2007). Thus FAP206 assembles independently of CSC complex and may be involved in

docking spoke 1 (Figure 3-7).

This study also raises the possibility that in spite of the large pool of small LC8 particles known to be present in the flagellar matrix (Rompolas et al., 2007) and the cell body (Puthalakath et al., 1999), certain target proteins do not bind LC8 until at particular timings or cellular compartments. For the RS, the most interesting scenario is that, like the spoke HSP40 (Yang et al., 2005; Yang et al., 2008), LC8 and precursor complexes enter flagella separately (Figure 4-2). Upon arrival at the tip of flagella, the N-terminus of RSP3 in the RS precursor becomes accessible to the copious amounts of LC8 and their interaction triggers a series of events: the formation of the basal part of the stalk; RSP3 phosphorylation by an unknown kinase; anchoring of the RIIa domain; and the interaction with the docking proteins.

This model explains that an additional tail at the LC8 C-terminus as seen in the *fla14-3* mutant may interfere with the stacking of multiple LC8 dimers, causing the low abundance, reduced stability and hypo-phosphorylation of the RSs (Yang et al., 2009). By the same token but to a lesser extent, the short length flagella of the *fla14-3* mutant suggests that the LC8 C-terminal tail also affects cytoplasmic dyneins that bind two LC8 dimers in tandem (Rompolas, et al., 2007) more than axonemal dyneins that bind to one LC8 dimer only. This model also explains the distinct morphologies of 12S and 20S spoke particles (Diener et al., 2011). In particular, the length of the stalk in the 12S is approximately half of that in the 20S RS on the axoneme or in the axonemal extract. The missing bottom part may contain the LC8-RSP3 complex and the docking proteins. This model is not necessarily applicable to all LC8-containing complexes in flagella. Some complexes are not assembled in the well-known tip-to-base direction as the RS (Johnson et al., 1999; Piperno et al., 1996), and LC8 also affects each complex differently (Yang et

al., 2009). Yet the series of reactions, triggered by LC8 for the assembly of a mature RS, may commonly occur in the final steps of the process of ciliogenesis.
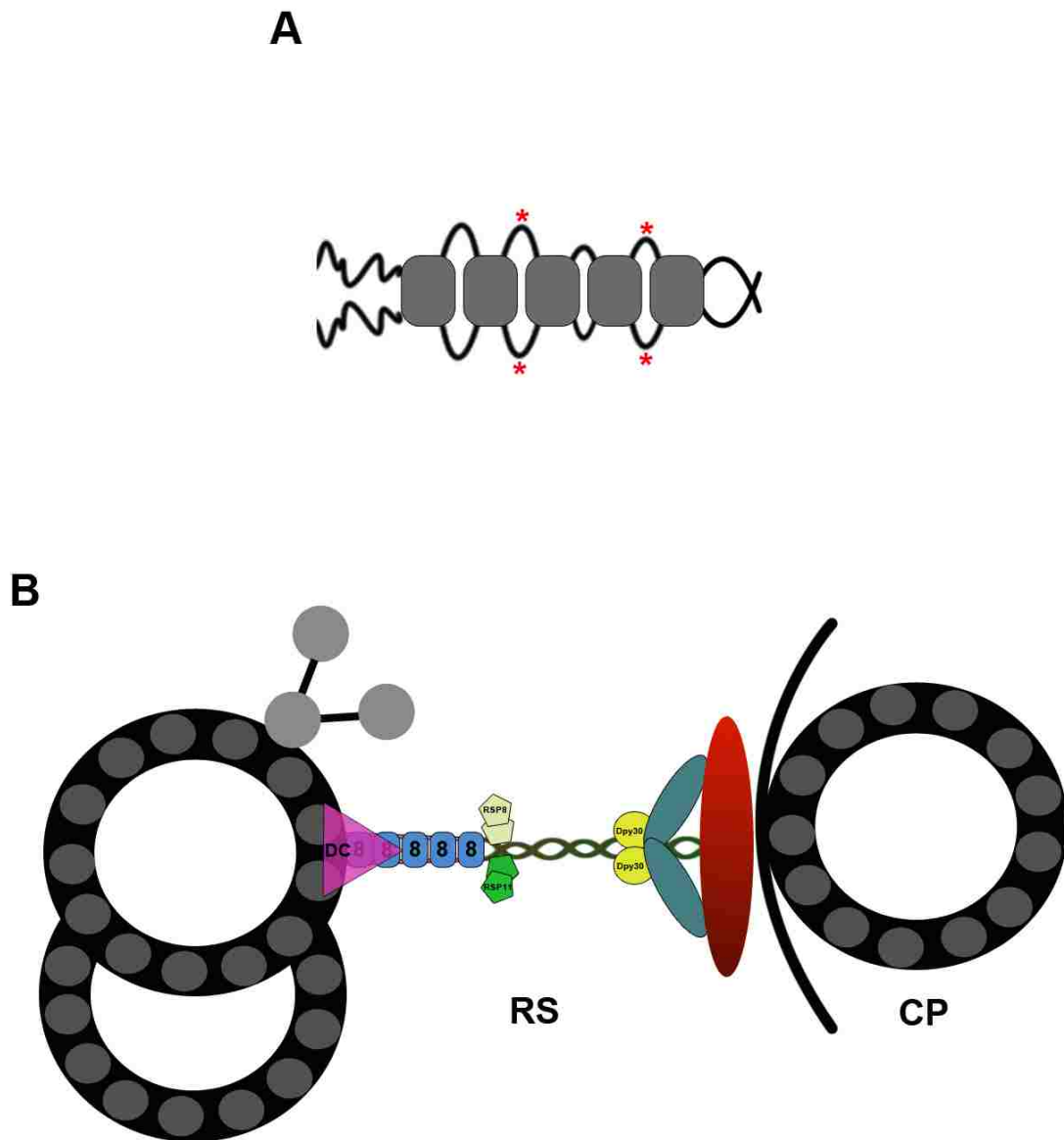
Figure 4-1. The model depicting the three effects of LC8 in the RS complex. A stack of 3-5 LC8 dimers binds to an RSP3 dimer to (A) form the basal part of the stalk; and enhance phosphorylation (asterisks); (B) to promote the RSP3-docking complex association.
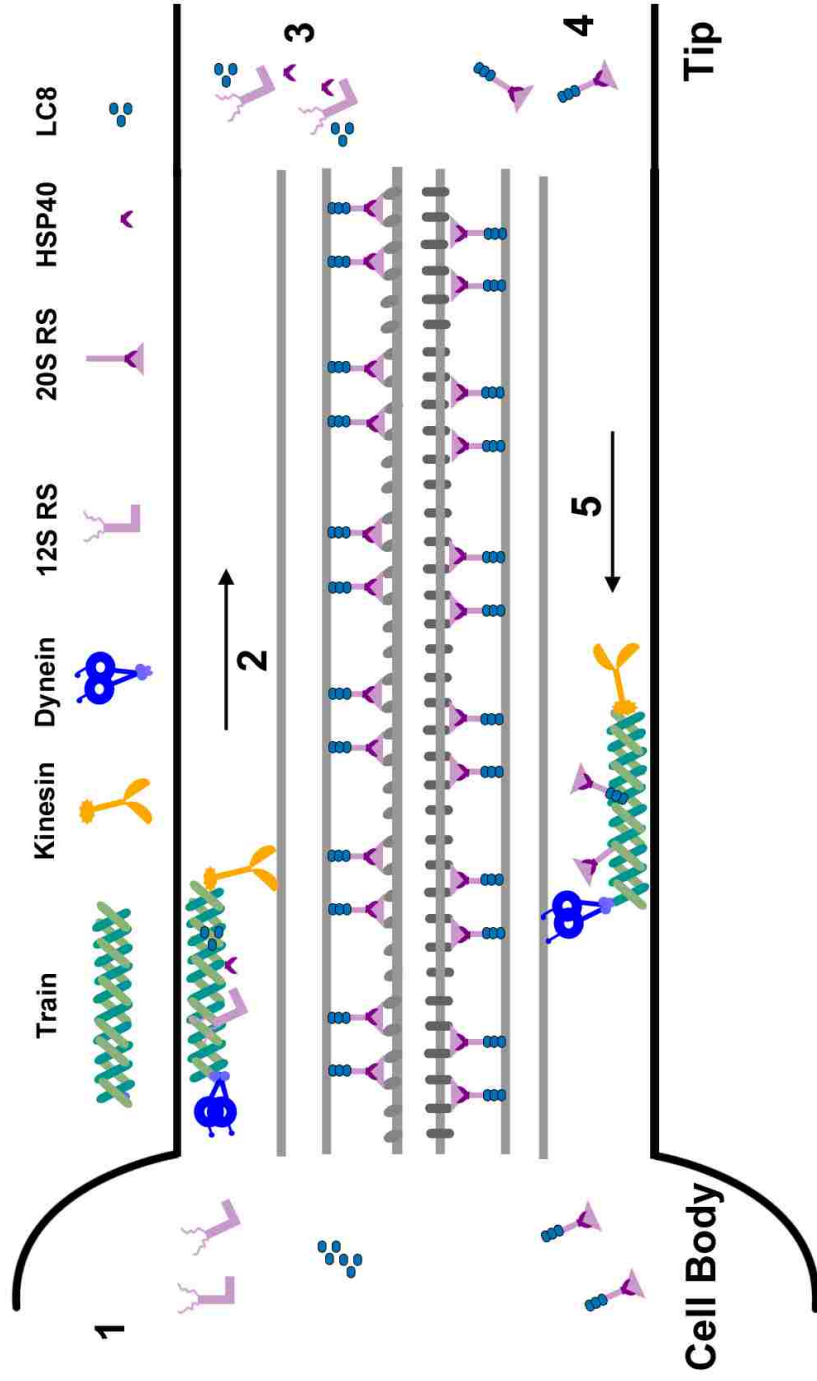
Figure 4-2. Model depicting the binding of LC8 at the tip of the flagella.

The LC8 like HSP40 is transported separately into the flagella. Upon arrival at the tip of flagella, the N-terminus of RSP3 in the RS precursor become accessible to the copious amounts of LC8 and their interactions trigger a series of events: the formation of the basal part of the stalk; RSP3 phosphorylation by an unknown kinase; anchoring of the RIIa domain; and the interaction with the docking proteins.

REFERENCES

Avidor-Reiss, T., A. M. Maer, et al. (2004). "Decoding cilia function: defining specialized genes required for compartmentalized cilia biogenesis." Cell 117(4): 527-39.

Barbar, E. (2008). "Dynein light chain LC8 is a dimerization hub essential in diverse protein networks." Biochemistry 47(2): 503-8.

Beckwith, S. M., C. H. Roghi, et al. (1998). "The "8-kD" cytoplasmic dynein light chain is required for nuclear migration and for dynein heavy chain localization in Aspergillus nidulans." J Cell Biol 143(5): 1239-47.

Benison, G., A. Nyarko, et al. (2006). "Heteronuclear NMR identifies a nascent helix in intrinsically disordered dynein intermediate chain: implications for folding and dimerization." J Mol Biol 362(5): 1082-93.

Benison, G., P. A. Karplus, et al. (2007). "Structure and dynamics of LC8 complexes with KXTQT-motif peptides: swallow and dynein intermediate chain compete for a common site." J Mol Biol 371(2): 457-68.

Bergen, J. M. and S. H. Pun (2007). "Evaluation of an LC8-binding peptide for the attachment of artificial cargo to dynein." Mol Pharm 4(1): 119-28.

Bregman, D. B., Bhattacharyya, N., and Rubin, C. S. (1989). "High affinity binding protein for the regulatory subunit of cAMP-dependent protein kinase II-B. Cloning, characterization, and expression of DNAs for rat brain P150." J. Biol. Chem. 264: 4648 56.

Casey, D. M., K. Inaba, et al. (2003). "DC3, the 21-kDa subunit of the outer dynein arm-docking complex (ODA-DC), is a novel EF-hand protein important for assembly of both the outer arm and the ODA-DC." Mol Biol Cell 14(9): 3650-63.

Cole, D. G. (2003). "The intraflagellar transport machinery of Chlamydomonas reinhardtii." Traffic 4(7): 435-42.

Cole, D. G., S. W. Chinn, et al. (1993). "Novel heterotrimeric kinesin-related protein purified from sea urchin eggs." Nature 366(6452): 268-70.

Curry, A. M. and J. L. Rosenbaum (1993). "Flagellar radial spoke: a model molecular genetic system for studying organelle assembly." Cell Motil Cytoskeleton 24(4): 224-32.

Davenport, J. R. and B. K. Yoder (2005). "An incredible decade for the primary cilium: a look at a once-forgotten organelle." Am J Physiol Renal Physiol 289(6): F1159-69.

Deane, J. A., D. G. Cole, et al. (2001). "Localization of intraflagellar transport protein IFT52 identifies basal body transitional fibers as the docking site for IFT particles." Curr Biol 11(20): 1586-90.

DiBella, L. M., O. Gorbatyuk, et al. (2005). "Differential light chain assembly influences outer arm dynein motor function." Mol Biol Cell 16(12): 5661-74.

DiBella, L. M., M. Sakato, et al. (2004). "The LC7 light chains of Chlamydomonas flagellar dyneins interact with components required for both motor assembly and regulation." Mol Biol Cell 15(10): 4633-46.

DiBella, L. M., E. F. Smith, et al. (2004). "A novel Tctex2-related light chain is required for stability of inner dynein arm I1 and motor function in the Chlamydomonas flagellum." J Biol Chem 279(20): 21666-76.

DiBella, L. M. and S. M. King (2001). "Dynein motors of the Chlamydomonas flagellum." Int Rev Cytol 210: 227-68.

Dick, T., K. Ray, et al. (1996). "Cytoplasmic dynein (ddlc1) mutations cause morphogenetic defects and apoptotic cell death in Drosophila melanogaster." Mol Cell Biol 16(5): 1966-77.

Diener, D. R., L. H. Ang, et al. (1993). "Assembly of flagellar radial spoke proteins in Chlamydomonas: identification of the axoneme binding domain of radial spoke protein 3." J Cell Biol 123(1): 183-90.

Diener, D. R., P. Yang, et al. (2011). "Sequential assembly of flagellar radial spokes." Cytoskeleton (Hoboken).

Dymek, E. E. and E. F. Smith (2007). "A conserved CaM- and radial spoke associated complex mediates regulation of flagellar dynein activity." J Cell Biol 179(3): 515-26.

Dymek, E. E., T. Heuser, et al. (2011) "The CSC is required for complete radial spoke assembly and wild-type ciliary motility." Mol Biol Cell.

Fejtova, A., D. Davydova, et al. (2009). "Dynein light chain regulates axonal trafficking and synaptic levels of Bassoon." J Cell Biol 185(2): 341-55.

Fan, J., Q. Zhang, et al. (2001). "Structural basis of diverse sequence-dependent target recognition by the 8 kDa dynein light chain." J Mol Biol 306(1): 97-108.

Gaillard, A. R., D. R. Diener, et al. (2001). "Flagellar radial spoke protein 3 is an A-kinase anchoring protein (AKAP)." J Cell Biol 153(2): 443-8.

Gaillard, A. R., L. A. Fox, et al. (2006). "Disruption of the A-kinase anchoring domain in flagellar radial spoke protein 3 results in unregulated axonemal cAMP-dependent protein kinase activity and abnormal flagellar motility." Mol Biol Cell 17(6): 2626-35.

Gardner, L. C., E. O'Toole, et al. (1994). "Components of a "dynein regulatory complex" are located at the junction between the radial spokes and the dynein arms in Chlamydomonas flagella." J Cell Biol 127(5): 1311-25.

Gerdes, J. M., E. E. Davis, et al. (2009). "The vertebrate primary cilium in development, homeostasis, and disease." Cell 137(1): 32-45.

Gibbons, B. H. and I. R. Gibbons (1972). "Flagellar movement and adenosine triphosphatase activity in sea urchin sperm extracted with triton X-100." J Cell Biol 54(1): 75-97.

Habermacher, G. and W. S. Sale (1995). "Regulation of dynein-driven microtubule sliding by an axonemal kinase and phosphatase in Chlamydomonas flagella." Cell Motil Cytoskeleton 32(2): 106-9.

Habermacher, G. and W. S. Sale (1997). "Regulation of flagellar dynein by phosphorylation of a 138-kD inner arm dynein intermediate chain." J Cell Biol 136(1): 167-76.

Hall, J., P. A. Karplus, et al. (2009). "Multivalency in the assembly of intrinsically disordered Dynein intermediate chain." J Biol Chem 284(48): 33115-21.

Harrison, A., P. Olds-Clarke, et al. (1998). "Identification of the t complex-encoded cytoplasmic dynein light chain tctex1 in inner arm I1 supports the involvement of flagellar dyneins in meiotic drive." J Cell Biol 140(5): 1137-47.

Harris, E. H. (2001). "Chlamydomonas as a Model Organism." Annu Rev Plant Physiol Plant Mol Biol 52: 363-406.

Hasegawa, E., H. Hayashi, et al. (1987). "Stimulation of in vitro motility of Chlamydomonas axonemes by inhibition of cAMP-dependent phosphorylation." Cell Motil Cytoskeleton 8(4): 302-11.

Hendrickson, T. W., C. A. Perrone, et al. (2004). "IC138 is a WD-repeat dynein intermediate chain required for light chain assembly and regulation of flagellar bending." Mol Biol Cell 15(12): 5431-42.

Hemmens, B., S. Woschitz, et al. (1998). "The protein inhibitor of neuronal nitric oxide synthase (PIN): characterization of its action on pure nitric oxide synthases." FEBS Lett 430(3): 397-400.

Hodi, Z., A. L. Nemeth, et al. (2006). "Alternatively spliced exon B of myosin Va is essential for binding the tail-associated light chain shared by dynein." Biochemistry 45(41): 12582-95.

Howard, D. R., G. Habermacher, et al. (1994). "Regulation of Chlamydomonas flagellar dynein by an axonemal protein kinase." J Cell Biol 127(6 Pt 1): 1683-92.

Huang, B., G. Piperno, et al. (1981). "Radial spokes of Chlamydomonas flagella: genetic analysis of assembly and function." J Cell Biol 88(1): 80-8.

Jacob, Y., H. Badrane, et al. (2000). "Cytoplasmic dynein LC8 interacts with lyssavirus phosphoprotein." J Virol 74(21): 10217-22.

Jaffrey, S. R. and S. H. Snyder (1996). "PIN: an associated protein inhibitor of neuronal nitric oxide synthase." Science 274(5288): 774-7.

Johnson, K. A. and J. L. Rosenbaum (1992). "Polarity of flagellar assembly in Chlamydomonas." J Cell Biol 119(6): 1605-11.

Jivan, A., S. Earnest, et al. (2009). "Radial spoke protein 3 is a mammalian protein kinase A-anchoring protein that binds ERK1/2." J Biol Chem 284(43): 29437-45.

Jung, Y., H. Kim, et al. (2008). "Dynein light chain LC8 negatively regulates NF-kappaB through the redox-dependent interaction with IkappaBalpha." J Biol Chem 283(35): 23863-71.

Kagami, O., S. Takada, et al. (1990). "Microtubule translocation caused by three subspecies of inner-arm dynein from Chlamydomonas flagella." FEBS Lett 264(2): 179-82.

Kagami, O. and R. Kamiya (1995). "Separation of dynein species by high-pressure liquid chromatography." Methods Cell Biol 47: 487-9.

Kamiya, R. (2002). "Functional diversity of axonemal dyneins as studied in Chlamydomonas mutants." Int Rev Cytol 219: 115-55.

Kamiya, R. and G. B. Witman (1984). "Submicromolar levels of calcium control the balance of beating between the two flagella in demembranated models of Chlamydomonas." J Cell Biol 98(1): 97-107.

Kindle, K. L. (1990). "High-frequency nuclear transformation of Chlamydomonas reinhardtii." Proc Natl Acad Sci U S A 87(3): 1228-32.

King, S. J. and S. K. Dutcher (1997). "Phosphoregulation of an inner dynein arm complex in Chlamydomonas reinhardtii is altered in phototactic mutant strains." J Cell Biol 136(1): 177-91.

King, S. M. and R. S. Patel-King (1995). "The M(r) = 8,000 and 11,000 outer arm dynein light chains from Chlamydomonas flagella have cytoplasmic homologues." J Biol Chem 270(19): 11445-52.

King, S.M. and Kamiya, R. (2009). "Assembly, Structure and force generation". In: The Chlamydomonas sourcebook: cell motility and behavior, vol. 3, ed. G.B. Witman, Oxford: Academic press, 131-208

Kohno, T., K. Wakabayashi, et al. "Subunit interactions within the Chlamydomonas flagellar spokehead." Cytoskeleton (Hoboken) 68(4): 237-46.

Kozminski, K. G., K. A. Johnson, et al. (1993). "A motility in the eukaryotic flagellum unrelated to flagellar beating." Proc Natl Acad Sci U S A 90(12): 5519-23.

Li, J. Y. and C. F. Wu (2003). "Perspectives on the origin of microfilaments, microtubules, the relevant chaperonin system and cytoskeletal motors--a commentary on the spirochaete origin of flagella." Cell Res 13(4): 219-27.

Li, J. B., J. M. Gerdes, et al. (2004). "Comparative genomics identifies a flagellar and basal body proteome that includes the BBS5 human disease gene." Cell 117(4): 541-52.

Lightcap, C. M., G. Kari, et al. (2009). "Interaction with LC8 is required for Pak1 nuclear import and is indispensable for zebrafish development." PLoS One 4(6): e6025.

Lindemann, C.B. and Lesich, K.A. (2010). "Flagellar and cilliary beating: the proven and the possible." J Cell Sci 123(4): 519-28.

Lechtreck, K. F. and G. B. Witman (2007). "Chlamydomonas reinhardtii hydin is a central pair protein required for flagellar motility." J Cell Biol 176(4): 473-82.

Lechtreck, K. F., P. Delmotte, et al. (2008). "Mutations in Hydin impair ciliary motility in mice." J Cell Biol 180(3): 633-43.

Liang, J., S. R. Jaffrey, et al. (1999). "Structure of the PIN/LC8 dimer with a bound peptide." Nat Struct Biol 6(8): 735-40.

Lo, K. W., H. M. Kan, et al. (2005). "The 8-kDa dynein light chain binds to p53-binding protein 1 and mediates DNA damage-induced p53 nuclear accumulation." J Biol Chem 280(9): 8172-9.

Lo, K. W., H. M. Kan, et al. (2006). "Identification of a novel region of the cytoplasmic Dynein intermediate chain important for dimerization in the absence of the light chains." J Biol Chem 281(14): 9552-9.

Lo, K. W., S. Naisbitt, et al. (2001). "The 8-kDa dynein light chain binds to its targets via a conserved (K/R)XTQT motif." J Biol Chem 276(17): 14059-66.

Marshall, W. F. (2008). "The cell biological basis of ciliary disease." J Cell Biol 180(1): 17-21.

Mitchell, D. R. and M. Nakatsugawa (2004). "Bend propagation drives central pair rotation in Chlamydomonas reinhardtii flagella." J Cell Biol 166(5): 709-15.

Mitchell, D. R. and W. S. Sale (1999). "Characterization of a Chlamydomonas insertional mutant that disrupts flagellar central pair microtubule-associated structures." J Cell Biol 144(2): 293-304.

Mitchell, D. R. and B. Smith (2009). "Analysis of the central pair microtubule complex in Chlamydomonas reinhardtii." Methods Cell Biol 92: 197-213.

Merchant, S. S., S. E. Prochnik, et al. (2007). "The Chlamydomonas genome reveals the evolution of key animal and plant functions." Science 318(5848): 245-50.

Mok, Y. K., K. W. Lo, et al. (2001). "Structure of Tctex-1 and its interaction with cytoplasmic dynein intermediate chain." J Biol Chem 276(17): 14067-74.

Naisbitt, S., J. Valtschanoff, et al. (2000). "Interaction of the postsynaptic density-95/guanylate kinase domain-associated protein complex with a light chain of myosin-V and dynein." J Neurosci 20(12): 4524-34.

Navarro-Lerida, I., M. Martinez Moreno, et al. (2004). "Proteomic identification of brain proteins that interact with dynein light chain LC8." Proteomics 4(2): 339-46.

Nicastro, D., J. R. McIntosh, et al. (2005). "3D structure of eukaryotic flagella in a quiescent state revealed by cryo-electron tomography." Proc Natl Acad Sci U S A 102(44): 15889-94.

Nicastro, D., C. Schwartz, et al. (2006). "The molecular architecture of axonemes revealed by cryoelectron tomography." Science 313(5789): 944-8.

Nyarko, A., J. Hall, et al (2011). "Conformational dynamics promote binding diversity of dynein light chain LC8." Biophys Chem.

Nyarko, A., M. Hare, et al. (2004). "The intermediate chain of cytoplasmic dynein is partially disordered and gains structure upon binding to light-chain LC8." Biochemistry 43(49): 15595-603.

Omoto, C. K. and C. J. Brokaw (1985). "Bending patterns of Chlamydomonas flagella: II. Calcium effects on reactivated Chlamydomonas flagella." Cell Motil 5(1): 53-60.

Omoto, C. K., I. R. Gibbons, et al. (1999). "Rotation of the central pair microtubules in eukaryotic flagella." Mol Biol Cell 10(1): 1-4.

O'Neill, M. J. and K. Artzt (1995). "Identification of a germ-cell-specific transcriptional repressor in the promoter of Tctex-1." Development 121(2): 561-8.

Pan, J. and W. Snell (2007). "The primary cilium: keeper of the key to cell division." Cell 129(7): 1255-7.

Patel-King, R. S., O. Gorbatyuk, et al. (2004). "Flagellar radial spokes contain a Ca2+-stimulated nucleoside diphosphate kinase." Mol Biol Cell 15(8): 3891-902.

Pazour, G. J., N. Agrin, et al. (2005). "Proteomic analysis of a eukaryotic cilium." J Cell Biol 170(1): 103-13.

Pazour, G. J. and G. B. Witman (2003). "The vertebrate primary cilium is a sensory organelle." Curr Opin Cell Biol 15(1): 105-10.

Pazour, G. J. and G. B. Witman (2009). "The Chlamydomonas flagellum as a model for human ciliary disease." In: The Chlamydomonas sourcebook: cell motility and behavior, vol. 3, ed. G.B. Witman, Oxford: Academic press, 445-468

Pazour, G. J., C. G. Wilkerson, et al. (1998). "A dynein light chain is essential for the retrograde particle movement of intraflagellar transport (IFT)." J Cell Biol 141(4): 979-92.

Pedersen, L. B., S. Geimer, et al. (2006). "Dissecting the molecular mechanisms of intraflagellar transport in chlamydomonas." Curr Biol 16(5): 450-9.

Pfister, K. K., P. R. Shah, et al. (2006). "Genetic analysis of the cytoplasmic dynein subunit families." PLoS Genet 2(1): e1.

Piperno, G. and Huang, B (1981). "Radial spokes of Chlamydomonas flagella: polypeptide composition and phosphorylation of stalk components." J Cell Biol 88: 73-79.

Piperno, G., K. Mead, et al. (1996). "Inner dynein arms but not outer dynein arms require the activity of kinesin homologue protein KHP1(FLA10) to reach the distal part of flagella in Chlamydomonas." J Cell Biol 133(2): 371-9.

Piperno, G., K. Mead, et al. (1994). "Mutations in the "dynein regulatory complex" alter the ATP-insensitive binding sites for inner arm dyneins in Chlamydomonas axonemes." J Cell Biol 125(5): 1109-17.

Piperno, G., K. Mead, et al. (1992). "The inner dynein arms I2 interact with a "dynein regulatory complex" in Chlamydomonas flagella." J Cell Biol 118(6): 1455-63.

Piperno, G., Z. Ramanis, et al. (1990). "Three distinct inner dynein arms in Chlamydomonas flagella: molecular composition and location in the axoneme." J Cell Biol 110(2): 379-89.

Puthalakath, H., D. C. Huang, et al. (1999). "The proapoptotic activity of the Bcl-2 family member Bim is regulated by interaction with the dynein motor complex." Mol Cell 3(3): 287-96.

Puthalakath, H., A. Villunger, et al. (2001). "Bmf: a proapoptotic BH3-only protein regulated by interaction with the myosin V actin motor complex, activated by anoikis." Science 293(5536): 1829-32.

Qin, H., D. R. Diener, et al. (2004). "Intraflagellar transport (IFT) cargo: IFT transports flagellar precursors to the tip and turnover products to the cell body." J Cell Biol 164(2): 255-66.

Rapali, P., L. Radnai, et al. "Directed evolution reveals the binding motif preference of the LC8/DYNLL hub protein and predicts large numbers of novel binders in the human proteome." PLoS One 6(4): e18818.

Raux, H., A. Flamand, et al. (2000). "Interaction of the rabies virus P protein with the LC8 dynein light chain." J Virol 74(21): 10212-6.

Regue, L., S. Sdelci, et al. "DYNLL/LC8 protein controls signal transduction through the Nek9/Nek6 signaling module by regulating Nek6 binding to Nek9." J Biol Chem 286(20): 18118-29.

Rodriguez-Crespo, I., B. Yelamos, et al. (2001). "Identification of novel cellular proteins that bind to the LC8 dynein light chain using a pepscan technique." FEBS Lett 503(2-3): 135-41.

Rodriguez-Crespo, I., W. Straub, et al. (1998). "Binding of dynein light chain (PIN) to neuronal nitric oxide synthase in the absence of inhibition." Arch Biochem Biophys 359(2): 297-304.

Rompolas, P., L. B. Pedersen, et al. (2007). "Chlamydomonas FAP133 is a dynein intermediate chain associated with the retrograde intraflagellar transport motor." J Cell Sci 120(Pt 20): 3653-65.

Rosenbaum, J. L. and G. B. Witman (2002). "Intraflagellar transport." Nat Rev Mol Cell Biol 3(11): 813-25.

Rupp, G. and M. E. Porter (2003). "A subunit of the dynein regulatory complex in Chlamydomonas is a homologue of a growth arrest-specific gene product." J Cell Biol 162(1): 47-57.

Salathe, M. (2007). "Regulation of mammalian ciliary beating." Annu Rev Physiol 69: 401-22.

Sakato, M. and S. M. King (2004). "Design and regulation of the AAA+ microtubule motor dynein." J Struct Biol 146(1-2): 58-71.

Satir, P. and S. T. Christensen (2007). "Overview of structure and function of mammalian cilia." Annu Rev Physiol 69: 377-400.

Scholey, J. M. and K. V. Anderson (2006). "Intraflagellar transport and cilium-based signaling." Cell 125(3): 439-42.

Segal, R. A., B. Huang, et al. (1984). "Mutant strains of Chlamydomonas reinhardtii that move backwards only." J Cell Biol 98(6): 2026-34.

Singla, V. and J. F. Reiter (2006). "The primary cilium as the cell's antenna: signaling at a sensory organelle." Science 313(5787): 629-33.

Silflow, C. D., P. A. Lefebvre, et al. (1982). "Expression of flagellar protein genes during flagellar regeneration in Chlamydomonas." Cold Spring Harb Symp Quant Biol 46 Pt 1: 157-69.

Snell, W. J., J. Pan, et al. (2004). "Cilia and flagella revealed: from flagellar assembly in Chlamydomonas to human obesity disorders." Cell 117(6): 693-7.

Smith, E. F. (2002). "Regulation of flagellar dynein by calcium and a role for an axonemal calmodulin and calmodulin-dependent kinase." Mol Biol Cell 13(9): 3303-13.

Smith, E. F. and P. Yang (2004). "The radial spokes and central apparatus: mechano-chemical transducers that regulate flagellar motility." Cell Motil Cytoskeleton 57(1): 8-17.

Sui, H. and K. H. Downing (2006). "Molecular architecture of axonemal microtubule doublets revealed by cryo-electron tomography." Nature 442(7101): 475-8.

Summers, K. E. and I. R. Gibbons (1971). "Adenosine triphosphate-induced sliding of tubules in trypsin-treated flagella of sea-urchin sperm." Proc Natl Acad Sci U S A 68(12): 3092-6.

Stelter, P., R. Kunze, et al. (2007). "Molecular basis for the functional interaction of dynein light chain with the nuclear-pore complex." Nat Cell Biol 9(7): 788-96.

Tan, G. S., M. A. Preuss, et al. (2007). "The dynein light chain 8 binding motif of rabies virus phosphoprotein promotes efficient viral transcription." Proc Natl Acad Sci U S A 104(17): 7229-34.

Vadlamudi, R. K., R. Bagheri-Yarmand, et al. (2004). "Dynein light chain 1, a p21-activated kinase 1-interacting substrate, promotes cancerous phenotypes." Cancer Cell 5(6): 575-85.

Wagner, W., E. Fodor, et al. (2006). "The binding of DYNLL2 to myosin Va requires alternatively spliced exon B and stabilizes a portion of the myosin's coiled-coil domain." Biochemistry 45(38): 11564-77.

Wang, L., M. Hare, et al. (2004). "Dynein light chain LC8 promotes assembly of the coiled-coil domain of swallow protein." Biochemistry 43(15): 4611-20.

Wakabayashi, K., T. Ide, et al. (2009). "Calcium-dependent flagellar motility activation in Chlamydomonas reinhardtii in response to mechanical agitation." Cell Motil Cytoskeleton 66(9): 736-42.

Wargo, M. J., E. E. Dymek, et al. (2005). "Calmodulin and PF6 are components of a complex that localizes to the C1 microtubule of the flagellar central apparatus." J Cell Sci 118(Pt 20): 4655-65.

Wargo, M. J., M. A. McPeek, et al. (2004). "Analysis of microtubule sliding patterns in Chlamydomonas flagellar axonemes reveals dynein activity on specific doublet microtubules." J Cell Sci 117(Pt 12): 2533-44.

Warner, F. D. and P. Satir (1974). "The structural basis of ciliary bend formation. Radial spoke positional changes accompanying microtubule sliding." J Cell Biol 63(1): 35-63.

Wei, M., P. Sivadas, et al. "Chlamydomonas mutants display reversible deficiencies in flagellar beating and axonemal assembly." Cytoskeleton (Hoboken) 67(2): 71-80.

Wilkerson, C. G., S. M. King, et al. (1995). "The 78,000 M(r) intermediate chain of Chlamydomonas outer arm dynein isa WD-repeat protein required for arm assembly." J Cell Biol 129(1): 169-78.

Williams, B. D., M. A. Velleca, et al. (1989). "Molecular cloning and sequence analysis of the Chlamydomonas gene coding for radial spoke protein 3: flagellar mutation pf-14 is an ochre allele." J Cell Biol 109(1): 235-45.

Williams, J. C., P. L. Roulhac, et al. (2007). "Structural and thermodynamic characterization of a cytoplasmic dynein light chain-intermediate chain complex." Proc Natl Acad Sci U S A 104(24): 10028-33.

Wilson, M. J., M. W. Salata, et al. (2001). "Light chains of mammalian cytoplasmic dynein: identification and characterization of a family of LC8 light chains." Cell Motil Cytoskeleton 49(4): 229-40.

Wirschell, M., F. Zhao, et al. (2008). "Building a radial spoke: flagellar radial spoke protein 3 (RSP3) is a dimer." Cell Motil Cytoskeleton 65(3): 238-48.

Wirschell, M., C. Yang, et al. (2009). "IC97 Is a Novel Intermediate Chain of I1 Dynein That Interacts with Tubulin and Regulates Interdoublet Sliding." Mol Biol Cell.

Wong, W. and J. D. Scott (2004). "AKAP signalling complexes: focal points in space and time." Nat Rev Mol Cell Biol 5(12): 959-70.

Yang, C., H. A. Owen, et al. (2008). "Dimeric heat shock protein 40 binds radial spokes for generating coupled power strokes and recovery strokes of 9 + 2 flagella." J Cell Biol 180(2): 403-15.

Yang, C., M. M. Compton, et al. (2005). "Dimeric novel HSP40 is incorporated into the radial spoke complex during the assembly process in flagella." Mol Biol Cell 16(2): 637-48.

Yang, P., D. R. Diener, et al. (2001). "Localization of calmodulin and dynein light chain LC8 in flagellar radial spokes." J Cell Biol 153(6): 1315-26.

Yang, P., D. R. Diener, et al. (2006). "Radial spoke proteins of Chlamydomonas flagella." J Cell Sci 119(Pt 6): 1165-74.

Yang, P. and W. S. Sale (1998). "The Mr 140,000 intermediate chain of Chlamydomonas flagellar inner arm dynein is a WD-repeat protein implicated in dynein arm anchoring." Mol Biol Cell 9(12): 3335-49.

Yang, P. and W. S. Sale (2000). "Casein kinase I is anchored on axonemal doublet microtubules and regulates flagellar dynein phosphorylation and activity." J Biol Chem 275(25): 18905-12.

Yang, P., C. Yang, et al. (2004). "Flagellar radial spoke protein 2 is a calmodulin binding protein required for motility in Chlamydomonas reinhardtii." Eukaryot Cell 3(1): 72-81.

Yang, C. and P. Yang (2006). "The flagellar motility of Chlamydomonas pf25 mutant lacking an AKAP-binding protein is overtly sensitive to medium conditions." Mol Biol Cell 17(1): 227-38.

Yang, P., C. Yang, et al. (2009). "Novel LC8 mutations have disparate effects on the assembly and stability of flagellar complexes." J Biol Chem 284(45): 31412-21.

Yang, P. and E.F. Smith (2009). "The flagellar radial spokes." In: The Chlamydomonas sourcebook: cell motility and behavior, vol. 3, ed. G.B. Witman, Oxford: Academic press, 209-229

Zhang, H. and D. R. Mitchell (2004). "Cpc1, a Chlamydomonas central pair protein with an adenylate kinase domain." J Cell Sci 117(Pt 18): 4179-88.